UC Santa Barbara

UC Santa Barbara Electronic Theses and Dissertations

Title

The Systematics, Evolutionary History, and Ecomorphology of Early Pan-pinnipeds

Permalink

https://escholarship.org/uc/item/3gg8q0fc

Author

Everett, Christopher John

Publication Date

2024

Peer reviewed|Thesis/dissertation

eScholarship.org Powered by the California Digital Library
University of California

UNIVERSITY OF CALIFORNIA

Santa Barbara

The Systematics, Evolutionary History, and Ecomorphology of Early Pan-pinnipeds

A dissertation submitted in partial satisfaction of the

requirements for the degree Doctor of Philosophy

in Earth Science

by

Christopher John Everett

Committee in charge:

Professor André Wyss, Chair

Professor Susannah Porter

Professor Bruce Tiffney

December 2024

The dissertation of Christopher John Everett is approved.

_____

Susannah Porter

_____

Bruce Tiffney

_____

André Wyss, Committee Chair

December 2024

VITA OF CHRISTOPHER JOHN EVERETT

December 2024

EDUCATION

Bachelor of Science in Molecular Environmental Biology, University of California, Berkeley, May 2015
Master of Science in Paleobiology, University of California, Santa Barbara, March 2020
Doctor of Philosophy in Paleobiology, University of California, Santa Barbara, December 2024 (expected)

PROFESSIONAL EMPLOYMENT

2016: Lead Fossil Preparator, Paleontology Department and PaleoServices, San Diego Natural History Museum
2017-2024: Teaching Assistant, Department of Earth Science, University of California, Santa Barbara
2019-2020: Fossil Preparator, Earth Sciences, Santa Barbara Museum of Natural History
2021-2023: Teaching Associate, Department of Earth Science, University of California, Santa Barbara
2024: Teaching Associate, Evolution, Ecology, and Marine Biology, University of California, Santa Barbara

PUBLICATIONS

Everett, C. J., Deméré, T. A., & Wyss, A. R. (2023). A new species of Pinnarctidion from the Pysht Formation of Washington State (USA) and a phylogenetic analysis of basal pan-pinnipeds (Eutheria, Carnivora). *Journal of Vertebrate Paleontology*, 42(3), e2178930.

AWARDS

Graduate Student Association Excellence in Teaching Award, April 2021

FIELDS OF STUDY

Major Fields: Paleobiology and Evolutionary Biology
Studies in Carnivoran Systematics and Paleobiology with Professor André Wyss

ABSTRACT

The Systematics, Evolutionary History, and Ecomorphology of Early Pan-pinnipeds

by

Christopher John Everett

Chapter 1 reports on several fossil pinnipedimorph specimens from the Pacific Northwest. Two new taxa ("*Enaliarctos" bertae* and *Proneotherium? borealis*) are described from the late Oligocene of Washington and early Miocene of Oregon. The former is known from a small partial skull and mandible from the Pysht Formation of Clallam County, Washington. This specimen, likely the smallest mature stem-pinniped known, has unusually large postcanine alveoli. *P. borealis* , known from a nearly complete cranium from the Astoria Formation of Lincoln County, Oregon, shares many features with *Pinnarctidion* and *Proneotherium*, but differs in the shape of the zygomatic arch, the size of the molar alveoli, and the shape of the auditory bulla. The newly described taxa possess mosaic features which simultaneously indicate the diversity of form and function of stem pinnipeds but also complicate our understanding of the details of their evolutionary history. This chapter also reports new specimens referable to previously known taxa, "*Enaliarctos" barnesi* and *Pinnarctidion iverseni*. The new *"E." barnesi* specimen preserves the basicranium–missing in the holotype–which thus helps refine how this taxon is related to other pinnipedimorphs. The new *P. iverseni* specimen preserves a nearly complete cranium, mandible, scapula, humerus, femur, tibia, and other elements yet to be prepared. This specimen adds important

anatomical information missing from the holotype , such as details of the facial sutures, lateral basicranium, and postcranial skeleton. Lastly, we report on several marked differences between the type specimens of "*Enaliarctos" mitchelli* and the referred specimen, which indicate that the latter should be recognized as a separate taxon, "*Enaliarctos" sullivani*.

Chapter 2 takes a comprehensive look at the evolutionary relationships of pan-pinnipeds and their arctoid relatives. A broad sampling of taxa were used to determine whether enigmatic taxa such as *Kolponomos*, *Amphicticeps*, amphicynodontids, *Potamotherium*, and *Puijila* are allied with pinnipeds, or if they fit elsewhere on the arctoid tree. A new composite matrix of characters was assembled to parse the differences between canids, ursids, musteloids, pinnipeds, and their extinct relatives. Our results support *Potamotherium* and *Puijila* as basal pan-pinnipeds and *Kolponomos* as an ursid. Although some trees place *Amphicticeps* within Pan-pinnipedia, most suggest it diverged, along with other amphicynodontids, before the arctoid common ancestor. Our results concord with molecular evidence placing pan-pinnipeds closer to mustelids than to ursids. Amphicyonids have mixed results, either diverging from the canid branch or between canids and arctoids. Among pan-pinnipeds, we find that "*Enaliarctos*" is a paraphyletic grade, *Prototaria* and *Proneotherium* diverge before crown pinnipeds, phocids are the earliest-diverging pinniped family, and desmatophocids may be paired with, or nested within, odobenids. A series of twelve trial analyses were run to assess how ordered characters, weighted characters, implied weights, and molecular backbone constraints affect the branch support values of resulting maximum parsimony trees. The only statistically significant effect came from implied weights, which display a strongly negative relationship between Bremer support and bootstrap support values.

Chapter 3 examines the dental disparity and varied diets of arctoid carnivorans (the group including bears, weasels, and seals). Their feliform and canid relatives tend to retain the ancestral carnassial dentition for shearing meat, whereas many arctoids – such as ursids, procyonids, and pinnipeds – possess modified post-canines to feed on plants, invertebrates, or fish. Details of these morphological and corresponding dietary shifts are poorly understood, but can be inferred from the fossil record. The upper fourth premolar (P4), which is preserved often and comparable across disparate groups, serves as a reliable proxy for diet in otherwise enigmatic fossil taxa. The P4s of a variety of extinct and extant arctoids were analyzed using 2D landmark morphometrics. Canids and many early arctoids retain carnassial-like premolars and cluster together as hypercarnivores. Some enigmatic early arctoids, such as *Kolponomos* and *Eoarctos*, occupy morphospace that overlaps with extant hypocarnivores, suggesting they may have eaten more plant material than previously believed. Among pan-pinnipeds, "*Enaliarctos"* species fit intermediately between invertebrate and fish consumers, whereas *Pinnarctidion* and other later-diverging pinnipedimorphs have more overlap with modern piscivorous pinnipeds.

TABLE OF CONTENTS

Chapter 1: New pinnipedimorph fossils from Oregon and Washington, USA

Introduction 1

Pinnipeds, a group of amphibious, typically marine, carnivoran mammals, include the extant walrus (Odobenidae), true seals (Phocidae), and eared seals (Otariidae). Details of their evolutionary history are still being revealed, with significant breakthroughs occurring in the last few decades (Repenning & Tedford, 1977; Wyss, 1988; Berta & Wyss, 1994; Deméré et al., 2003; Berta et al., 2018; Park et al., 2024). Living pinniped families are widely viewed as sharing a common ancestor that diverged from other arctoids (bears, weasels, and their extinct relatives) in the late Eocene or earliest Oligocene (Arnason et al., 2006; Higdon et al., 2007; Nyakatura & Bininda-Emonds, 2012). The pinniped total group, Pan-Pinnipedia, includes all taxa more closely related to pinnipeds than to any other extant mammal (Wolsan et al., 2020). Pinnipedimorpha, sometimes incorrectly used to describe the pinniped total group, is a slightly more exclusive clade that includes all descendants of the last common ancestor of *"Enaliarctos"* and pinnipeds (Berta, 1991) and can be diagnosed by apomorphies of the upper first molar (Everett et al., 2023). At least 12 basal pan-pinniped species have been formally recognized (*Potamotherium valletoni* Geoffroy, 1833; "*Enaliarctos" mealsi* Mitchell and Tedford, 1973; "*Enaliarctos" mitchelli* and *Pinnarctidion bishopi* Barnes, 1979; *Pteronarctos goedertae* Barnes, 1989; *"E." barnesi, "E." emlongi,* and *"E." tedfordi* Berta, 1991; *Pacificotaria hadromma* Barnes, 1992; *Pinnarctidion rayi* Berta, 1994a; *Puijila darwini* Rybczynski et al., 2009; *Pinnarctidion iverseni* Everett et al., 2023). This study adds three new taxa to this list and suggests that some putative odobenids may have diverged earlier than previously thought.

An early leading hypothesis regarding pinniped origins held that two independent aquatic invasions occurred in pinniped carnivorans (McLaren, 1960; Tedford, 1976; de Muizon, 1982). According to this "diphyly" hypothesis, phocids diverged from mustelids whereas otariids (plus odobenids) diverged from ursids. The rise of cladistics (Hennig, 1966), and its role in taxonomy (de Quieroz & Gauthier, 1990), allowed for rigorous testing of hypotheses surrounding pan-pinniped origin(s) and relationships. By considering a broad set of morphological characters – notably those of the dentition, auditory region, and flippers (Wyss, 1987; Wyss, 1988) – in a cladistic framework, the synapomorphies uniting crown pinnipeds came into focus (Berta & Wyss, 1994). Sparse sampling of characters and outgroup taxa, however, led to misinformed hypotheses about which characters were thought to be plesiomorphic, and inflated confidence that groups such as "*Enaliarctos*" (Berta, 1991) and early odobenids (Kohno et al., 1994) were monophyletic. The accumulation of formally described fossil taxa allowed more comprehensive analyses to clarify relationships among early diverging pan-pinnipeds. This progressively refined cladistic framework informs the naming of fossil taxa, often supporting traditional group names but sometimes revealing paraphyly or other shortcomings. Many studies that have described new basal pan-pinnipeds in a phylogenetic context sampled only a subset of early forms, often including a composite "*Enaliarctos*" taxonomic unit, *Pteronarctos goedertae*, and/or *Pinnarctidion spp.* as outgroup(s) to crown Pinnipedia (Rybczynski et al., 2009; Tanaka & Kohno, 2015; Boessenecker & Churchill, 2018). To test the placement of new taxa within the pan-pinniped tree, a wider range of early-diverging taxa has been included here.

Other factors, such as sexual dimorphism, ontogenetic change, and incomplete preservation, complicate the taxonomy of fossil pan-pinnipeds. Sexual dimorphism among early pinnipedimorphs has been reported in "*Enaliarctos" emlongi* (Cullen et al., 2014) and *Pteronarctos goedertae* (Berta, 1994b). However, such inferences are hindered by small sample sizes, lack of postcranial material, and a poor understanding of intraspecific variation. The ontogenetic age of pinnipedimorph fossils is most reliably estimated by determining the number of cranial sutures fused by the time of death (Sivertsen, 1954; Audibert et al., 2017; Kahle et al., 2022). This is useful when dealing with particularly small or morphologically unusual skulls, or when the dentition is missing and cannot illuminate patterns of tooth eruption or wear. Early pan-pinnipeds are known mainly from cranial material, often missing some or all of the teeth. Fortunately, some fossils preserve associated postcranial material, providing important information about early pinnipedimorph locomotory adaptations to aquatic environments (Berta et al., 1989; Berta, 1994a; Rybczynski et al., 2009). Isolated pan-pinniped postcrania have been described, but generally cannot be identified to genus or species (Churchill & Uhen, 2019). Hence, skulls remain the most valuable source of data on pan-pinniped evolution, while postcranial material provides important functional information.

Most early pinnipedimorphs are known from the late Oligocene and early Miocene of California, Oregon, and Washington. The North Pacific seems to be the region of origin for pinnipedimorphs (Repenning et al., 1979; Miyazaki et al., 1995; Deméré et al., 2003), although earlier-diverging pan-pinnipeds such as *Potamotherium* and *Puijila* originated in the Atlantic (Deméré et al., 2003). Recent investigation of pan-pinniped biogeography supports

the hypotheses that Otarioidea (the clade including eared seals and walruses) originated in the North Pacific and Phocidae (true seals) in the North Atlantic, yet the ancestral home of the earliest pan-pinnipeds remains inconclusive (Park et al., 2024). Although the present study does not solve the pan-pinniped origin problem, it corroborates the view that early pinnipedimorphs evolved in the North Pacific.

This work introduces four previously undescribed specimens, three of which represent new basal pinnipedimorph species. The incorporation of these new taxa in an updated character-taxon matrix results in the most detailed consideration of early pinnipedimorph relationships to date, addressing some of the taxonomic challenges posed by paraphyletic genera such as "*Enaliarctos*." These specimens contribute new morphological data that augments our understanding of pinnipedimorph character evolution and may facilitate future study of dimorphism, ontogeny, and intraspecific variation.

Abbreviations

LACM: Natural History Museum of Los Angeles County, Section of Vertebrate Paleontology, Los Angeles, California, U.S.A.

SBMNH: Santa Barbara Museum of Natural History, Santa Barbara, California, U.S.A.

SDSNH: San Diego Society of Natural History, San Diego, California, U.S.A.

UCMP: University of California Museum of Paleontology, Berkeley, California, U.S.A.

USNM: United States National Museum of Natural History, Washington, D.C., U.S.A.

Methods 1

The four specimens presented here were examined in detail at their corresponding institutions. LACM 128004 and LACM 127974 are housed at the Natural History Museum of Los Angeles County. LACM 128004 was previously mentioned and figured in a paper about arctoid basicranial morphology (Hunt & Barnes, 1994), but a detailed description or consideration of its systematic affinities was never published. LACM 127974 was also studied by Barnes, but his notes and manuscript outlines on the specimen were never published. USNM 335376 and USNM 314312 are housed at the Smithsonian National Museum of Natural History. USNM 335376 was cataloged as "Genus indet. sp. indet." in the fossil pinniped collections, and previous researchers had left notes with the accession records that tentatively identify the specimen as "*Enaliarctos" barnesi* (Berta, 1991). USNM 314312 was originally labeled by Douglas Emlong as an undetermined pinniped. Later, David Bohaska identified the specimen as a desmatophocid, and it was stored in the corresponding cabinet. Initial inspection led the author to identify USNM 314312 as *Pinnarctidion iverseni* (Everett et al., 2023). Specimens were photographed digitally and compared to potentially related early pan-pinniped specimens described in the literature (Condon, 1906; Mitchell & Tedford, 1973; Barnes, 1979, 1989; Berta, 1991, 1994a; Everett et al., 2023).

A phylogenetic analysis of early pan-pinnipeds was carried out to facilitate various taxonomic decisions. A matrix of 48 caniform taxa and 184 morphological characters modified from Everett et al. (2023) was analyzed using the New Technology parsimony tree search function in TNT 1.6 (Goloboff & Morales, 2023). Multistate characters that form a linear sequence were treated as ordered characters in the analysis.

Stem-pinniped phylogeny

The phylogenetic analysis produced 14 maximally parsimonious trees of 1224 steps each. The strict consensus tree (Figure 1.1) indicates uncertainty in many relationships. Notably, a polytomy unites "*Enaliarctos" bertae*, *"E." mitchelli*, *Prototaria*, *Pinnarctidion*, *Proneotherium*, the *Neotherium*-*Pteronarctos* clade, and Pinnipedia. All other "*Enaliarctos*" species form a paraphyletic grade that branches sequentially after the common ancestor with the early-diverging pan-pinniped, *Puijila*. Although poorly resolved, *Proneotherium repenningi* specimens group with *Proneotherium? borealis.* The tree also supports the monophyly of taxa represented by multiple specimens. USNM 335376 is well-supported as the sister to "*Enaliarctos" barnesi*, suggesting they are conspecific. The same is true for *Pinnarctidion rayi* specimens, as well as USNM 314312 referred to *Pinnarctidion iverseni*. The two specimens of "*Enaliarctos" mitchelli*, however, do not pair and likely warrant separate taxonomic designations.

The topology of the majority rule tree (Figure 1.2) agrees with over half of the maximum parsimony trees, but still includes two polytomies, one composed of *Prototaria*, *Pinnarctidion*, and a clade including *Proneotherium*, *Neotherium*, and *Pteronarctos*. The other polytomy concerns the uncertain placement of "*Enaliarctos" bertae* (LACM 128004). In half of the maximally parsimonious trees, *"E." bertae* diverged before the seemingly monophyletic *Prototaria* + *Pinnarctidion* + *Proneotherium* + *Pteronarctos* clade, which supports the specimen's conservative referral to the paraphyletic "*Enaliarctos*." In the other

half of parsimony trees, *"E." bertae* is more closely related to *Pinnarctidion* than to crown pinnipeds.

A single tree (Figure 1.3) with the greatest congruence with other analyses (see Chapter 2) was chosen from among fourteen maximally parsimonious trees to represent a likely phylogenetic hypothesis for taxonomic comparisons. Strangely, the musteloid outgroups are recovered as paraphyletic, with *Neovison* placed closest to the pan-pinniped clade. *Potamotherium* and *Puijila* are the earliest-diverging pan-pinnipeds. The sequence of branching among the paraphyletic grade of *"Enaliarctos"* species is as follows: *"E." mealsi*, *"E." barnesi*, *"E." tedfordi*, *"E." emlongi*, *"E." sullivani*, *"E." mitchelli*, and finally *"E." bertae*. *Pinnarctidion*, *Prototaria*, *Proneotherium*, and *Pteronarctos* form a monophyletic clade that branched just before the crown clade.

Systematic Paleontology

Disclaimer: the new taxonomic names proposed in this chapter (*Proneotherium? borealis*, *"Enaliarctos" bertae*, and *"Enaliarctos" sullivani*) are disclaimed for nomenclatural purposes, according to the International Code of Zoological Nomenclature section 8.3, and are not available until they are presented in peer-reviewed publication.

LACM 127974

CARNIVORA Bowditch, 1821

PAN-PINNIPEDIA Wolsan et al., 2020

PINNIPEDIMORPHA Everett et al., 2023

PRONEOTHERIUM Kohno et al., 1994

PRONEOTHERIUM? BOREALIS, sp. nov.

Holotype—LACM 127974, a nearly-complete cranium.

Locality—The type specimen was collected by Guy E. Pierson on June 13, 1984, from the Astoria Formation in Lincoln County, Oregon. The specimen was recovered as float at LACM Locality 4850, immediately north of Schooner Point, near the town of Agate Beach.

Stratigraphy and Age—LACM Locality 4850 occurs in a green-gray, well-cemented siltstone with associated mollusc fragments (based on matrix conserved with the holotype). The specimen was recovered adjacent to an exposure of the Iron Mountain Bed of the Astoria Formation (Armentrout, 1981), the source of several other early pan-pinnipeds, including the type specimens of *Proneotherium repenningi*, *Pacificotaria hadromma*, and *Desmatophoca oregonensis*, as well as multiple specimens of *Pteronarctos* and "*Enaliarctos*". Paleomagnetic correlation from the Iron Mountain Bed gives an estimated age of 17.3–16.6 Ma (Prothero et al., 2001), making it late Burdigalian in age (lower Miocene).

Diagnosis—*Proneotherium? borealis* is distinguished from other pinnipedimorphs by its steeply sloping premaxilla that contacts the frontal posteriorly, lack of antorbital process on the maxilla or postorbital process on the jugal, thin pterygoid strut in ventral view, bulla that underlaps the basioccipital, reduced preglenoid process, and reduced mastoid process.

Description of LACM 127974

LACM 127974 is a nearly complete, well-preserved skull missing only the anterior portion of the rostrum supporting the incisors, right zygomatic arch posterior to the postorbital process, and left occipital condyle. A few other peripheral portions of the skull are slightly abraded, but it is otherwise well-preserved. Beyond alveoli, the dentition is represented by a partial left P2 crown and right P2 root. The cranium is 174 mm long, which is smaller than the holotype crania of its close relatives *Pinnarctidion bishopi* (180 mm), *Pinnarctidion rayi* (189), *Pteronarctos goedertae* (207 mm) and *Proneotherium repenningi* (256 mm).

Rostrum—The rostrum is short and narrow for an early pinnipedimorph. The anterior narial opening is 20 mm tall and wide. The anteroventral-most portion of the rostrum is lost to abrasion. In the dorsal view, the anterior tips of the nasals form a subdued "w" shape. The medial suture and lateral edges of these elements are equal in length (26.2 mm). The nasal-frontal suture also forms a "w" shape, as a medial projection of the frontals extends a short distance between the nasals. The frontal-nasal suture is positioned nearly level with or slightly posterior to the frontal-maxilla suture. On the left side, a very thin strip of the frontal projects anteriorly between the maxilla and the nasal, meeting the posterior tip of the premaxilla and thereby interrupting the maxilla-nasal suture. Anteriorly, the frontal is slightly cleft, following the suture line of the nasals. The premaxilla contacts the nasal along roughly 60% of the latter's length. The dorsal portion of the right maxilla is dorsally displaced along its natural margins relative to the nasals, and is slightly abraded between the infraorbital foramen and canine. A subtle nasolabialis fossa is represented by a slight anteroventrally-angled ridge on the maxilla anterior to the orbit.

Orbits—The orbits are large (37 mm at their greatest diameter), as is common among pan-pinnipeds. The antorbital process is indistinct. A small lacrimal foramen lies within the

anterior orbital rim. The supraorbital process is low and rounded; subtle supraorbital ridges contour posteromedially and meet at the midline immediately anterior of the braincase. The supraorbital process lies closer to the anterior orbital margin than to the anterior margin of the braincase. The interorbital region is constant in width (~20 mm) anterior and posterior to the supraorbital processes.

Zygoma—The zygomatic arch, preserved completely on the left side of the specimen, is dorsoventrally thin and weakly arched dorsally. The small but distinct postorbital process, directed dorsomedially, is located midway along the arch between the anterior orbital margin and the glenoid fossa. The zygoma is unarched posterior to the postorbital process. The greatest transverse distance from the external face of the left arch to the skull midline is 46 mm, just anterior to the glenoid fossa. The squamosal-jugal articulation is evident only anteriorly; there is no indication that the jugal process reaches the postorbital process, unlike the weakly mortised arrangement of these elements in *Pinnarctidion* species. The anterior zygomatic root, positioned ventrally, bears a shallow fossa that trends posterolaterally and extends the length of the infraorbital foramen. The infraorbital foramen is large (8.6 mm wide) and most deeply excavated at its ventromedial corner.

Palate—The palate of LACM 127974 widens posteriorly, from 26 mm across the labial margins of the left and right P1 alveoli, to 39 mm across the labial margins of the M1 alveoli. Shallow embrasure pits occur only between P4 and M1. The palate arches slightly transversely. The two primary palatal foramina are associated with moderately deep sulci which terminate ~4 mm from a slightly curved maxillary-palatine suture that divides the palate posteromedial to M1.

The palatal process forms a 33 mm-wide shelf posterior to M2. This shelf, which extends posteriorly 4 mm from M2, has obliquely angled posterolateral corners. A 20 mm-wide pterygoid-palatine bridge occurs posterior to the palatal shelf ventral to an equally narrow choana. The notch between the posterior margin of this bridge and the medial margins of the pterygoid struts is narrower than the one in *Pinnarctidion bishopi* or *P. iverseni* (Fig. 1.4B).

Dentition—The dentition of LACM 127974 is represented mainly by alveoli, a partial left P2 and heavily abraded right P2 being the only preserved crowns. The alveoli show an identical root count and similar shape to those of species of *Pinnarctidion*. Neither the anterior portions of the premaxillae, nor the incisors, are preserved. The small diameter of the canine alveoli, and subdued lateral bulge in the rostrum indicate that these teeth were small. The medial margins of the canine alveoli are 33.0 mm apart, while each alveolus is 6.2 mm wide. The first premolar, represented by alveoli on both sides of the specimen, was the only single-rooted cheek tooth and was likely smaller than the other premolars. The crown of LP2 is abraded to the level of the cingulum; its lingual face curves medially, slightly overhanging the palate. Only the roots of the P2 remain, the posterior of which is larger. The P3 alveoli exhibit a similar pattern. The posterior alveolus of P4 is bilobed and transversely oriented, suggesting that a protocone shelf occurred postero-lingually, as in species of *Pinnarctidion*. As in P4, the alveoli of M1 are double-rooted; the bilobed posterior root is oriented posteromedially, indicating a posteriorly placed protocone. The small anterior alveolus likely indicates that the metacone was more prominent than the paracone, as in *P. bishopi*. The single M2 alveolus is undivided. The long axis of its elliptical aperture is oriented antero-posteriorly, although its posterolabial margin is not fully closed by the maxilla.

Basicranium—The glenoid fossa is shallow compared to that of *P. bishopi*. The preglenoid process is indistinct. The postglenoid process is rounded with no distinct lateral or medial prominences. A medial ridge bisects the basioccipital. The basicranium is 70 mm wide across the external auditory meati. The oval auditory bullae, moderately inflated, are oriented slightly anteromedially. The ventral walls of both bullae are damaged, revealing a matrix-filled middle ear cavity within the left bulla with no discernable petrosal morphology. The posterior lacerate foramen (PLF) is large. The large posterior carotid foramen (PCF) is partially separated from the PLF by the entotympanic.

Braincase—Anterolaterally, the braincase forms an obtuse-angled corner. A pseudosylvian sulcus extends postero-dorsally from the glenoid fossa to the nuchal region. Near the middle of the dorsal surface of the cranium, just posterior to the junction of the supraorbital ridges, occurs a rounded, bilobed sagittal crest. Posterior to this low crest, the cranium is abraded to reveal a scaffolded layer of cortical bone. No evidence of a posterior sagittal crest or nuchal crests remains. Although the posterior portion of the cranium is missing, the occipital region can be roughly described. The nearly round foramen magnum is 24 mm wide and 22 mm tall.

Taxonomic considerations

LACM 127974 is recovered as the sister to *Proneotherium repenningi*, albeit with low branch support, in each maximum parsimony tree found in the present analysis (Figure 1.1). Yet some trees produced in Chapter 2 place the specimen closer to *Pinnarctidion* or to Pinnipedia, making it prudent to name this taxon with caution. Here, LACM 127974 is referred to *Proneotherium?*, with a query, or "sign of uncertainty" (sensu Matthews, 1973; Sigovini et al., 2016), calling attention to the uncertainty of its generic level affinity. Barnes

tentatively referred the specimen to *Pinnarctidion* in his unpublished notes, a reasonable interpretation given the few other stem pinniped genera known at the time, and one that is supported by a minority of trees (5 out of 12) in Chapter 2. Regardless of which genus it belongs to, LACM 127974 represents a new species diagnosed by several apomorphies including a slender cranium with generally reduced processes. LACM 127974 cannot be referred to *Proneotherium repenningi*, however, because all sampled *P. repenningi* specimens are consistently recovered as monophyletic whereas many trees separate LACM 127974 from the rest of *Proneotherium*. In naming the new species, we honor the work of Barnes by keeping his tentative species name of *borealis*, reflecting the taxon's northerly provenance of Oregon. LACM 127974 is here formally named a new taxon with uncertain generic affinity, *Proneotherium? borealis*. When additional fossils or additional characters constrain its phylogenetic position, this uncertainty may eventually be resolved.

LACM 128004

"ENALIARCTOS" Mitchell and Tedford, 1973

Type species—"*Enaliarctos" mealsi* Mitchell and Tedford, 1973.

Included species—"*Enaliarctos" mealsi* Mitchelli and Tedford, 1973; *"E." mitchelli* Barnes 1979; *"E." emlongi* Berta, 1991; *"E." barnesi* Berta, 1991; *"E." tedfordi* Berta, 1991; *"E." bertae*, sp. nov.

"ENALIARCTOS" BERTAE, sp. nov.

Holotype—LACM 128004, a nearly complete cranium, incomplete edentulous left dentary, and a partial right dentary bearing only the canine and i3.

Etymology—The species name honors Annalisa Berta for her foundational contributions to the study of fossil pan-pinnipeds.

Locality—The type specimen was collected by J. L. Goedert on June 8, 1985, from LACM locality 5561 in the Pysht Formation, Clallam County, Washington. Based on field notes, LACM locality 5561 at Merrick's Bay is likely equivalent to SDSNH locality 7283 (the type locality of *Pinnarctidion iverseni*, Everett et al., 2023). Most fossil material from this locality has been recovered from eroded concretions (closely matching those occurring in the Pysht Formation) resting on the intertidal wave-cut platform.

Stratigraphy and Age—Although the provenance of LACM 128004 is imprecisely known, the gray siltstone matrix adhering to it strongly suggests a Pysht Formation source (Snavely et al., 1978). The overlying Clallam Formation is mapped as the primary unit at Merrick's Bay (Schasse, 2003). Paleomagnetic data indicate that the age of the uppermost Pysht and lowermost Clallam formations fall within the error range of one another, correlating with Chron C6Cr to C6Cn3n (23.7-24.7 Ma) and Chron C6Cn3n to C6Cn2r (23.8-24.2 Ma), respectively (Prothero et al., 2001). Therefore, LACM 128004 is most likely late Chattian in age.

Diagnosis—"*Enaliarctos" bertae* is distinguished from other early pinnipedimorphs by its lack of supraorbital processes, infraorbital foramen that is most deeply excavated mediodorsally, braincase that is elevated above the interorbital region, short and posteriorly bifurcating sagittal crest, strongly divergent palate, presence of a postglenoid foramen, and double-rooted M2.

Description of LACM 128004

LACM 128004 consists of a well-preserved nearly complete cranium, an incomplete edentulous left dentary, and a partial right dentary bearing the canine and i3. The partial cranium includes nearly complete zygomatic arches, a palate with alveoli for P1-M2, and a well-preserved basicranium. The portion of the rostrum anterior of the canines and the braincase posterior of roughly the mastoid processes are missing. The cranium appears undeformed.

Rostrum—Even taking into account its missing anterior portion, the rostrum is unusually short for an early pinnipedimorph. In anterior view, the narial opening is wider (17.1 mm) than high (12.9 mm). The anterior margins of the nasals are "w" shaped. The medial suture (20.6 mm long) reaches as far anteriorly as the elements' lateral edges, the latter of which contact the premaxillae. The nasal-frontal and maxillary-frontal sutures are highly "interfingered." The slender premaxillae contact the nasals along nearly 50% of the latter elements' length. Subtle nasolabialis fossae occur on the maxillae anterior to the orbital margins, as do low antorbital ridges.

Orbits—The orbits are large (29 mm at their widest) relative to the size of the cranium. The interorbital constriction varies little in width. It widens gradually anteriorly at the level of the nasal-frontal suture, and abruptly posteriorly at the anterolateral margin of the braincase. The antorbital process is greatly reduced, forming little more than a low ridge that appears undiminished by abrasion. The supraorbital processes form nearly indistinguishable lateral bulges. From these processes begin two low, posteromedially-oriented ridges that converge near the anterior expansion of the braincase, and continue posteriorly as a low, broad sagittal crest.

Zygomatic arch—The dorsoventrally narrow zygomatic arch bends little dorsally at its center. The postorbital process marks its most dorsal point. The arch bends steeply ventrally anterior of a line joining the postorbital processes, and more gradually posteriorly. The greatest transverse width between the external surfaces of the arches is 80 mm, ~10 mm anterior of the glenoid fossae. The round infraorbital foramen, 6.4 mm in diameter, is less triangular than in most early diverging pinnipedimorphs. The prominent postorbital process of the zygomatic arch projects dorsally and slightly medially. It is located near the midpoint of the arch, between the anterior orbital margin and the glenoid fossa. The thin squamosal and jugal processes have a linear, splint-like contact. The anterior end of squamosal terminates posterior to the postorbital process, unlike in *"E." emlongi* and *Pinnarctidion spp*. where it extends farther anteriorly. The anterior zygomatic root, flat ventrally, is positioned on roughly the same transverse plane as the palate. Ventrally, a shallow fossa trends posterolaterally and extends the length of the ventral wall of the infraorbital foramen.

Palate—The palate is short, broad, and strongly divergent posteriorly. It diverges starting at the level of the P2 alveoli and ending at the anterior M1 alveoli, then narrows posteriorly medial to the M1-2 alveoli. The palate is 23 mm wide across the outer margins of the P1 alveoli, 40 mm across the M1 alveoli, and 31 mm across the M2 alveoli. Deep embrasure pits lie medial to P4 and M1, and shallower ones medial to P2-3 and P3-4. The palate arches weakly transversely. The maxilla-palatine suture is even with the anterior root of M2. Two primary palatal foramina open near this suture, each with a broad palatine sulcus extending anteriorly. The right palatal foramen opens anterior to the maxilla-palatine suture, whereas the left one originates posterior to the suture. A palatal process forms a 26-mm-wide shelf posterior to M2. This shelf extends posteromedially 4.5 mm from the M2 alveoli, and has an

obliquely angled corner. Posterior of the palatal shelf lies a 17.4-mm-wide pterygoid-palatine bridge flooring the choana. The posterior margin of this bridge, and the medial margins of the pterygoid struts, form a tight u-shape in ventral view.

Dentition—The upper dentition is represented only by alveoli. Those for I1-2 are completely missing, but a cross-section of the lingual portion of the I3 alveolus is visible in anterior view. The nearly complete right canine alveolus is 6.4 mm in diameter, and the deeply abraded left one is preserved only proximally.

Judging from their alveoli, the cheek teeth were large and closely packed. P1 is the sole single-rooted cheek tooth. The orientation of its alveolus indicates that the crown was canted anteriorly. The posterior of the two equally-sized P2 alveoli is laterally positioned relative to the anterior, reflecting the posterior widening of the palate. Of the two roots of P3, the posterior one is larger and weakly bilobed. The three roots of P4 form an equilateral triangle. The broad medial alveolus is positioned midway between the other two, suggesting that a large protocone cusp or shelf was present, as in "*Enaliarctos" barnesi, "E." tedfordi,* and *"E." mitchelli*. In contrast, the protocone shelf is positioned more anteriorly in *"E." mealsi* and *"E." emlongi*, and more posteriorly in *Pinnarctidion spp.* The posterior of the two M1 alveoli is bilobed. The metacone root is smaller and medially compressed. The M2 alveoli, both of the same size and distinctly smaller than those of the other cheek teeth, are aligned posteromedially along the edge of the palate.

Basicranium—The incompletely preserved basicranium (along with the posterodorsal cranium) is truncated posterior to the level of the posterior lacerate foramina. The broad, concave pterygoid struts bear lateral processes as seen in *Pinnarctidion* and many odobenids.

Prominent yet delicate pterygoid hamuli project posteroventrally. The alisphenoid canal is enclosed within a thick lateral wall. The postglenoid process is prominent medially, whereas the preglenoid process is weak.

Bullae—The auditory bullae are moderately inflated. Two small processes project anteromedially from the open anterior aperture of each bulla. A small postglenoid foramen is present. A gap separates the medial edge of the entotympanic and basioccipital, making the carotid canal visible along the entire medial margin of the bullae. This does not appear taphonomic, so it may either represent an immature suture condition or an autapomorphy of this taxon.

Braincase—The anterior half of the "box-like" braincase is preserved. It expands abruptly laterally at its anterior end, forms an obtuse corner at its anterolateral extremity, and gently curves posteriorly. The condition of the pseudosylvian sulcus, lambdoidal crests, or occipital condyles cannot be determined.

Dentaries—The partial left dentary preserves the alveoli of i2-m1. Judging from them, the cheek teeth were double-rooted and evidently similar in size, apart from p3, the alveoli of which are slightly enlarged. The dentary is broken posterior to the initial ascent of the coronoid process, leaving evidence of a shallow masseteric fossa. The coronoid, condylar, and angular processes are not preserved.

The right dentary preserves only the portion anterior to P3. The crowns of the canine and i3, plus alveoli of the p1 and p2, are preserved. The canine and i3 crowns are appressed at their bases, though the left dentary reveals that i3 has a distinct alveolus. The i2 alveolus closely

abuts that of i3, and is at least as large. The ventral portion of the right dentary is heavily abraded, revealing the robust canine root, but no others in cross-section.

Taxonomic considerations

LACM 128004 displays several unique features that warrant its referral to a new species ("*Enaliarctos" bertae*). LACM 128004 is the smallest fossil pinnipedimorph cranium known, raising the question of which ontogenetic stage it represents. Because the consequences of allometry and other ontogenetic changes are difficult to account for in conventional phylogenetic methods, the potential effects are qualified herein.

The best evidence for ontogenetic age in fossil mammals are patterns of tooth eruption and cranial suture fusion. Unfortunately, only the lower right i3 and canine teeth are preserved in LACM 128004, and there is no evidence of unerupted adult teeth within the maxillae. The lower canine appears worn, but it is unclear whether this wear occurred pre- or post-mortem. Fortunately, the specimen preserves several unfused cranial sutures. A standard for cranial suture age has been established for pinnipeds (Sivertsen, 1954). Recent studies of modern seals (Kahle et al., 2022) and sea lions (Audibert et al., 2017) confirm that suture closure patterns correlate well with age of death in these taxa. Both of those studies measured a series of nine sutures (Sivertsen, 1954) that close in sequential order as an individual ages. Each suture is assigned a score of 1 to 4 depending on the degree of fusion, allowing for a possible total score range from 9 to 36, with adults typically scoring ≥19.

The condition and corresponding scores of these sutures in LACM 128004 are listed here. The occipito-parietal suture (I) is not preserved, score unknown; the squamoso-parietal suture

(II) is partially unfused, score of 3; the interparietal suture (III) is fused, score of 4; the interfrontal suture (IV) is fused, score of 4; the coronal suture (V) is fused, score of 4; the basioccipito-basisphenoid suture (VI) is narrowly unfused, score of 2; the maxillary suture (VII) is partially unfused toward the anterior end, score of 3; the basisphenoid-presphenoid suture (VIII) is widely unfused, score of 1; and the premaxillary-maxillary suture (IX) is unfused, score of 1. The total score for LACM 128004 is between 23-26 (depending on the unknown occipito-parietal suture), which falls on the low end of the range for an adult pinniped. Indeed, seals and sea lions show slightly different patterns of suture fusion, and even conspecific males and females can show different patterns (Kahle et al., 2022). Early pinnipedimorphs could differ even more widely, but this specimen seems to be a young adult judging from suture closure, our best means of inference. Therefore, the unusual apomorphies of LACM 128004 are not likely immaturities, but rather are diagnostic, of "*Enaliarctos" bertae*.

USNM 175637

"ENALIARCTOS" SULLIVANI, sp. nov.

Holotype—USNM 175637, nearly complete cranium missing the right wall of the braincase and squamosals, originally referred to *"E." mitchelli* and described in detail by Berta (1991).

Locality—The anterior and posterior portions of USNM 175637 were collected separately as float concretions by Douglas Emlong. The braincase was collected in 1970 from float material associated with exposed strata south of the mouth of Thiel Creek, Lincoln County, Oregon. The rostrum was collected in 1974 near the same locality as the braincase.

Stratigraphy and Age—The locality falls within the lower section of the Nye Mudstone near its contact with the Yaquina Formation. This portion of the Nye Mudstone has been correlated with upper Oligocene polarity chrons C9n-C8n (Prothero et al., 2001), dated to 27.3-25.3 Ma (Ogg et al., 2016), making these deposits early Chattian in age.

Diagnosis—"*Enaliarctos" sullivani* is distinguished from other species of "*Enaliarctos*" by its strongly arched zygomatic portion of the jugal, a narrow but continuous lateral palatine process, a more posteriorly placed pterygoid hamulus, and an auditory bulla that contacts the postglenoid process more closely.

Reevaluation of "*Enaliarctos" mitchelli* and taxonomic distinction of *"E." sullivani*

"Enaliarctos" mitchelli was described by Barnes (1979) from two specimens: holotype UCMP 100391, the anterior half of a cranium lacking teeth, and paratype UCMP 80943, a partial palate with canines. Despite the non-preservation of teeth and basicranial regions, the morphological similarity of the two UCMP specimens makes their reference to the same taxon plausible. However, a third specimen, USNM 175637, referred to *"E." mitchelli* by Berta (1991), exhibits some notable differences. Although USNM 175637 shares similarities with the type material and is likely fairly closely related, it is marked by several unique apomorphies, and it is never recovered as *"E." mitchelli*'s closest relative in phylogenetic analyses. Rather, in the strict consensus of maximally parsimonious trees (Figure 1.1), USNM 175637 diverges before the *"E." mitchelli* type specimen, meaning none of the parsimony trees pair them together.

Accordingly, USNM 175637 is referred to a distinct taxon, "*Enaliarctos" sullivani*, sp. nov., named after the late Gladwyn "Tut" Sullivan, a Smithsonian fossil preparator whose skillful work on the Emlong collection illuminated many valuable specimens. "*Enaliarctos*" is still used here, despite its apparent paraphyletic nature, because of the remaining uncertainty surrounding early pinnipedimorph relationships (i.e., some "*Enaliarctos"* species form a monophyletic group when certain characters are weighted; see Figures 2.5–2.8). There is also a convenient utility to using the name "*Enaliarctos*" to describe this particular window of pinniped evolutionary history, as long as we acknowledge it is probably not monophyletic.

USNM 335376

"ENALIARCTOS" BARNESI Berta, 1991

Holotype—USNM 314295, anterior portion of cranium and nearly complete lower left and right mandibles.

Referred specimen—USNM 335376, nearly-complete cranium.

Locality—Referred specimen USNM 335376 was collected by Douglas Emlong from an unnamed locality roughly one-third of a mile south of the mouth of Beaver Creek, which lies between Yaquina and Alsea bays, in Lincoln County, Oregon. This locality is very close to the type localities for "*Enaliarctos" barnesi* and *"E." tedfordi* (Berta, 1991).

Stratigraphy and Age—The provenance of USNM 335376 is most likely the upper Yaquina Formation, which is exposed along the coastal bluffs south of Beaver Creek (Snavely et al.,1976). The Yaquina Formation has been correlated with lower Oligocene polarity chrons

C12n-C9r (Prothero et al., 2001), which are dated to 31.0-27.3 Ma (Ogg et al., 2016), from the late Rupelian Age.

Amended Diagnosis—"*Enaliarctos" barnesi* is distinguished from other species of "*Enaliarctos*" by its prominent prenarial process of the premaxilla, zygomatic arch that is nearly equal in width at both anterior and posterior ends, embrasure pits present between the premolars, cuspate lingual cingula on the premolars, M1 that is oriented in parallel with the other cheek teeth, and a M2 that is less medially offset. USNM 335376 differs from the holotype in possessing a narrower P3 lingual cingulum, P3 roots that are comparatively reduced, and a zygomatic root of the maxilla that joins the palate more anteriorly.

Description of USNM 335376

USNM 335376 is a nearly-complete cranium, preserving both canines and P3s. The portion of the premaxilla bearing I1-2 and the majority of the zygomatic arches are missing. The cranium is slightly compressed dorsoventrally and heavily cracked on its dorsal and ventral surfaces. Judging from fusion of most skull sutures and the degree of tooth wear, this was likely a fully mature individual.

Rostrum—The snout is broad and narrows only slightly anteriorly. The narial opening is much wider than tall in anterior view. The maxillae bulge anterolaterally around the moderately large canines. The premaxillae converge anteroventrally as in the holotype, but their tips are not preserved. The posterior margins of the premaxillae contact the nasals along about a quarter of the latter's length. Anteriorly, the nasals form a concave margin with a very slight medial bulge. The nasal-frontal suture is indistinct due to the maturity of the individual and post-depositional fracturing of the skull. The maxillae possess deep

nasolabialis fossae bordered by a pronounced ridge anteriorly and a large antorbital process posteriorly, a distinctive feature of *"E." barnesi*.

Orbits—Although the orbits are preserved only medially, as the zygomatic arches are missing, they seem proportioned as in the holotype. A pair of short but robust supraorbital processes flank the frontals. The distance between the antorbital and supraorbital processes is very short (15 mm), as in the holotypes of *"E." barnesi*, *"E." mealsi,* and *"E." tedfordi*. In some terrestrial arctoids, a forward-placed supraorbital process is correlated with smaller orbits, but this not true for "*Enaliarctos*" species, which tend to have a posteriorly-placed postorbital process of the jugal, giving them relatively large orbits for an arctoid.

Zygomatic arch—Only the extreme posterior end of the squamosal's contribution of the zygomatic arch is preserved. The transverse width of the skull across the zygomatic arches widens more gradually and would be widest at a level anterior to the glenoid fossa, rather than widest at the level of the glenoid fossa as in *"E." tedfordi* and many other early-diverging pan-pinnipeds. The *"E." barnesi* holotype, USNM 314295, does not preserve the posterior portion of the arch, but the remaining portion forms a rounded bracket-shaped lateral margin. The glenoid fossae of USNM 335376 bear prominent pre- and postglenoid processes. The anterior portion of the arch is only represented by a short segment near the jugal-maxillary suture. The orientation of this segment suggests the jugal was placed high on the skull, comparable to other early-diverging pan-pinnipeds, but differing from the lower and flatter contact of later-diverging forms such as *Pinnarctidion*.

Palate—The palate is elongate and slightly arched transversely. Its surface is cracked, but preserves original grooves and pits, some of which remain filled with sediment. Two parallel

incisive foramina occur between the canines. Shallow grooves line the lateral sides of the palate, the right of which deepens parallel to P4 and M1. The posterolateral margins of the palate abruptly deflect medially directly posterior to M2, then extend posteriorly to the pterygoids. The palatine extends 20 mm posteriorly and terminates as a weakly V-shaped shelf above the internal choana.

Dentition—USNM 335376 preserves both canines and P2s, along with alveoli for all other teeth except the left I1-2 and the right I1. The I2 alveolus is transversely compressed. The I3 alveolus is round and moderately larger than I2.

The canines are larger and broader than those of the holotype, lack posterior cristae, and are deeply worn—the left one in particular to a blunt, rounded apex. This wear pattern is nearly uniform around the tooth, except for a smooth anteromedial indentation that likely resulted from contact with the lower canine. Curiously, the right canine is not rounded; instead, its apex is broken at an anteroventral angle. Whether this break occurred pre- or post mortem is uncertain.

The premolar rows diverge slightly posteriorly, but the molars deflect medially as in other basal pan-pinnipeds. The single-rooted P1 was likely about half the size of the other premolars. The alveoli for P2 are poorly preserved, but those on the right side indicate the tooth was double-rooted. The P3 crowns are narrow and blade-like, bearing very thin labial, and thicker lingual, cingula. A small but distinct “metacone” forms the tooth’s posterior heel. It is unclear whether the protocone cusp and shelf are completely missing inherently (which would be unusual for a basal pan-pinniped) or have simply been worn away. The P4 alveoli are better preserved on the right side, where three roots form a nearly equilateral triangle.

Judging from these alveoli, P4 was perhaps slightly larger than P3, but would have had a moderate protocone shelf. The left P4 alveoli are mostly obliterated, although widely-spaced, shallow pits suggest this tooth was slightly larger than the right.

Normally, three M1 roots are to be expected for "*Enaliarctos*," but there is only clear evidence for two here. The pair of M1 root alveoli begin directly posterior to the distal P4 alveolus; their orientation shows that roots were directed mesiodistally. The basis for inferring the morphology of the lingual portion of the tooth is limited. A seemingly deep pit filled with matrix lies mesiolingual to the right M1's mesial alveolus. In other basal pinnipedimorphs, this position (directly anterior to a lingually-placed M1 protocone alveolus) is usually occupied by a deep embrasure pit. Potential candidates for the M1 protocone alveolus include a narrow matrix-filled groove on the right side, or a small hole in the palate on the left. M2 is represented by a distinct, single, oval-shaped alveolus on the left, and an incomplete one on the right.

Basicranium—The basicranium is complete aside from minor damage to the pterygoids, bullae, and basisphenoid. Its overall morphology is very similar to the holotype of *"E." tedfordi* (USNM 206273), although USNM 335376 differs in its less inflated bullae and smaller posterior lacerate foramina.

The pterygoids are moderately broad, but do not form the distinct lateral processes seen in some other basal pinnipedimorphs. Their ventral surface is damaged, but they appear weakly concave. The thick-walled alisphenoid canals open posterolaterally. The foramen ovale is indistinct.

Bullae—The auditory bullae are small and weakly inflated. The right bulla is largely made up of a fractured ectotympanic. The left bulla is more damaged, exposing some of the middle ear cavity, although the promontorium remains obscured by matrix. The gently sloping entotympanic is roughly continuous with the lateral margins of the basioccipital across a thin suture. Anteriorly, each bulla forms a smoothly concave shelf over the canalis musculotubarius.

Braincase—The braincase of USNM 335376 is complete but heavily fractured along most of its dorsal and lateral surfaces. The anterior expansion of the braincase meets the interorbital region at an obtuse angle and curves convexly posteriorly. A distinct pair of pseudosylvian sulci run posterodorsally from the anterior end of the undivided squamosal fossae. A low, narrow sagittal crest runs along the dorsal surface of the skull from a level medial to the supraorbital processes to the posteromedial vertex of the nuchal crests. The nuchal crests are pronounced, overhanging much of the occipital and flaring laterally. A moderately broad foramen magnum opens between a pair of robust ventromedially-canted occipital condyles.

USNM 314312

PINNARCTIDION Barnes, 1979

Type species—*Pinnarctidion bishopi* Barnes, 1979

Included species—*Pinnarctidion bishopi* Barnes, 1979; *Pinnarctidion rayi* Berta, 1994a; *P. iverseni* Everett, 2023

PINNARCTIDION IVERSENI Everett et al., 2023

Holotype—SDSNH 146624, a nearly-complete cranium, cervical vertebra, partial right humerus, and rib fragments.

Referred specimen—USNM PAL 314312, a nearly complete cranium, partial left and right mandibles, right scapula, right humerus, left and right femora, left tibia, and fragmentary ribs. The specimen is currently filed in the collection database as *Callophoca sp.*, although this taxon name is now considered dubious (Rule et al., 2020). The only mention of this specimen in the literature refers it to *Desmatophoca oregonensis* (Boessenecker and Churchill, 2015).

Locality—USNM 314312 was collected by Douglas Emlong about 120 meters south of the mouth of Moore Creek, which is ~6 kms south of Yaquina Bay, in Newport, Oregon, U.S.A. Emlong noted collecting the anterior half of the bisected cranium in a concretion on the beach. Upon further investigation, the posterior half of the cranium and remaining elements of the specimen were recovered in situ from bedrock near the low tide line.

Stratigraphy and Age—Strata outcropping along the coast from Henderson Creek to Beaver Creek (between which lies Moore Creek) are mapped as Nye Mudstone (Snavely et al., 1976). The dark-olive-gray sandy siltstone lithology characteristic of the Nye matches the matrix sample associated with USNM 314312. The locality likely lies within the lower section of the Nye Mudstone as it is near the contact with the conformably underlying Yaquina Formation (Snavely et al., 1976). The lower portion of the Nye Mudstone has been correlated with upper Oligocene polarity chrons C9n-C8n (Prothero et al., 2001), which are dated to 27.3-25.3 Ma (Ogg et al., 2016), making these deposits early Chattian in age.

Amended diagnosis—*Pinnarctidion iverseni* is distinguished from other early pinnipedimorphs in having an interorbital constriction that is thinnest at its anterior end, and a lateral border of the basioccipital that is distinct from the bulla and flared ventrally. USNM 314312 differs from the holotype in possessing a thinner zygomatic arch, accessory cusps on the P2 rather than the P3-4, and no embrasure pits between any of the cheek teeth.

Description of USNM 314312

USNM 314312 consists of a nearly complete cranium, partial left and right mandibles, scapula, humerus, both femora, tibia, and ribs. The cranium is broken across a transverse plane near the posterior margin of the palatine ventrally and just anterior to the braincase dorsally; very little seems to be missing due to this breakage. The referred skull is ~180 mm long, compared with the 145 mm long skull (missing occipital condyles) of SDSNH 146624. Considering that the occipital condyles typically account for about 15-20 mm of total skull length, the skull of USNM 314312 would still have been slightly longer than that of the *P. iverseni* holotype. Only the earliest-closing skull sutures are fused, but the dentition appears permanent, indicating this individual was a subadult.

Rostrum—The snout is narrow and short, although the anterior-most portion is incomplete. The premaxilla, best observed on the right side, forms a short anterior shelf and slopes postero-dorsally at a ~45° angle in lateral view. In anterior view, the narial opening appears wider than it is tall; however, the anterior half of the cranium is dorsoventrally compressed making this character uncertain. In dorsal view, the anterior nasal margin is weakly w-shaped. The premaxillae extend laterally along at least half the length of the nasals. The nasal-frontal suture is interdigitated by several 5-mm-deep projections of each bone.

Interdigitating sutures at the anterior margin of the frontals also occur in the *P. bishopi* holotype (Barnes, 1979).

Orbits—The large orbits of USNM 314312 compare favorably to the holotype. The antorbital processes are formed by slightly raised, rugose suturing of the frontals and maxillae. A small lacrimal foramen occurs within the anteromedial margin of the left orbit. Reduced supraorbital processes lie roughly midway along the anteriorly-narrowing interorbital region of the frontals. The unfused suture between the frontals forms a medial furrow. The posterior portion of the interorbital region is missing, but it appears to gradually widen posteriorly.

Zygoma—The nearly complete right zygomatic arch is broken posterior to the small, medially-directed postorbital process of the jugal. The anterior squamosal process is 'mortised' with the postorbital process of the jugal. The large orbit is more than one-third as long as the zygomatic arch, as in other species of *Pinnarctidion*, a few other early pan-pinnipeds, and most crown pinnipeds. The widest part of the arch lies directly anterior to the glenoid fossa. The zygomatic arch is wider dorsoventrally than in the type of *P. iverseni*, more resembling the condition in *P. rayi*.

Palate—The palate of USNM 314312 is similar in most aspects to that of the holotype. The toothrows diverge evenly from P1 to M2. On the right side, an oval-shaped incisive foramen lies medial to the canine root. The palate is cracked and slightly distorted, but it appears moderately arched transversely. The interpalatine and maxillo-palatine sutures are unfused. The expanded and cornered posterolateral margins of the palate extend ~10 mm posterior of M2. The posterior margin of the palate is incomplete, but judging from its width across the

pterygoids, the shelf above the posterior choana was broad, as is characteristic of *Pinnarctidion* species.

Dentition—The right P2-4 crowns are preserved along with alveoli for I1-3, the canine, and P1. The left side is missing the incisor-bearing portion of the premaxilla, but alveoli for the canine, P1-4, and M1-2 are intact. The alveoli for the right I1-2 are poorly preserved, but indicate transversely compressed roots. The right I3 alveolus is slightly larger than those of the other incisors. The canine alveolus, relatively small for a pan-pinniped, is distorted, forming a nearly hourglass shape in outline.

The P1 alveolus is only slightly larger than the anterior alveolus of P2, suggesting that P1 was about half the size of the other premolars. The P2-4 crowns are blade-like and gently recurved apically, closely resembling their counterparts in the holotype except that they lack the accessory cuspules on the distal carinae seen on the holotype. The premolars bear cuspate lingual cingula with distinct mesial and distal cuspules. P2 is transversely narrow with a lingually-placed mesial cuspule. The distal root of the double-rooted P2 is slightly broader than the mesial root. P3 is similar to P2 but has a posteriorly-placed incipient protocone shelf. P3 is double-rooted with a smaller mesial root and a broader distal root. P4 is similar in length to the other premolars, but the protocone shelf is moderately-expanded. The vertex of this shelf is placed posteriorly, as in *P. bishopi* and the holotype of *P. iverseni*, whereas these shelves lie in an intermediate position directly lingual to the paracone in *P. rayi* and other earlier-diverging pan-pinnipeds. Although its alveolus is partially crushed, the left P4 appears to have been double-rooted.

Judging from its alveoli, M1 was double-rooted with a broad, bilobed distal root. Its position parallel to the rest of the toothrow, distolingually placed protocone alveolus, and small size are similar to those of *P. bishopi* and *P. iverseni*. The right M2 alveolus, positioned in-line with the remaining cheek teeth, is oblong in shape, oriented at an anteromedial angle, and about half the size of the M1 alveolus. Overall, the teeth and alveoli of USNM 314312 most closely resemble those of *P. iverseni*, with the notable exception that the former lacks accessory cuspules on P3-4.

Basicranium—The basicranium is generally well-preserved, with sutures between elements clearly visible. Each pterygoid is thin anteriorly, fans out posteriorly, and terminates in a ventromedially-canted arc with both ventral and lateral vertices. The left pterygoid appears anterolaterally displaced from breakage. The presphenoid loosely contacts the basisphenoid between the pterygoids. The caudal alar foramina emerge from thick-walled alisphenoid canals and small foramina ovale share the same relatively shallow fossae posteriorly. Lateral to these foramina, on the right side, lies a relatively deep glenoid fossa with a medially-prominent postglenoid process and a reduced preglenoid process. No postglenoid foramen is present. The mastoid processes form distinct bulges laterally, but these are less prominent than in "*Enaliarctos*" or *Pteronarctos*; they more closely resemble those of *P. bishopi*. On the better-preserved right side, a narrow ridge connects the mastoid process to the relatively narrow, pointed paroccipital process. An unfused basispheno-basioccipital suture occurs between the bullae. The lateral margins of the basioccipital are distinct from the bullae, forming ridges that flare ventrally, as in the *P. iverseni* holotype. Also similar to the holotype, the basioccipital of USNM 314312 possesses embayments and tuberosities associated with the rectus capitis muscles. The posterior lacerate foramina are large and only

connected to the posterior carotid canals anteriorly by a small fissure. The hypoglossal foramina lie anterior to the ventral condyloid fossa and are not closely associated with the posterior lacerate foramina. The well-preserved occipital condyles angle dorsolaterally and project posteromedially, bordering a nearly circular foramen magnum.

Bullae—The right bulla is slightly damaged posterolaterally, yet it seems to have been only slightly inflated. The left bulla is missing the ectotympanic, revealing most of the middle ear cavity.

Mandibles—USNM 314312 includes a partial left and nearly complete right mandible, bearing the right p1 and p4 crowns. The left mandible is missing the tooth crowns and the anterior half of the body. The right mandible is missing a majority of the teeth and portions of the intermandibular joint region.

Scapula—The right scapula is complete and well-preserved. The glenoid fossa is broad and moderately concave, very similar in shape to that of *P. rayi*. The anterior and dorsal borders of the scapula form a continuous rounded arc, which ends at a cornered posterodorsal process but does not curve posteriorly to a sharp point as would be expected for other pinnipedimorphs (except *Odobenus*). It is difficult to confirm whether USNM 314312 lacks a postscapular fossa, or if that portion is not preserved. The scapular spine is most prominent along its center and tapers out before it reaches the dorsal border. At the distal end of the spine, adjacent to the knob-like acromion process, is a prominent metacromion process that overhangs the posterior border. The supraspinous fossa occupies a much greater area than the infraspinous fossa, as in other pinnipedimorphs, with the exception of some phocids.

Humerus—The right humerus is largely preserved, missing only the proximal epiphysis and anterior edge of the deltopectoral crest. The proximal edge of the metaphysis indicates that the head would have been posteriorly offset and overhung the shaft, as in other pan-pinnipeds. The missing epiphysis prohibits characterization of the greater or lesser tuberosities. The shaft is similarly slender in anterior view as in *P. rayi* and less broad than in *"E." mealsi.* The deltopectoral ridge is broken along its entire length, but it was clearly robust and extends three-quarters of the length of the shaft, as in other non-phocine pinnipedimorphs. The lateral supracondylar ridge is prominent, but less so than in *E mealsi* or *P. rayi*. By contrast, the medial epicondylar ridge is more prominent than in *P. rayi*.

Femora—Both the left and right femora are mostly complete. The left element is missing the proximal portion of the capitulum and both are missing the distal epiphyses and much of their greater trochanters. The fovea capitis is hemispherical and the collum femoris is broad and short. Due to damage to the greater trochanters, the depth of the trochanteric fossa is not visible. The preserved portion of the greater trochanter suggests it was equal or higher (more proximal) than the capitulum, a common feature in pan-pinnipeds. The lesser trochanter – vestigial in crown pinnipeds – is smaller than in *"E." mealsi*, *"E." emlongi*, or *P. rayi*, but it is similarly medially-directed in USNM 314312. The shaft is short and mediolaterally broad, as in other pinnipedimorphs. The broadly-set distal condyles slightly bifurcate at their midpoint to accommodate the patellar facet. The condyles are medially inclined, as is characteristic of pinnipedimorphs.

Tibia—The left tibia is completely preserved. Though no fibula is preserved, the tibia bears no evidence of fusion of the two elements. The proximal condyles are missing the epiphysis, but the remaining surface is convex with a slight concavity between the two condyles. The

articular surface for the fibula is not as indented as in *P. rayi*, rather the medial edge of the condyle joins the shaft along a continuous slope. The shaft is laterally concave and triangular in cross-section, but the tibial tuberosity is not as pronounced as in *P. rayi*. The inflection point of the lateral concavity is positioned more proximally than in *P. rayi*, a condition more similar to that of *"E." emlongi*. The distal end is gradually inclined toward the medial malleolus, but is less pronounced than in *"E." mealsi*.

Conclusions 1

New pinnipedimorph specimens from the Oligocene and Miocene of Oregon and Washington described above represent three new taxa (*Proneotherium? borealis*, "*Enaliarctos" bertae*, and "*Enaliarctos" sullivani*) and provide important reference material that expands our knowledge of "*Enaliarctos" barnesi* and *Pinnarctidion iverseni*. Our growing knowledge of early pinnipedimorph diversity makes it exceedingly clear that the North Pacific was the group's center of origin, and that these taxa were occupying marine carnivoran niches long before seals or sea lions arose. New species add data points for study of phylogeny and diversity. Duplicate specimens are also valuable as they often reveal previously unknown morphological features and increase sample sizes for investigation of sexual dimorphism, ontogenetic change, and intra-specific variation.

The new specimens described here offer more information for our models of pinnipedimorph phylogeny. USNM 335376 affirms the near-basal position of *"E." barnesi* among pinnipedimorphs, illuminates the posterior portion of the cranium that was missing from the holotype, and poses new questions about the taxon's worn dentition. *"E." bertae* and *"E."*

sullivani underscore recent findings that "*Enaliarctos*" is a paraphyletic grade rather than a clade (Paterson et al., 2020; Everett et al., 2023). Perhaps it will become desirable to erect separate genus names for each species, but the present study opts to maintain the traditional "*Enaliarctos*" genus designation to avoid confusion. Although it poses a naming problem for taxonomists, the "*Enaliarctos*" paraphyletic grade is significant because it illuminates the sequence in which apomorphies diagnostic of pinnipeds and their closest allies were acquired.

The recognition of *Proneotherium? borealis* strengthens the notion that the early- to middle-Miocene pinnipedimorphs *Prototaria, Proneotherium,* and *Neotherium* diverged prior to the origin of crown pinnipeds, indicating that they are not odobenids as has been widely held (Kohno et al., 1994; Deméré & Berta, 2001; Boessenecker & Churchill, 2013; Boessenecker et al., 2024). The precise position of these taxa is not consistently resolved, but they may belong to a monophyletic clade that also includes *Pinnarctidion* and *Pteronarctos*. USNM 314312 reaffirms previous conclusions that *Pinnarctidion iverseni* is more closely related to *P. bishopi* than to *P. rayi* (Everett et al., 2023) and includes rare associated postcranial material.

Given their diversity, one might question why the record of stem pinnipeds ends in the middle Miocene, and what causes changes in pinnipedimorph diversity through time (Berta & Lanzetti, 2020; Park et al., 2024). Paleoclimate models indicate a peak in sea surface temperatures in the early Miocene, followed by an inflection toward colder temperatures in the middle Miocene (Flower & Kennett, 1994; Steinthorsdottir et al., 2021). This shift likely

disrupted the stability of marine ecosystems to which early pinnipedimorphs had adapted, leaving ecological niches open for early crown pinnipeds to specialize and radiate.

Figures 1

Figure 1.1. Strict consensus of maximally parsimonious trees. Numbers represent relative Bremer support values.

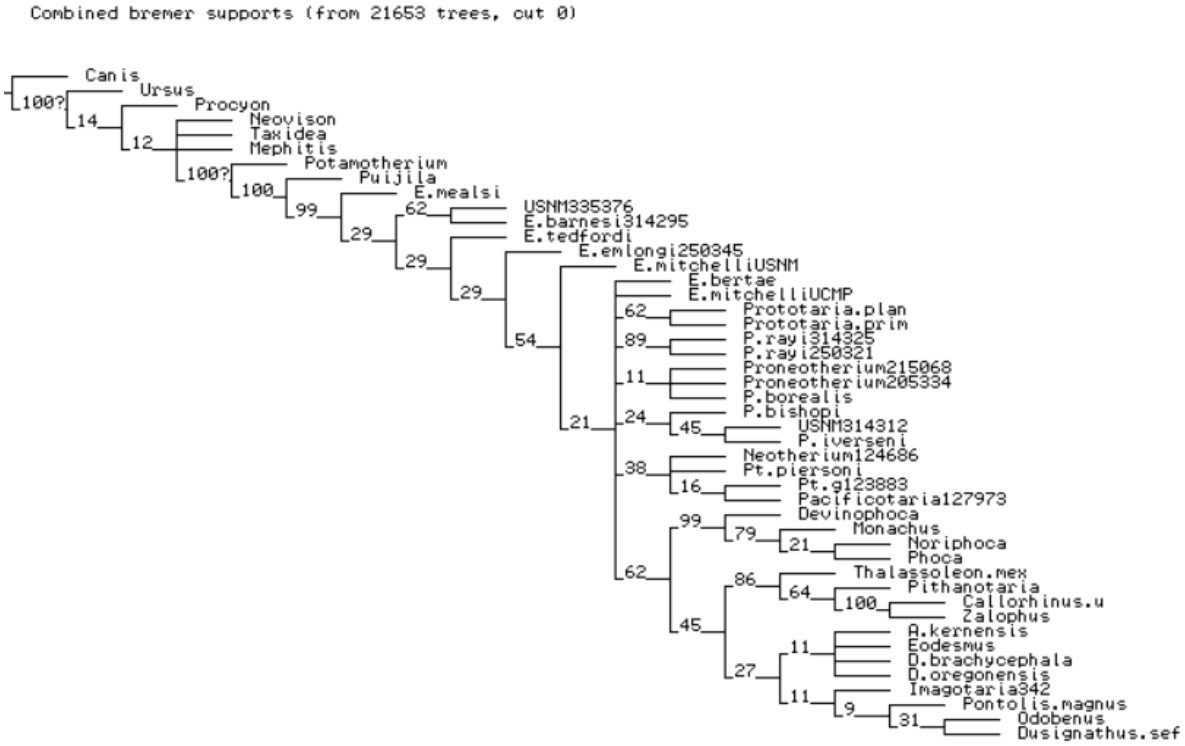

Figure 1.2. Majority rule tree. Numbers represent the percentage of maximally parsimonious trees that resolve that branch.

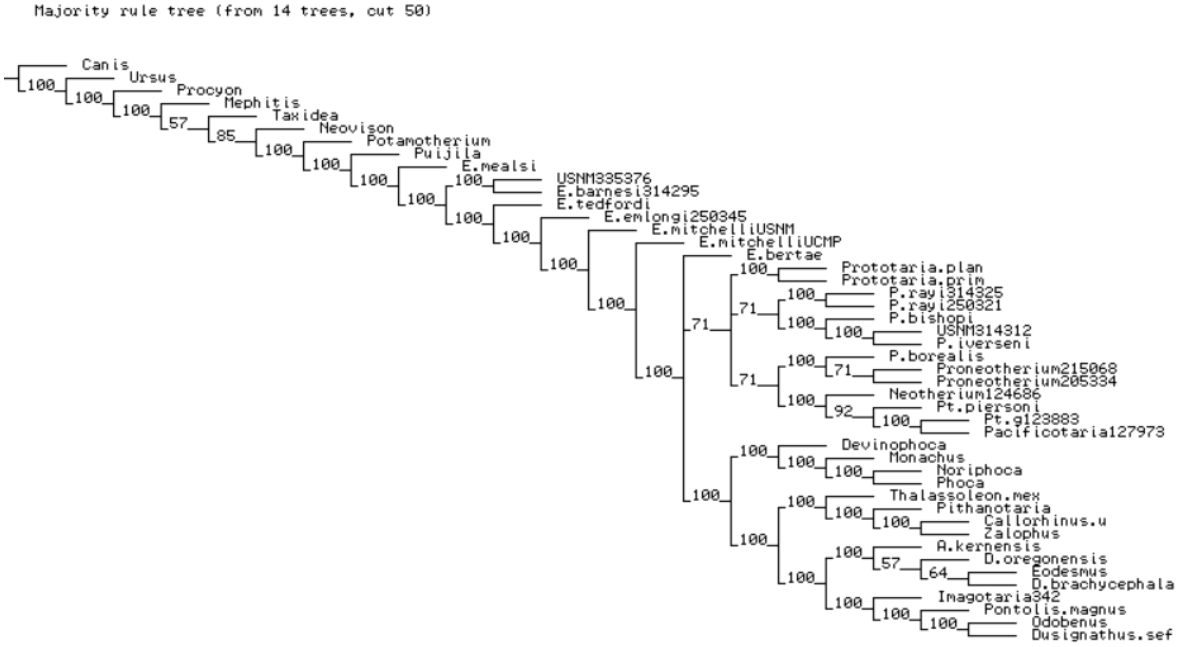

Figure 1.3. Parsimony tree with closest topology to the majority rule tree.

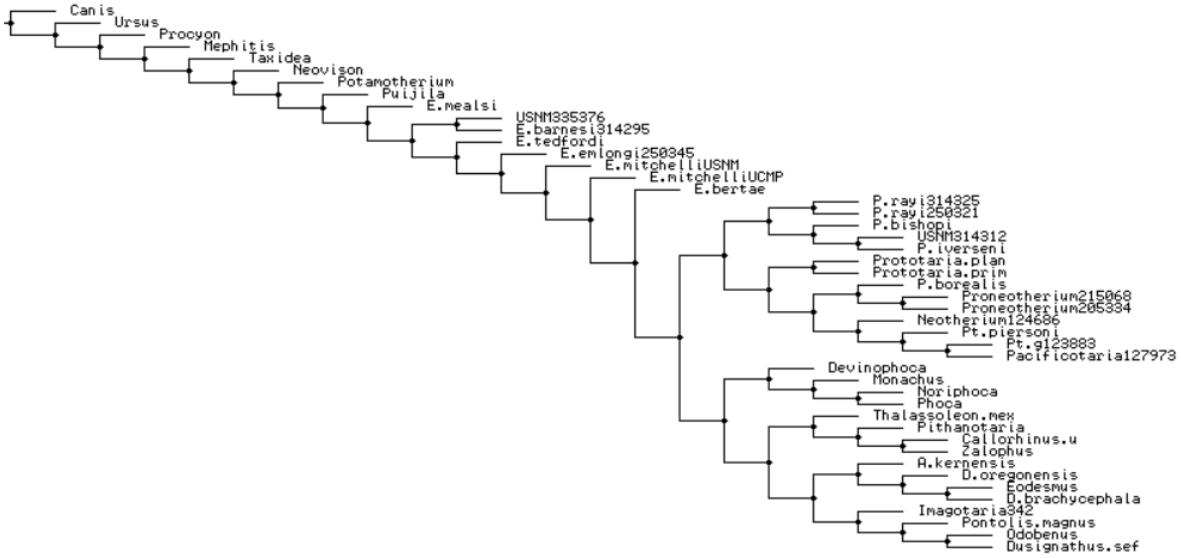

Figure 1.4. LACM 127974, *Proneotherium? borealis*, sp. Nov., cranium in (A) dorsal, (B) ventral, and (C) lateral views.

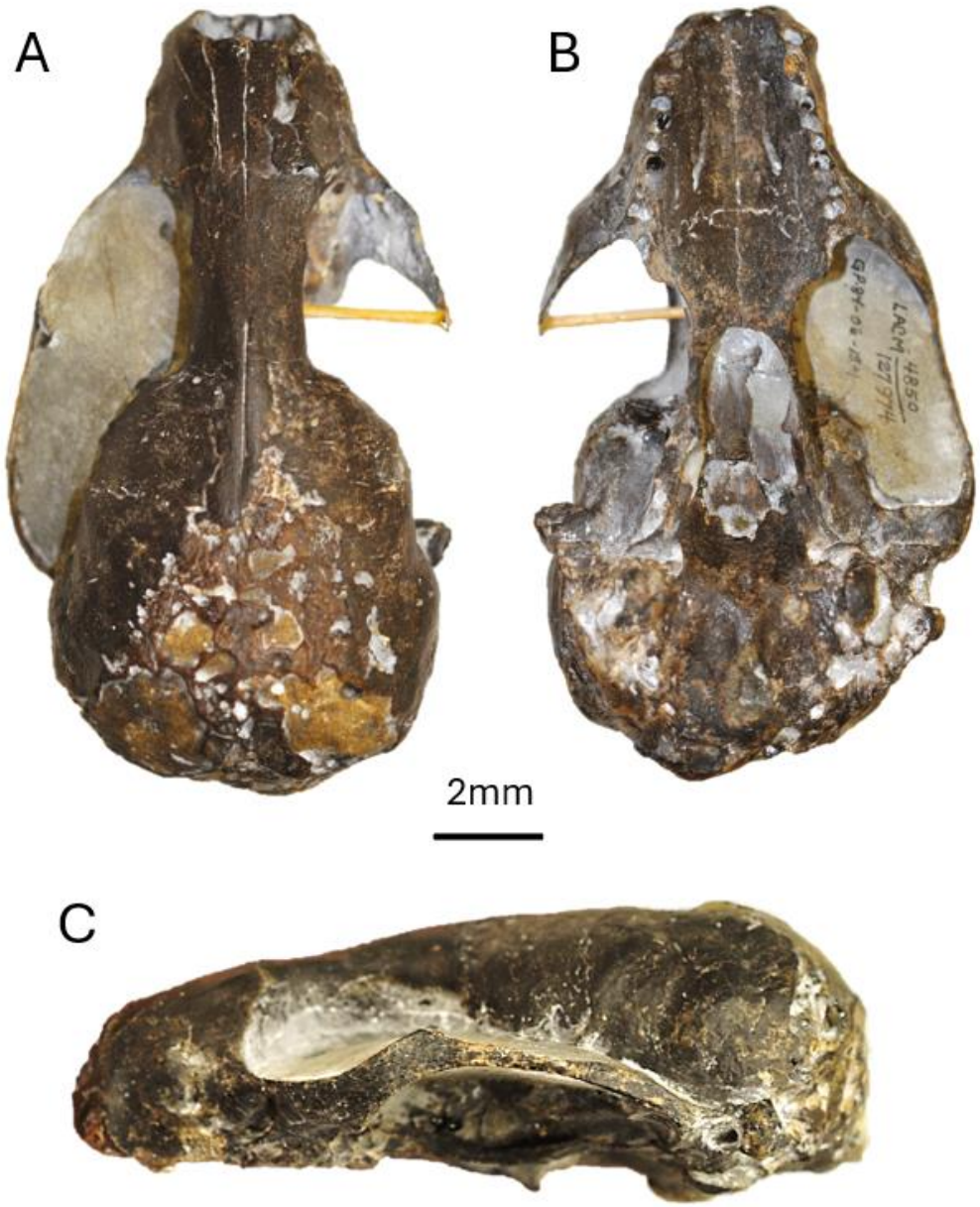

Figure 1.5. LACM 128004, "*Enaliarctos" bertae*, sp. nov., cranium in (A) dorsal, (B) ventral, and (C) lateral views.

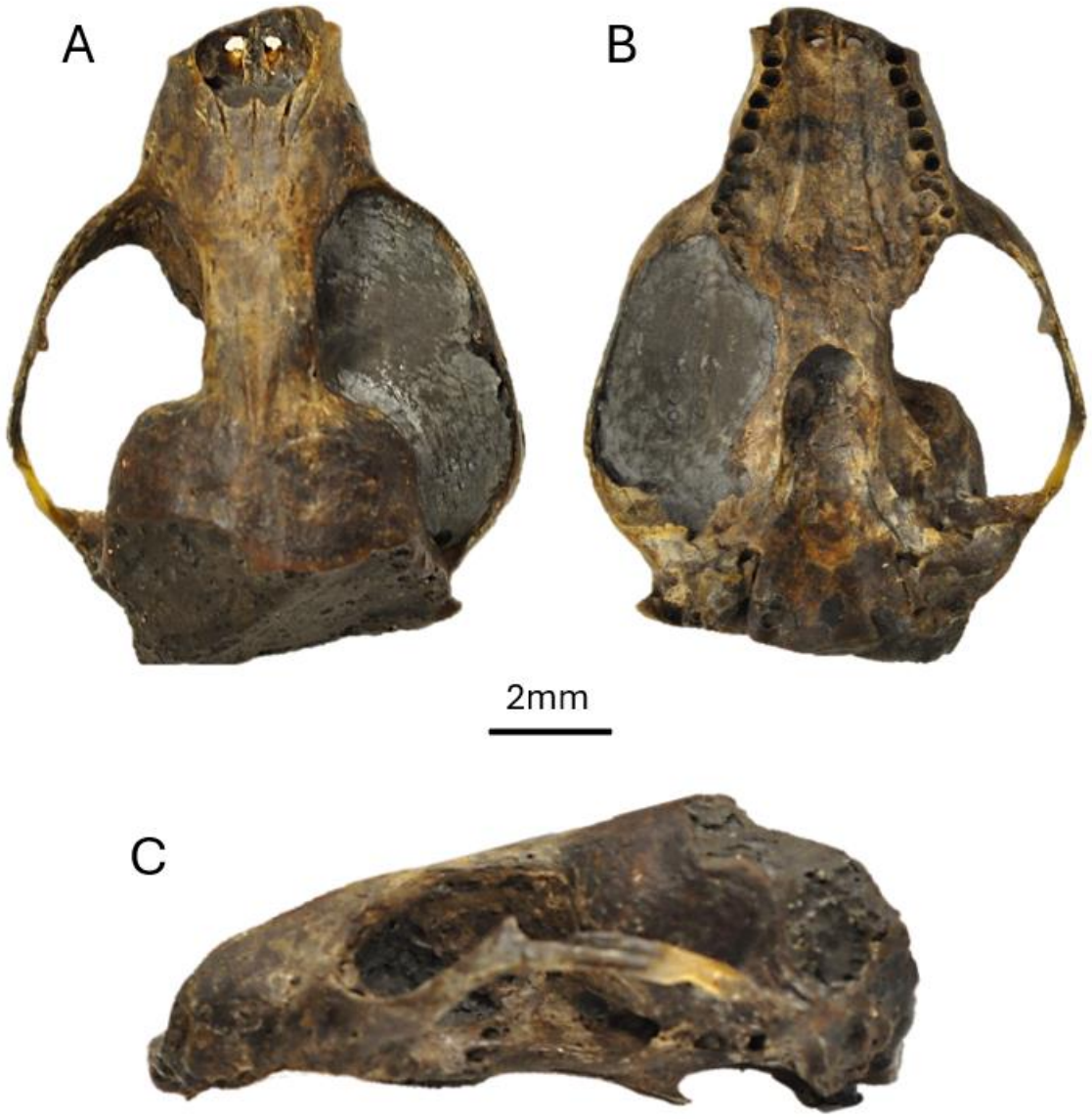

Figure 1.6. Dorsal view of (A) "*Enaliarctos" sullivani* and (B) "*Enaliarctos" mitchelli* holotype crania (modified from Barnes, 1979). Scale bar is 2mm.

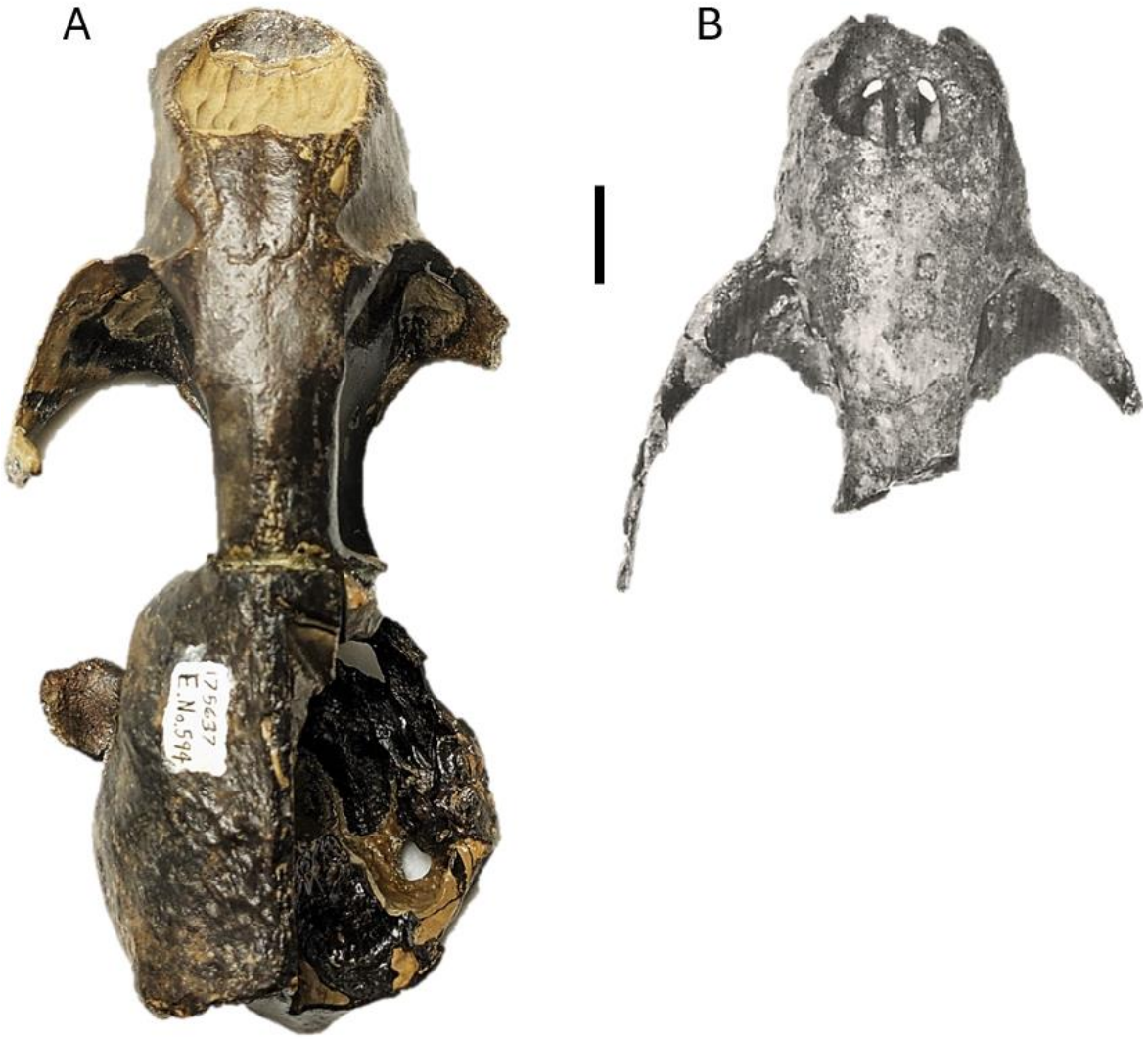

Figure 1.7. Ventral view of (A) "*Enaliarctos" sullivani* and (B) "*Enaliarctos" mitchelli* holotype crania (modified from Barnes, 1979). Scale bar is 2mm.

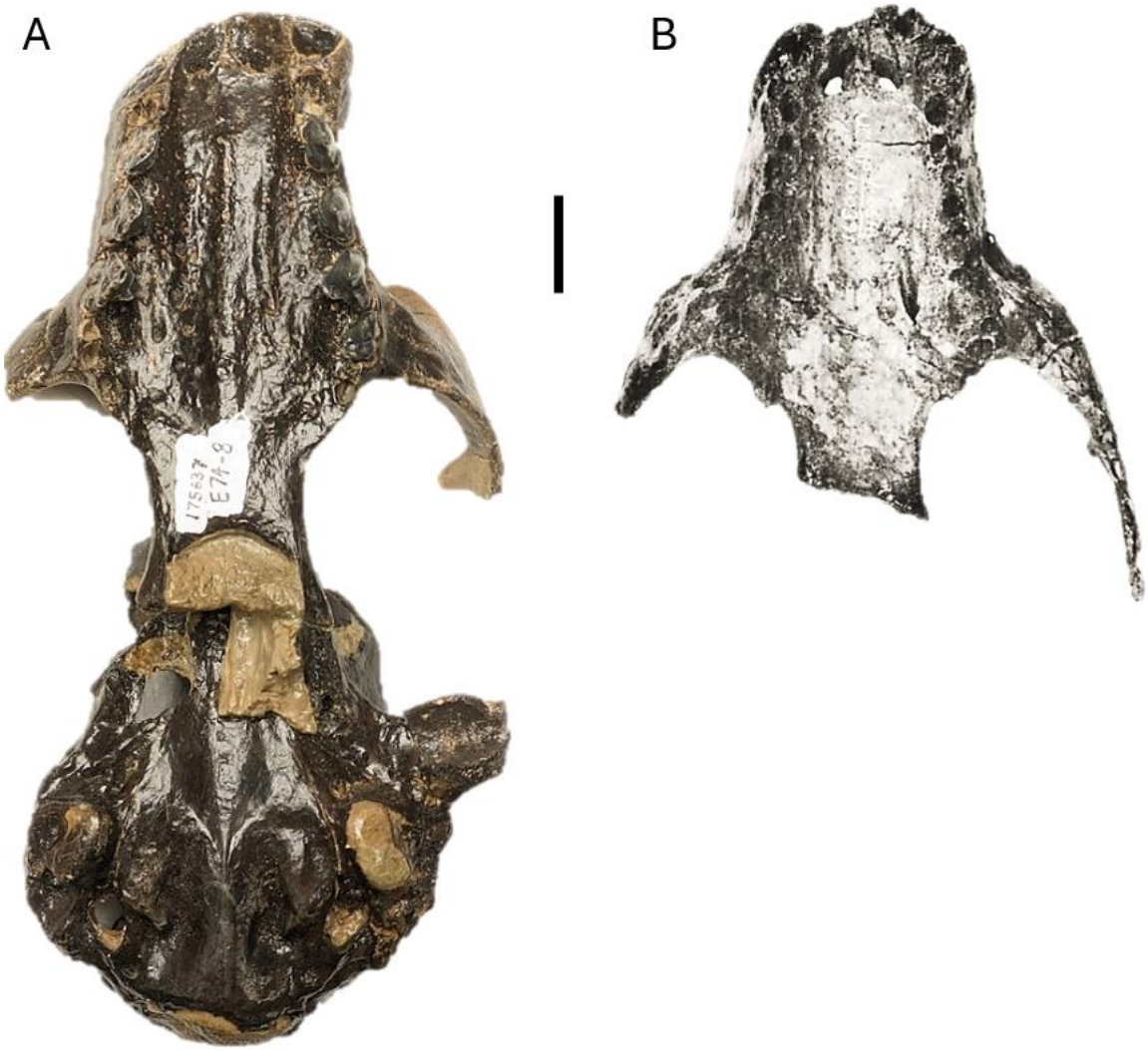

Figure 1.8. Lateral view of (A) "*Enaliarctos" sullivani* and (B) "*Enaliarctos" mitchelli* holotype crania (modified from Barnes, 1979). Scale bar is 2mm.

Figure 1.9. USNM 335376, referred to "*Enaliarctos" barnesi*, cranium in (A) dorsal and (B) ventral views.

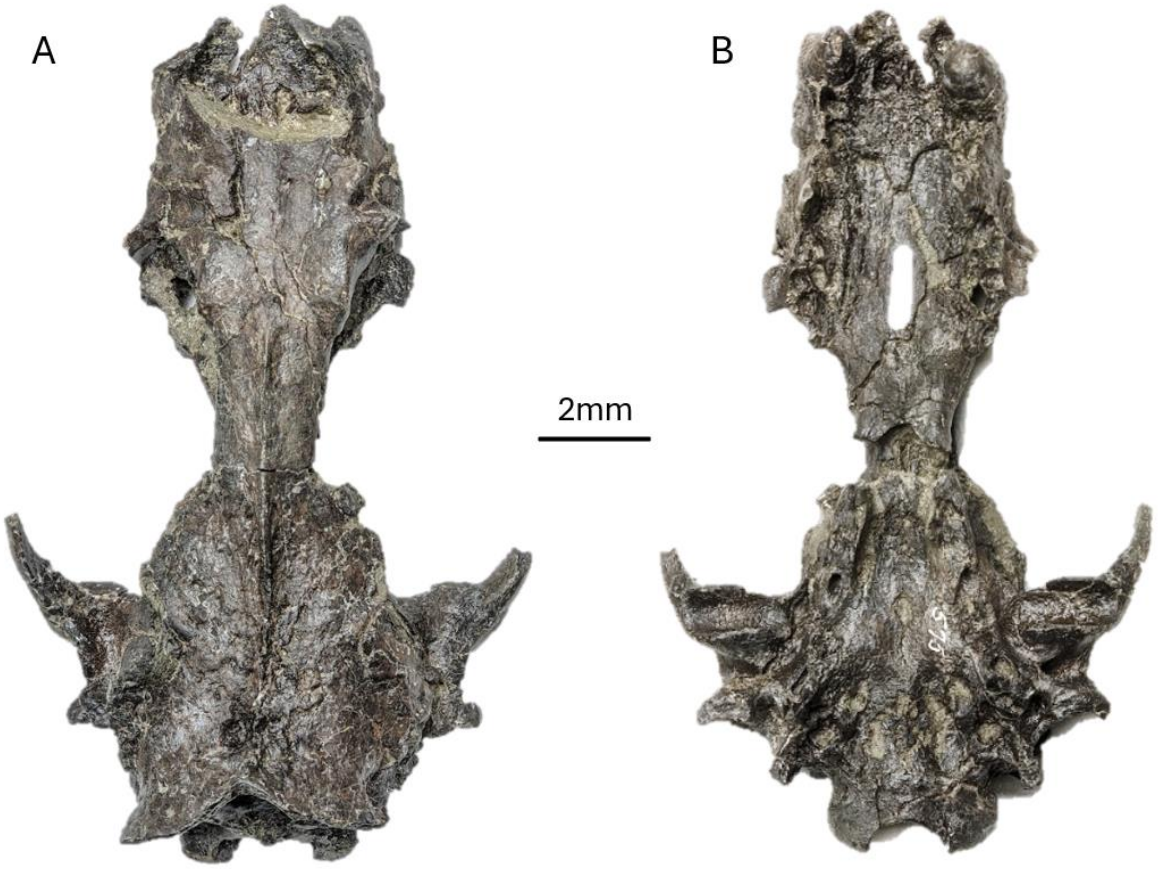

Figure 1.10. USNM 314312, referred to *Pinnarctidion iverseni*, cranium in (A) dorsal and (B) ventral views.

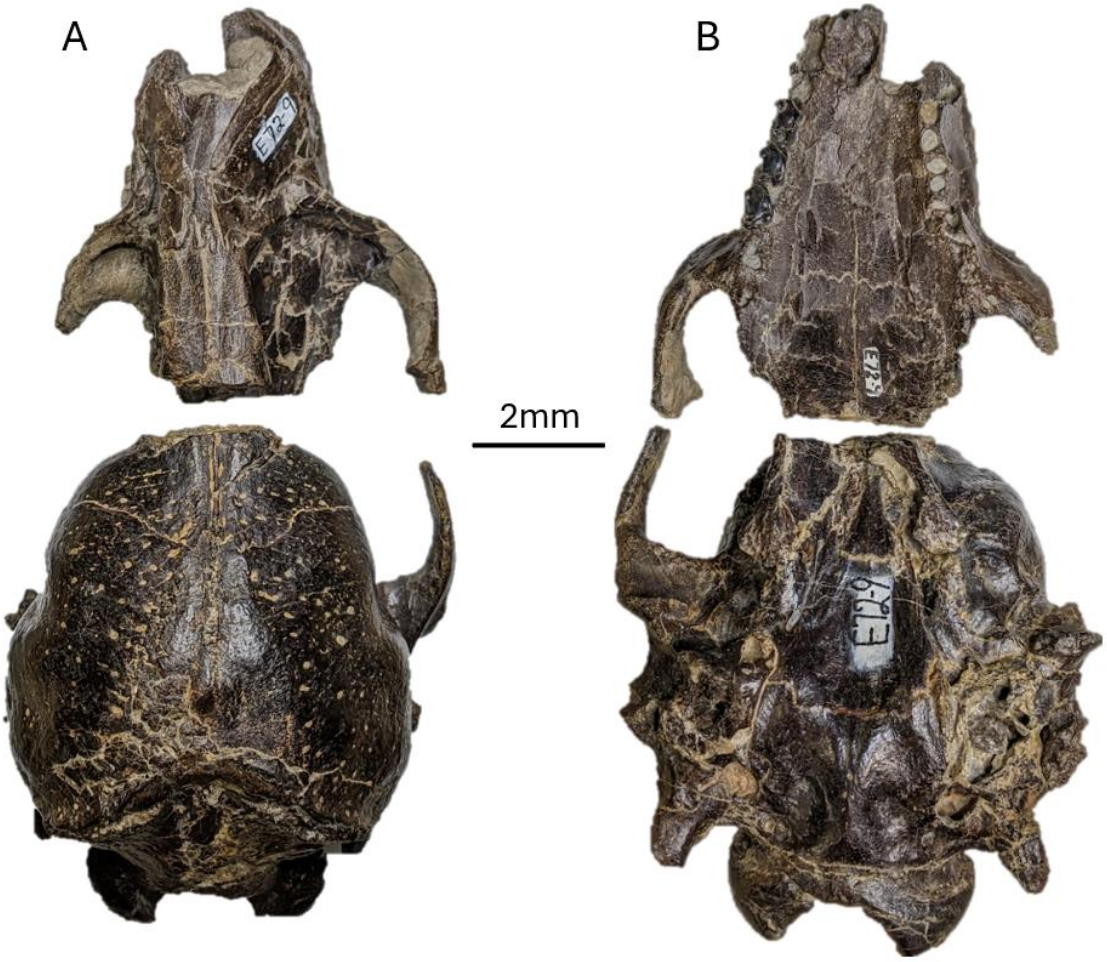

Figure 1.11. USNM 314312, referred to *Pinnarctidion iverseni*, cranium in right lateral view.

Figure 1.12. USNM 314312, referred to *Pinnarctidion iverseni*, (A) left and (B) right mandibles.

Figure 1.13. USNM 314312, referred to *Pinnarctidion iverseni*, right scapula in lateral view.

Figure 1.14. USNM 314312, referred to *Pinnarctidion iverseni*, right humerus in (A) anterior and (B) posterior views.

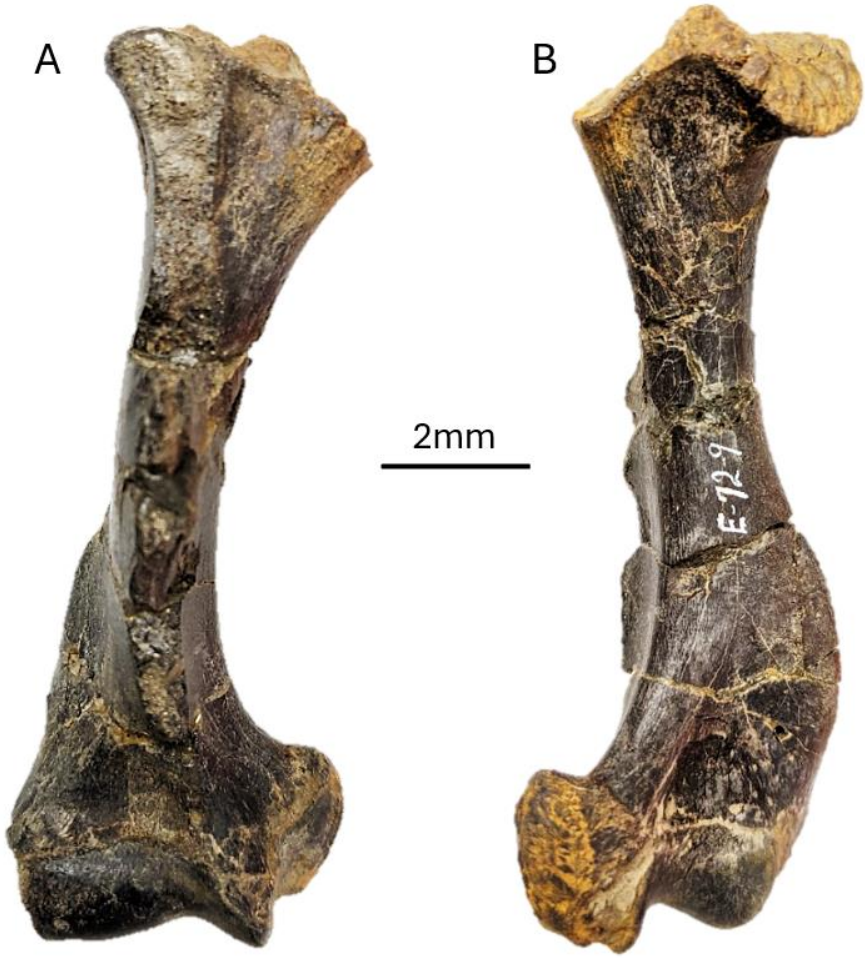

Figure 1.15. USNM 314312, referred to *Pinnarctidion iverseni*, (A) left and (B) right femora in posterior view.

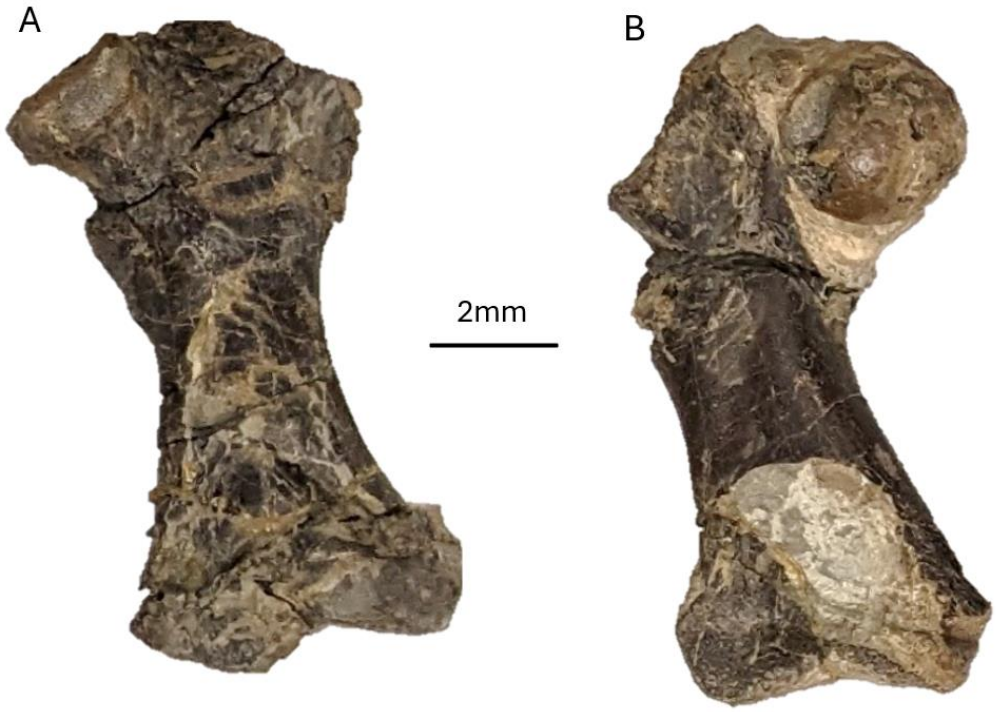

References 1

Armentrout, J. M. 1981. Correlation and ages of Cenozoic stratigraphic units in Oregon and Washington; pp. 137–148 in J. M. Armentrout (ed.), *Pacific Northwest Cenozoic Biostratigraphy*. Geological Society of America, Boulder, Colorado.

Arnason, U., Gullberg, A., Janke, A., Kullberg, M., Lehman, N., Petrov, E. A., & Väinölä, R. (2006). Pinniped phylogeny and a new hypothesis for their origin and dispersal. Molecular Phylogenetics and Evolution, 41(2), 345–354.

Audibert, P., Drehmer, C., Danilewicz, D., & De Oliveira, L. (2017). Do cranial suture age and growth layer groups correlate in southAmerican pinnipeds? *Journal of the Marine Biological Association of the United Kingdom*, 98:635–644.

Barnes, L. G. (1979). Fossil Enaliarctine Pinnipeds (Mammalia: Otariidae) from Pyramid Hill, Kern County, California. *Contributions in Science, Natural History Museum of Los Angeles County 318*, 1–41.

Barnes, L. G. (1989). A new enaliarctine pinniped from the Astoria Formation, Oregon, and a classification of the Otariidae (Mammalia: Carnivora). *Contributions in Science, Natural History Museum of Los Angeles County 403*, 1–26.

Barnes, L. G. (1992). A new genus and species of middle Miocene enaliarctine pinniped (Mammalia: Carnivora) from the Astoria Formation in Coastal Oregon. *Contributions in Science, Natural History Museum of Los Angeles County* 431.

Berta, A., Ray, C.E.,Wyss, A.R. (1989). Skeleton of the oldest known pinniped, *Enaliarctos mealsi*. *Science 244*:60–62.

Berta, A. (1991). New *Enaliarctos* (Pinnipedimorpha) from the Oligocene and Miocene of Oregon and the role of "Enaliarctids" in pinniped phylogeny. *Smithsonian Contributions to Paleobiology 69*, 1–36.

Berta, A. (1994a). A new species of phocoid pinniped *Pinnarctidion* from the early Miocene of Oregon. *Journal of Vertebrate Paleontology 14*, 405–13.

Berta, A. (1994b). New Specimens of the Pinnipediform *Pteronarctos* from the Miocene of Oregon. *Smithsonian Contributions to Paleobiology 78*.

Berta, A., Churchill, M., & Boessenecker, R. W. (2018). The origin and evolutionary biology of pinnipeds: seals, sea lions, and walruses. Annual Review of Earth and Planetary Sciences, 46(1), 203–228. https://doi.org/10.1146/annurev-earth-082517-010009

Berta, A., & Lanzetti, A. (2020). Feeding in marine mammals: an integration of evolution and ecology through time. *Paleontologica Electronica*. 23(2):a40 https://doi.org/10.26879/951

Boessenecker, R. W. and Churchill, M. (2015). The oldest known fur seal. *Biology Letters* 11: 20140835.

Boessenecker, R.W., & Churchill, M. (2018). The last of the desmatophocid seals: a new species of *Allodesmus* from the upper Miocene of Washington, USA, and a revision of the taxonomy of Desmatophocidae. *Zoological Journal of the Linnean Society 184*:211–35.

Bowditch, T. E. 1821. An Analysis of the Natural Classifications of Mammalia for the Use of Students and Travelers. J. Smith, Paris.

Churchill, M. & Uhen, M.D. (2019). Taxonomic implications of morphometric analysis of earless seal limb bones. *Acta Palaeontologica Polonica 64*(2):213–230.

Condon, T. (1906). A new fossil pinniped (*Desmatophoca oregonensis*) from the Miocene of the Oregon coast. *University of Oregon Bulletin* 3: 1–14.

Cullen, T. M., Fraser, D., Rybczynski, N., & Schroder-Adams, C. (2014). Early evolution of sexual dimorphism and polygyny in Pinnipedia. *Evolution 68*, 1469–84.

Deméré, T. A., & Berta, A. (2001). A reevaluation of *Proneotherium repenningi* from the Miocene Astoria Formation of Oregon and its position as a basal odobenid (Pinnipedia: Mammalia). *Journal of Vertebrate Paleontology*, 21(2): 279–310.

Deméré, T. A., Berta, A., & Adam, P. J. (2003). Chapter 3: Pinnipedimorph evolutionary biogeography. Bulletin of the American Museum of Natural History, 279, 32–76.

de Muizon, C. (1982). Phocid phylogeny and dispersal. *Annals of the South African Museum, 89(2)*:175–213.

Everett, C. J., Deméré, T. A., & Wyss, A. R. (2023). A New Species of Pinnarctidion from the Pysht Formation of Washington State (U.S.A.) and a Phylogenetic Analysis of Basal Pan-Pinnipeds (Eutheria, Carnivora). *Journal of Vertebrate Paleontology 42(3)*.

Flower, B. P., & Kennett, J. P. (1994). The middle Miocene climatic transition: East Antarctic ice sheet development, deep ocean circulation and global carbon cycling. *Palaeogeography, Palaeoclimatology, Palaeoecology*, 108(3–4), 537–555.

Geoffroy St. Hilaire, E. 1833. Revue encyclopédique, Paris 59, 80–81.

Goloboff, P. A. & Morales, M. E. (2023). TNT version 1.6, with a graphical interface for MacOS and Linux, including new routines in parallel. *Cladistics*, 39: 144–153.

Hennig, W. (1966). Phylogenetic Systematics. University of Illinois Press

Higdon, J. W., Bininda-Emonds, O. R., Beck, R. M., & Ferguson, S. H. (2007). Phylogeny and divergence of the pinnipeds (Carnivora: Mammalia) assessed using a multigene dataset. *BMC Evolutionary Biology*, 7, 1–19.

Hunt, R. M., and L. G. Barnes. 1994. Basicranial evidence for ursid affinity of the oldest pinnipeds; pp. 57–67 in A. Berta and T.A. Deméré (eds.), Contributions in marine mammal paleontology honoring Frank C. Whitmore, Jr. *Proceedings of the San Diego Society of Natural History* 29.

Kahle, P., Gallus, M., Kierdorf, H., & Kierdorf, U. (2023). Age estimation in the harbour seal (*Phoca vitulina*) based on the closure of skull sutures and synchondroses. *Anatomia, Histologia, Embryologia*, 52:300–311.

Kohno, N., Barnes, L. G., & Hirota, K. (1994). Miocene fossil pinnipeds of the genera *Prototaria* and *Neotherium* (Carnivora; Otariidae; Imagotariinae) in the North Pacific Ocean: evolution, relationships and distribution. *Island Arc* 3:285–308.

Matthews, S.C. (1973). Notes on Open Nomenclature and on synonymy lists. *Palaeontology*, 16,713–719.

McLaren, I.A. (1960). Are the Pinnipedia biphyletic? *Systematic Zoology*, 9:18-28.

Mitchell, E. D., & Tedford, R. H. (1973). The Enaliarctinae: a new group of extinct aquatic Carnivora and a consideration of the origin of the Otariidae. *Bulletin of the American Museum of Natural History 151*, 201–284.

Miyazaki, S., Horikawa, H., Kohno, N., Hirota, K., Kimura, M., Hasegawa, Y., Tomida, Y., Barnes, L.G., & Ray, C.E. (1995). Summary of the fossil record of pinnipeds of Japan, and comparisons with that from the eastern North Pacific. *Island Arc* 3:361–72.

Nyakatura, K. & Bininda-Emonds, O. R. P. (2012). Updating the evolutionary history of Carnivora (Mammalia): a new species-level supertree complete with divergence time estimates. *BMC Evolutionary Biology 10*.

Ogg, J. G., Ogg, G. M., & Grandstein, F. M. 2016. A Concise Geologic Timescale: Chapter 14 - Paleogene. *Elsevier*. DOI: https://doi.org/10.1016/C2009-0-64442-1

Park, T., Burin, G., Lazo-Cancino, D., Rees, J. P. G., Rule, J. P., Slater, G. J., Cooper, N. (2024). Charting the course of pinniped evolution: insights from molecular phylogeny and fossil record integration. *Evolution* 78(7):1212–1226.

Prothero, D. R., A. Streig. and C. Burns. 2001. Magnetic stratigraphy and tectonic rotation of the upper Oligocene Pysht Formation, Clallam County, Washington, p.p. 224–233. In

Prothero, D.R. (ed.) Magnetic stratigraphy of the Pacific Coast. The Pacific Section SEPM, Santa Fe Springs, CA.

Repenning, C.A., Ray, C.E. & Grigorescu, D. (1979). Pinniped biogeography. In Historical Biogeography, Plate Tectonics, and the Changing Environment, ed. J Gray, AJ Boucot, pp. 357–69. Corvallis: Oregon State University Press

Repenning, C.A. & Tedford, R.H. (1977). Otarioid seals of the Neogene. Professional Paper 992, US Geological Survey, Washington, DC.

Rule, J. P., Adams, J. W., Rovinsky, D. S., Hocking, D. P., Evans, A. R., & Fitzgerald, E. M. G. 2020. A new large-bodied Pliocene seal with unusual cutting teeth. *Royal Society Open Science* 7201591201591.

Rybczynski N, Dawson, M. R., & Tedford, R. H. (2009). A semi-aquatic Arctic mammalian carnivore from the Miocene epoch and origin of Pinnipedia. *Nature 458*, 1021–24.

Schasse, H. W. 2003. Geologic map of the Washington portion of the Cape Flattery 1:100,000 quadrangle: Washington Division of Geology and Earth Resources Open File Report 2003-5, 1 sheet, scale 1:100,000.

Sigovini, M., Keppel, E., & Tagliapietra, D. (2016). Open Nomenclature in the biodiversity era. *Methods in Ecology and Evolution*, 7:1217–1225.

Sivertsen, E. (1954). A survey of the eared seals (family Otariidae) with remarks on the Antarctic seals collected by M/K "Norvegia" in1928–1929. In Scientific results of the Norwegian Antarctic expeditions 1927–1928, et sqq., instituted and financed by consul Lars Christensen (Vol. 36). Det Norske Videnskaps-Akademi i Oslo.

Snavely, P. D., MacLeod, N. S., Wagner, H. C., and Rau, W. W. 1976. Geologic map of the Yaquina and Toledo quadrangles, Lincoln County, Oregon. U.S. Geological Survey, Miscellaneous Investigation Series Map I-867.

Snavely, P., A. Niem, and J. Pearl. 1978. Twin River Group (Upper Eocene to Lower Miocene) defined to include the Hoko River, Makah, and Pysht Formations, Clallam County, Washington. In Sohl, N., and Wright, W. (ed.) Changes in Stratigraphic Nomenclature by the U.S. Geological Survey, 1977. Geological Survey Bulletin 1457A:111–20.

Steinthorsdottir, M., Coxall, H.K., Boer, A.M., de Huber, M., Barbolini, N., Bradshaw, C.D., Burls, N.J., Feakins, S.J., Gasson, E., Henderiks, J., Holbourn, A.E., Kiel, S., Kohn, M.J., Knorr, G., Kürschner, W.M., Lear, C.H., Liebrand, D., Lunt, D.J., Mörs, T., Pearson, P.N., Pound, M.J., Stoll, H., Strömberg, C.E. (2021). The Miocene: The future of the past. *Paleoceanography and Paleoclimatology* 36: e2020PA004037.

Tanaka, Y., & Kohno, N. (2015). A New Late Miocene Odobenid (Mammalia: Carnivora) from Hokkaido, Japan Suggests Rapid Diversification of Basal Miocene Odobenids. *PLoS ONE 10(8)*: e0131856.

Tate-Jones M.K., Peredo, C.M., Marshall, C.D., Hopkins, S.S.B. (2020). The dawn of Desmatophocidae: a new species of basal desmatophocid seal (Mammalia, Carnivora) from the Miocene of Oregon, U.S.A. *Journal of Vertebrate Paleontology* 40(4).

Tedford, R. H. (1976). Relationships of pinnipeds to other carnivores (Mammalia). *Systematic Zoology 25*, 363–74.

Wolsan, M., Wyss, A. R., Berta, A., & Flynn, J. J. (2020). Pan-Pinnipedia, new clade name. *Phylonyms: A Companion to PhyloCode.*

Wyss, A. R. (1987). The walrus auditory region and monophyly of pinnipeds. *American Museum Novitates* 2871:1–31.

Wyss, A. R. (1988). Evidence from flipper structure for a single origin of pinnipeds. *Nature* 334: 427–428.

Chapter 2: The phylogeny of arctoid carnivorans with emphasis on pan-pinniped relationships

Introduction 2

Pinnipeds, the "flipper-footed" carnivores, returned to the aquatic realm more recently (Nyakatura & Bininda-Emonds, 2012) and retained a closer resemblance to their terrestrial cousins than cetaceans (Uhen, 2010) or sirenians (Domning, 2018). Pinnipeds rely on land or ice territories for breeding, which imposes unique functional tradeoffs on their aquatic adaptations (Reichmuth et al., 2013; Tennett et al., 2018; Esteban et al., 2023). Extant pinnipeds inherited many of those adaptations from their most recent common ancestor, so details of their aquatic transition are buried with their fossil relatives. A growing number of early pan-pinnipeds have been recovered from the North Pacific (Mitchell and Tedford, 1973; Barnes, 1979; Barnes, 1989; Berta, 1991, 1994a; Everett et al., 2023) and Atlantic (Rybczynski et al., 2009), and possible pan-pinnipeds are found in Eurasia (Geoffroy, 1833; Matthew & Granger, 1924). To assemble a robust phylogeny of pan-pinnipeds and determine the sequence of character state transitions leading to the crown group, a wide range of in-group and out-group taxa must be sampled. Accordingly, this study performs a comprehensive examination of the phylogeny of pan-pinnipeds and other arctoids.

Arctoid carnivorans, which include ursids, musteloids, and pinnipeds, fill a wide variety of ecological roles and display a correspondingly disparate array of adaptations. Wholly extinct carnivorans such as amphicyonids (Trouessart, 1885) and amphicynodontids (Simpson, 1945) have also been considered arctoids. Molecular clock analyses suggest that the arctoid

common ancestor originated in the late Eocene (Nyakatura & Bininda-Emonds, 2012). Relationships among arctoids have been scrutinized from both morphological (Tedford, 1976; Wolsan, 1993; Wyss & Flynn, 1993; Wang et al., 2005a; Wesley-Hunt & Flynn, 2005; Tomiya & Tseng, 2016; Wang et al., 2023) and molecular perspectives (Delisle & Strobeck, 2005; Flynn et al., 2005; Arnason et al., 2006; Yu & Zhang, 2006; Finarelli, 2008; Sato et al., 2009; Nyakatura & Bininda-Emonds, 2012; Luan et al., 2013; Hassanin et al., 2021). Several previously controversial relationships have been consistently supported in recent studies. These include the monophyly of Pinnipedia, the placement of *Ailuropoda* within ursids, and the monophyly of Musteloidea composed of mustelids, procyonids, mephitids, and ailurids. Yet, uncertainties remain, especially regarding fossil taxa.

Outstanding questions to be addressed in this analysis include: (1) the relationships of the enigmatic arctoids *Puijila*, *Potamotherium*, and *Amphicticeps*; (2) the branching sequence of the five or more species of "*Enaliarctos*," along with two other pinnipedimorph genera, *Pteronarctos* and *Pinnarctidion*; (3) the affinities of *Prototaria*, *Proneotherium*, and *Neotherium*, heretofore considered odobenids; (4) the placement of *Kolponomos*, variably considered a procyonid (Stirton, 1960), pan-pinniped (Paterson et al., 2020), or amphicynodontid (Tedford et al., 1994); and (5) the position of the extinct Amphicynodontidae–variously considered pan-pinnipeds (Wang et al., 2005a) or ursoids (Tedford et al., 1994; Finarelli, 2008; Wang et al., 2023). A clearer understanding of the phylogeny of pan-pinnipeds will also illuminate the ancestral character states and sequence of character transitions leading to Pinnipedia.

Methods 2

A total of 186 morphological characters were scored for 111 caniform OTUs, including a significant sampling of extant taxa to allow comparison with molecular results. The characters scored and taxa compared in this study are listed in Appendix 2. The character-taxon matrix was modified from one used in a previous study of pan-pinniped relationships (Everett et al., 2023). Characters were compiled from previous studies (Berta and Wyss, 1994; Wesley-Hunt and Flynn, 2005; Tomiya and Tseng, 2016; Boessenecker and Churchill, 2018; Paterson et al., 2020) and modified to be more broadly compatible with such a range of taxa. Several novel characters were also included. Parsimony analysis was performed in TNT version 1.6 (Goloboff & Morales, 2023) using a new technology search of Wagner trees.

The selection and description of characters have a significant influence on the quality of information contained in morphological character matrices. Character descriptions were informed by Sereno (2007), Brazeau (2011), and Simões et al. (2017), who offer specific recommendations for avoiding problematic characters, such as uninformative compound multistate characters, pseudo-ordering of asymmetric transformations, and absent character states. The compilation of characters from previous matrices often involved modifying character state descriptions to avoid those issues. Ordered characters were limited to multistate characters that exhibit morphoclines in size, shape, or quantity.

A secondary goal of this study was to assess how ordered characters, weighted characters, implied weights, and molecular evidence-based group constraints affect branch support values in maximum parsimony analyses. A series of 12 trial analyses (see Table 2.1) were

performed to compare the effects of different combinations of these parameters on combined Bremer support and bootstrap support values.

The ordered characters parameter of TNT instructs the parsimony algorithm to treat each step in an additive sequence as its own character state change, favoring a series of stepwise evolutionary transitions rather than a series of unordered changes. Eighty-five characters were selected as ordered for trials 2, 4, 6, 8, 10, and 12 (see Appendix for annotated character list).

The 'force' command function in TNT (Goloboff & Morales, 2023) was used to constrain the parsimony tree search according to a predetermined tree structure based on molecular evidence (Finarelli, 2008; Sato et al., 2009; Flynn et al., 2010; Nyakatura & Bininda-Emonds, 2012; Law et al., 2017; Hassanin et al., 2021). The group constraint function 'force /' is used here to accommodate the uncertain relationships among fossil taxa. The positive group constraint function favors the predetermined tree structure by treating group membership variables as additional characters affecting tree length. Thus, a penalty is imposed on trees that violate the constraints. This method differs from the tree constraint function 'force =', which forces a specific tree topology but excludes unknown taxa from that monophyletic group. The following code line was used to guide which clade relationships should be favored in the tree search:

force / (Canis Urocyon) ((Ailuropoda (Tremarctos Ursus)) ((Monachus (Mirounga (Leptonychotes))) (Erignathus (Cystophora (Phoca))) (Odobenus (Callorhinus ((Eumetopias

Zalophus) (Otaria Arctocephalus))))) (Mephitis Ailurus ((Taxidea (Meles ((Gulo Martes) (Melogale (Galictis Neovison (Lontra Enhydra)))))) (Potos (Procyon Bassariscus)))))

The weighted characters parameter assigns a higher step cost to the state transformations of certain characters, based on assumptions that those characters are more evolutionarily significant and/or may be less subject to homoplasy. Here, a factor increase (k value) of 3 is imposed. Twenty-nine characters (see list in Appendix) were selected as sufficiently informative to be weighted more highly, based on how consistently they are observed to diagnose previously well-established clades.

Implied weighting instructs the tree search algorithm to downweight potentially homoplastic characters using *a posteriori* assumptions developed from simulated results from a subset of parsimony trees. Implied weighting applies to the entire matrix and does not require data manipulations or decisions to be made in advance.

	No manipulation	Ordered characters	Group constraints	Weighted characters	Implied weights
Trial 1	yes				
Trial 2		yes			
Trial 3			yes		
Trial 4		yes	yes		
Trial 5				yes	
Trial 6		yes		yes	

Trial 7			yes	yes	
Trial 8		yes	yes	yes	
Trial 9					yes
Trial 10		yes			yes
Trial 11			yes		yes
Trial 12		yes	yes		yes

Table 2.1. Trials to compare the effects of different tree search criteria.

The results of each trial are presented as a strict consensus tree with Bremer support values and a bootstrap resampling tree (see Figures 2 section).

Bremer support provides a measure of robustness for each branch by quantifying how many extra steps would need to be added to the most parsimonious tree that does not resolve that branch (Bremer, 1994). Combined Bremer support (CBS) is a more comprehensive support metric that combines both absolute and relative Bremer supports and is often consistent with jackknife frequencies (Goloboff, 2014). Absolute, relative, and CBS values are compared across all trials.

Bootstrap resampling (Felsenstein, 1985) generates trees from repeated subsets of the original character data. Bootstrap values represent the proportion of resampled trees that reproduce a given branch. These values tend to be more deflated (i.e., more of an underestimate of true support) with increasing numbers of characters and taxa (Zharkikh & Li, 1992), with values lower than 70 generally implying low support.

Statistical analysis

The two chosen measures of tree robustness and precision – Bremer support index and bootstrap resampling value, here both acting as dependent variables – were subjected to a Spearman's Rank Correlation test.

To test the influence of each model parameter on the dependent variables, support values for trials with and without each manipulated variable are compared by t test. Then, all four variables (ordered characters, group constraints, weighted characters, and implied weights) are compared using an ANOVA.

Results 2

For each of the twelve trial runs, two resulting trees are compared, the strict consensus of the maximally parsimonious trees, and the tree produced from bootstrap resampling. Branch supports are assessed quantitatively and differences in topology are assessed qualitatively. The total support index, the sum of all branch support values divided by the branch length of the most parsimonious tree(s), is an approximation of overall tree stability and resolution (Bremer 1994). Although Bremer (1994) initially suggested using absolute support value to inform total support, combined Bremer support (CBS) is used here because it takes into account relative fit differences which are necessary to assess trees yielded by implied weighting analyses.

Bremer supports for Trials 9-12 are rescaled because the implied weights parameter inherently rescales the branch length contribution of all characters around a constant of k=3.

Trial 1

A parsimony analysis with no parameter manipulations, Trial 1, yielded 12 equally parsimonious trees of 2555 steps each. A strict consensus of these trees (Figure 2.1) has a total support index of 1.147, ranking the lowest of any trial. *Gustafsonia*, *Daphoenus*, *Paradaphoenus*, and *Cynodictis* are recovered as the successively more basal caniforms. The rest of the tree is composed of two branches – one of pinniped-line taxa, and another of all "fissiped" caniforms. Canidae includes the extinct *Epicyon*, *Hesperocyon*, and *Lycophocyon*. An amphicyonid clade is sister to the canids. An ursid clade is nested within a paraphyletic procyonid group, sister to the remaining musteloids. *Allocyon*, *Cephalogale*, *Amphicticeps*, *Potamotherium*, and *Puijila* successively form the base of Pan-Pinnipedia. Many early-diverging pan-pinnipeds remain unresolved, but five clades can be distinguished within the broader polytomy. *Pinnarctidion rayi*, *P. bishopi*, and *P. iverseni* form a monophyletic group. Crown otariids and *Callorhinus gilmorei* pair, but *Thalassoleon* and *Pithanotaria* (traditionally considered otariids) fall into the basal pinniped polytomy. Desmatophocids are monophyletic. The Odobeninae (Mitchell, 1968; Boessenecker et al., 2024) – which include the tusked Odobenini plus *Ontocetus*, *Protodobenus*, and *Aivukus* – are monophyletic and sister to the dusignathines (excluding *Pontolis*). However, all other putative odobenids form a polytomy with other crown pinnipeds. Phocids, also part of the pinniped polytomy, are the best-supported clade.

The resampled tree yielded a total bootstrap value of 2303, ranking the sixth highest of all trials. *Gustafsonia*, *Daphoenus*, *Paradaphoenus*, and *Cynodictis* are here recovered as a

distinct basal clade, unlike the paraphyletic grade they formed in the parsimony trees. The major caniform clades mostly form a broad polytomy, with ursids nested within the musteloids. *Potamotherium* is the earliest member of the pan-pinniped clade to diverge. Pan-pinniped relationships are better resolved than in the parsimony trees. Notably, *Neotherium* and its tentative ally, LACM 124686, are nearest to the crown, which is a polytomy formed by monophyletic otariid, phocid, and desmatophocid clades, along with multiple conventionally odobenid branches.

Trial 2

The analysis in which all logical multistate characters were ordered, Trial 2, yielded 8 maximally parsimonious trees of 2618 steps each. A strict consensus of these trees (Figure 2.2) has a total support index of 1.640, ranking the sixth highest among consensus trees. The basal portion of this tree differs in significant ways from Trial 1. Ursids are nested within an amphicyonid clade that is sister to canids. A monophyletic musteloid clade is sister to Pan-Pinnipedia. *Pachycynodon* is the basalmost pan-pinniped. In this tree, pan-pinnipeds are reasonably well-resolved, with the crown composed of phocid and otarioid clades that includes a monophyletic desmatophocid group nested within odobenids.

The resampled tree yielded a total bootstrap value of 2487, ranking #3. This tree is very similar to the resampled tree from Trial 1, mainly having basal arctoids more fully resolved. *Amphicticeps* is resolved as the basalmost pan-pinniped.

Trial 3

The analysis with only group constraints applied, Trial 3, yielded 12 maximally parsimonious trees of 2569 steps each. A strict consensus of these trees (Figure 2.3) has a support index of 1.616, ranking the seventh highest among consensus trees. These trees place canids and amphicyonids as sister to one another. As in Trial 1, an ursid clade is nested within a paraphyletic procyonid group, sister to the remaining musteloids. Relationships among pan-pinnipeds are nearly identical to those in Trial 1, which implies that group constraints have a lesser effect on tree topology than ordered characters.

The resampled tree yielded a total bootstrap value of 2389, ranking #5; it is significantly different from previous trees because it recovers an otariid plus phocid clade in a polytomy with odobenids and desmatophocids. Basal caniforms remain poorly resolved.

Trial 4

The analysis with ordered characters and group constraints applied, Trial 4, yielded 11 equally parsimonious trees of 2634 steps each. A strict consensus of these trees (Figure 2.4) has a total support index of 1.333, ranking the tenth highest among consensus trees. The Trial 4 consensus tree contrasts with that of Trial 1 by resolving pan-pinnipeds quite well, but leaving most of the earlier-diverging lineages unresolved. The branches it does support well are similar to those of Trial 2. Canids and musteloids are almost fully collapsed into polytomy, but ursids are fully resolved. *Potamotherium* is confidently resolved as the earliest pan-pinniped. *Pinnarctidion* is monophyletic. Crown pinnipeds are resolved nearly identically to Trial 2.

The resampled tree yielded a total bootstrap value of 2552, ranking #1 of all trials. The Trial 4 resampled tree closely resembles that of Trial 2. The branching pattern of canids is more consistent with other analyses, but that of musteloids is less so. *Amphicticeps* is no longer recovered as a pan-pinniped. Crown pinnipeds are much better resolved than, yet follow a similar pattern to, the Trial 4 parsimony trees.

Trial 5

The analysis with only weighted characters applied, Trial 5, yielded 1 parsimony tree with 3373 steps. This tree (Figure 2.5) has a support index of 1.697, ranking the fifth highest among consensus trees. This tree places amphicynodontids basal to other caniforms. Canids, ursids, and an unusual amphicyonid-like group share a branch. Musteloids form a paraphyletic grade along the pan-pinniped branch. Basal pan-pinnipeds are mostly contained in two sequentially-branching clades – one with most "*Enaliarctos*" species and another with *Pteronarctos*, *Prototaria*, *Proneotherium*, and *Pinnarctidion*. Phocids branch separately from a reasonably well-resolved otarioid clade.

The resampled tree yielded a total bootstrap value of 2058, ranking #8. This poorly resolved tree is not significantly different from previous resampled trees. It does indicate very low support for a pairing of phocids plus otariids.

Trial 6

The analysis with ordered characters and weighted characters applied, Trial 6, yielded 6 equally parsimonious trees of 3367 steps each. A strict consensus of these trees (Figure 2.6) has a support index value of 1.397, ranking the eighth highest among consensus trees. The branching pattern of these trees differs significantly from those of previous trials. The basal caniforms form a clade, as in some of the bootstrap trees. Canids are nested within an amphicyonid clade. Amphicynodonts are polyphyletic, some closer to *Subparictis* and others closer to ursids. Musteloids and many other arctoids form a paraphyletic grade leading to pan-pinnipeds, which conflicts with molecular and other morphological analyses. Stem pinnipeds are moderately resolved, with a monophyletic grouping of *Prototaria*, *Proneotherium*, *Pinnarctidion*, "*Enaliarctos*" *bertae*, and *P. borealis*. Phocids diverge first of the crown families, and otariids are sister to odobenids and desmatophocids. The traditional odobenids would be monophyletic except desmatophocids are nested within them.

The resampled tree yielded a total bootstrap value of 2248, ranking #7. This tree places mustelids sister to pan-pinnipeds, but excludes procyonids. Most other basal caniform lineages form a polytomy. Pan-pinnipeds are resolved similarly to previous resampled trees.

Trial 7

The analysis with group constraints and weighted characters, Trial 7, yielded 6 equally parsimonious trees of 3287 steps each. The consensus of these trees (Figure 2.7) has a support index of 1.219, ranking the eleventh highest among consensus trees. This analysis resulted in better resolution of the basal portion of the tree than in Trials 6 or 8, but the pan-

pinniped branch is much more poorly resolved. It shows an early diverging grade of caniforms, as in Trial 1, then a clade of amphicynodontids, then a clade that includes canids, amphicyonids, and ursids. As in Trials 6 and 8, musteloids form a poorly resolved highly paraphyletic grade basal to pan-pinnipeds. Few clades are resolved among non-crown pan-pinnipeds. Most "*Enaliarctos*" species form a monophyletic grouping and *Prototaria*, *Proneotherium*, and *Pinnarctidion* are united. At the crown level, only phocids are robustly supported as a monophyletic group. Phocids, desmatophocids, some odobenids, some otariids, and nine other pinniped taxa share a polytomy.

The resampled tree yielded a total bootstrap support value of 2399, ranking #4. In this tree, musteloids are better resolved than in Trials 6 or 8. The pan-pinniped portion is similar to that in Trial 6, but less well resolved than in Trial 8.

Trial 8

The analysis with ordered characters, weighted characters, and group constraints, Trial 8, yielded 9 equally parsimonious trees of 3383 steps each. A strict consensus of these trees (Figure 2.8) has a support index of 1.390, ranking the ninth highest among consensus trees. The consensus of these trees places amphicyonids with canids, amphicynodontids with ursids, and musteloids as a paraphyletic grade closer to pan-pinnipeds. Among pan-pinnipeds, it is notable that "*Enaliarctos*" is nearly monophyletic and *Prototaria*, *Proneotherium*, and *Pinnarctidion* form a clade. Crown pinnipeds are separated into Phocidae and Otarioidea, the latter containing a monophyletic Otariidae. Desmatophocids are nested within an odobenid polytomy.

The resampled tree yielded a total bootstrap value of 2517, ranking #2. This tree preserves monophyletic canid and ursid clades, but most other early caniform relationships are unresolved. Pan-pinniped relationships are better resolved than most other resampled trees. Like the Trial 8 parsimony tree, phocids are separate from other crown pinnipeds. This otarioid clade consists of an unresolved polytomy of otariids, desmatophocids, odobenine and dusignathine walruses, and various other supposed walruses.

Trial 9

The final analysis that includes only implied weighting, Trial 9, yielded 1 most parsimonious tree (Figure 2.9) with 128.61 steps. This tree has the lowest support index of the three implied weight trials, 5.466. There are some similarities to previous trials, such as the canid clade, but several differences are worth noting. Most of the amphicyonids and amphicynodontids have very different placements; for instance, *Amphicyon* diverges earlier than canids, but most others form a paraphyletic grade leading to arctoids. Ursids are nested within musteloids, not closest to procyonids as they are in other implied weight trees. *Neovison* and *Lontra* are closer to pinnipeds, but *Oaxacagale* is not. Most of the pan-pinniped branch is similar to other trials, with otariids branching first among crown pinnipeds as in Trials 10 and 12. However, the rest of the crown is much different. *Pinnarctidion rayi* is allied with allodesmines, *Desmatophoca* species group together but are more closely related to phocids than to allodesmines, and odobenids are more paraphyletic than in other implied weight trials.

The resampled tree yielded a total bootstrap value of 1526, ranking #12. This tree resolves basal caniform relationships better than the previous implied weight resampled trees, but pan-pinnipeds are more poorly resolved. For instance, the crown pinniped node is a 13-way polytomy, whereas only 5 branches emanate from this node in Trial 12. As in the parsimony tree, *Desmatophoca brachycephala* is sister to *D. oregonensis*. However, the position of desmatophocids is unclear and odobenids are poorly resolved.

Trial 10

The analysis with ordered characters and implied weighting, Trial 10, yielded 1 most parsimonious tree (Figure 2.10) with 150.30 steps. This tree has an adjusted support index of 2.236. This implied weight parsimony tree is very different from any of the previous trials. The basal portion of the tree is a mix of enigmatic clades of early caniforms, but still preserves the monophyly of canids and ursids. Ursids are nested within the paraphyletic musteloids, with *Oaxacagale*, *Lontra*, and *Neovison* notably relegated to the pinniped stem. *"Enaliarctos" bertae* is placed basally, between *Puijila* and *"E." mealsi*, unlike its more crownward placement in other trials. With the exception of phocids and odobenines, the pinniped crown is poorly resolved. *Pinnarctidion rayi* is sister to *Desmatophoca brachycephala*, by contrast to its placement alongside other members of *Pinnarctidion* in prior trials. Desmatophocids form a weakly supported paraphyletic relationship with phocids, contrary to their placement near odobenids in prior trials.

The resampled tree yielded a total bootstrap value of 1740, ranking #11. Basal caniforms are poorly resolved in this tree, maintaining some traditional clades but uniting some unusual

taxa such as *Enhydra* with *Taxidea* + *Gulo*. The pinniped crown is comparatively well resolved, with desmatophocids sister to phocids and most later diverging odobenids forming a monophyletic group.

Trial 11

The analysis with group constraints and implied weights, Trial 11, yielded 1 most parsimonious tree (Figure 2.11) with 128.08 steps. This tree has an adjusted support index of 1.765. Most differences from other implied weight trees occur in the basal portion of the tree, with slight rearrangements of early caniforms compared to Trial 9. Ursids are still nested within musteloids, and *Neovison* and *Lontra* fall along the pan-pinniped branch. The most significant difference in this tree is the sequence of branching of crown pinnipeds. Phocids diverge first, followed by an otariioid clade that also includes desmatophocids. This is more similar to Trials 2, 3, 4, 5, 6, and 8 than to the other implied weight trees, which place otariids as the outgroup to other crown pinnipeds.

The resampled tree yielded a total bootstrap value of 1741, ranking #10. The topology is similar to Trial 9, with higher support but still very limited resolution for most clades. A notable difference from other similar trees is that *Pinnarctidion rayi* is separated from *Desmatophoca brachycephala*.

Trial 12

The analysis with ordered characters, group constraints, and implied weighting, Trial 12, yielded 1 most parsimonious tree (Figure 2.12) with 150.59 steps. This tree has an adjusted

support index of 2.51. Relationships are nearly identical to Trial 10. There are slight differences in the placement of *Subparictis*, some musteloids, some odobenids, and *Eodesmus*.

The resampled tree (Trial 12 Bootstrap) yielded a total bootstrap value of 1967, ranking #9. The topology of this tree is nearly identical to the resampled tree in Trial 10.

Statistical analysis of Bremer support and bootstrap results

A Spearman's Rank Correlation test was conducted to compare Bremer support indices and bootstrap values. When all 12 trials are included, these values are significantly negatively correlated at the .05 alpha level ($r = -0.748$, critical value= 0.587). When the implied weight data (Trials 9-12) are excluded, the correlation is no longer statistically significant, but still shows a negative relationship. One might expect weighted characters to exaggerate Bremer supports because the weights are artificially inflating the steps needed to collapse branches.

Each of the four parameters – ordered characters, group constraints, weighted characters, and implied weights – were tested to determine if their use resulted in a significant difference in support values. The variances of all samples did not differ significantly. The results of a series of t-tests show no significant influence from ordered characters, group constraints, or weighted characters. Implied weighting had a significantly positive effect on Bremer supports ($t = 4.613$, critical value= 2.228), and a significantly negative effect on bootstrap values ($t = -6.649$, critical value= 2.228).

All four parameters were tested by ANOVA to determine if any of the means exceed the normal variation. The Bremer support index ANOVA found no significant difference among the parameter test treatments (F= 1.725, critical value= 3.24). However, the bootstrap value ANOVA identified a weakly significant difference (F= 3.6, critical value= 3.24). Although this test does not indicate which variable is responsible for this difference, the expected culprit would be the implied weights treatments that yielded particularly low bootstrap values.

Discussion 2A: Character parameter manipulations

Ordered characters

Initial study of the effects of ordered characters was mixed or neutral, casting doubt on the usefulness of assuming that evolution proceeds in a linear series as opposed to multi-step leaps (Hauser & Presch, 1991). Ordered character matrices can produce more highly resolved trees, but not necessarily greater congruence, than unordered matrices (Slowinski, 1993). Grand et al. (2013) summarize attitudes about ordering characters that form a morphocline (e.g., a linear series of state transitions such as small-medium-large), pointing out that this practice was commonplace at the advent of computational cladistics but fell out of favor over time. Their simulated results showed that ordered characters lead to greater resolution and lower artifactual effects compared to unordered data, although results based on empirical data were far less consistent (Grand et al. 2013). The aversion to ordered characters may partly stem from the challenge of choosing which characters are suited for such a designation. Early studies (Hauser & Presch, 1991) took a less selective approach, treating all

multistate characters as ordered regardless of suitability. More recently, it is recommended that only the best-suited morphoclinal characters be treated as ordered and the more complex multistate characters be treated as unordered (Slowinski, 1993).

In the present study, ordered characters were carefully selected and applied in Trials 2, 4, 6, 8, 10, and 12. The Bremer support indices and bootstrap values yielded by these trials were slightly, but not significantly, higher than the others. This supports the notion that ordered characters can improve resolution, but are not necessary to produce a well-supported phylogenetic tree.

Positive group constraints

The positive group constraint function favors trees that more closely match a predetermined tree structure (based on molecular data) by treating group membership variables as additional characters that influence tree length. Information about positive group constraints is limited to TNT guide documentation, and it appears this method has not been widely implemented in the systematic paleontological literature. In the current study, group constraints were applied in Trials 3, 4, 7, 8, 11, and 12, a manipulation that had little effect on Bremer support, but did lead to higher support values – albeit insignificantly so – from bootstrap resampling. The tree topology between Trial 6 (no constraints) and Trial 8 (group constraints applied) differs very little, meaning that the constraints had a negligible effect on the tree search. It thus seems the stricter tree constraint method, which uses the 'force =' command, is necessary to enforce well-established relationships among extant taxa.

Weighted characters

Cladists were originally opposed to ad hoc character weighting, but early proponents found support for successive weighting with computer simulation data (Farris, 1969) and suggested explicit criteria for weighting characters only after traditional parsimony methods have failed to resolve a given tree (Wheeler, 1986). Later workers favored equal weighting of ostensibly informative characters selected based on prior knowledge and/or biological assumptions (Sereno, 2007). In the present study, weighted characters had little effect on Bremer or bootstrap support values, and this method may even produce tree topologies (see Trials 5-8) that stray further from those informed by molecular evidence than do unweighted analyses.

Implied weights

Theoretical models using implied weights have been shown to be inconsistent with empirical genetic results, despite producing trees with high consistency indices and support values (Congreve & Lamsdell, 2016). By contrast, other simulations have shown that implied weights parsimony can produce trees closer to a model tree than equal-weights parsimony, maximum likelihood, or Bayesian analyses (Goloboff et al., 2018). The parsimony trees derived from implied weighting – Trials 9, 10, 11, and 12 – differ substantially from those found in the other trials or in previous studies. If implied weights are meant to reduce the signal of homoplastic characters, this goal seems not to have been met in the present analysis. This may be an artifact of poor character sampling, but traditional equal-weight methods seem to handle potential homoplasy just as well as implied weights. Another weakness of implied weighting is that usually only a single most parsimonious tree is identified, obscuring

other potential trees of nearly the same length. The very low bootstrap values yielded by resampling indicate low reliability compared to other methods.

Discussion 2B: Phylogenetic results of non-pinniped caniforms

The relationships of basal caniforms and arctoids vary widely between trial analyses. For instance, some analyses place ursids as sister to canids (Trials 2, 5, 7) or musteloids (Trials 1, 3) rather than as sister to musteloids plus pan-pinnipeds (Trials 6, 8), and some nest pan-pinnipeds within musteloids (Trials 5, 6, 7, 8, 9, 10, 11, 12) rather than as sister to them (Trials 1, 2, 3). These unusual results may indicate that additional characters should be added to the matrix to improve the resolution of basal caniform relationships in future analyses. Below is a reconciliation of the uncertain placements of many basal caniforms, including comparisons to previous studies.

Outgroups

Outgroups must be similar enough to share most homologous features with the target group, but different enough to fall unequivocally outside that group. Choosing a proper outgroup is critical when using programs such as TNT that treat the chosen outgroup as fixed and only search for trees rooted by that group.

Tapocyon robustus, a carnivoramorph often recovered near crown Carnivora (Flynn et al., 2005; Wesley-Hunt & Flynn, 2005; Finarelli, 2008), was chosen as the best outgroup taxon because it lived during the middle Eocene, close in time to the likely origin of carnivorans,

and it is known from relatively complete material (Wesley & Flynn, 2003). *Gustafsonia cognita*, originally in the wastebasket genus "*Miacis*" and sometimes considered an amphicyonid (Tomiya & Tseng, 2016), consistently falls outside the caniform clade in this study and would be another good outgroup candidate.

Canids

Canids are nearly universally considered to be the earliest-diverging extant caniform (Wyss & Flynn, 1993; Flynn et al., 2005; Hassanin et al., 2021), and this is the most frequent result from the present analyses (Trials 6, 8, 9, 10, 11, 12). By contrast, some analyses place canids closer to ursids than to mustelids or pinnipeds (Trials 2, 5, 7). Some even recover a clade that includes canids, ursids, and mustelids, to the exclusion of pinnipeds (Trials 1, 3). Of these conflicting analyses, all but Trial 2 used unordered multistate characters.

Two extant canids (*Canis lupus* and *Urocyon cinereoargenteus*) and three extinct canids (*Epicyon haydeni*, *Enhydrocyon* , and *Hesperocyon*) were included in the analyses. These five taxa were recovered as a monophyletic group in all but Trials 1 & 3 (*Enhydrocyon* recovered closer to amphicyonids) and Trial 4 (part of a basal polytomy). *Temnocyon altigens* and *Lycophocyon hutchisoni*, also included, showed inconsistent affinities with canids or amphicyonids.

Ursids

In all trials, *Ursus*, *Tremarctos*, *Ailuropoda*, and *Kolponomos* form a monophyletic group. This result is expected for the extant taxa, whereas *Kolponomos* has remained enigmatic.

Previous workers regarded *Kolponomos* as an amphicynodontid (Tedford et al., 1994; Hunt, 1998a) or a pan-pinniped (Paterson et al., 2020), but those interpretations are questionable. Amphicynodontids are found to be paraphyletic in this study and others (Cirot & Bonis, 1992; Wang et al., 2005; Finarelli, 2008), and have been diagnosed by largely plesiomorphic characteristics. Pan-pinnipeds are more closely related to musteloids than to ursids, and the similarities they share with *Kolponomos* are most likely convergent. *Kolponomos* shares many characteristics with ursids and is recovered closest to *Ailuropoda* in most analyses.

The position of ursids relative to other arctoids is poorly constrained in this study. Only Trials 6 and 8 resolve ursids in the traditional position of diverging after canids but before musteloids. The other consensus trees ally ursids with canids (Trials 2, 5, 7) or nest them within musteloids (Trials 1, 3, 9, 10, 11, 12). Some studies have found ursids to be sister to (Delisle & Strobeck, 2005), or nested within (Wyss & Flynn, 1993; Spaulding & Flynn, 2012), musteloids. Unlike some previous studies (Flynn et al., 1988; Wyss & Flynn, 1993), none of the consensus trees in this study placed ursids sister to pinnipeds.

Musteloids

Although some morphological studies have found musteloids to be paraphyletic (Flynn et al., 1988; Wyss & Flynn, 1993), the recent consensus supports a monophyletic clade composed of mustelids, procyonids, mephitids, and ailurids (Flynn et al., 2005; Hassanin et al., 2021).

The tendency of *Lontra*, *Neovison*, and other musteloids to appear more closely related to pan-pinnipeds is most likely due to the otter-like nature of the basal pan-pinnipeds

Potamotherium and *Puijila*. Pan-pinnipeds are closely related to musteloids (Finarelli, 2008; Nyakatura & Bininda-Emonds, 2012; Hassanin et al., 2021; Wang et al., 2023), so it is no surprise that they share many characteristics in common. Yet there are a surprising number of convergent features between mustelids and phocids, and between otters and *Potamotherium* and *Puijila*. Most studies focused on pinnipeds consider *Potamotherium* and *Puijila* to be pan-pinnipeds (Paterson et al., 2020; Park et al., 2024), whereas studies focused on musteloid interrelationships tend to place *Potamotherium* within mustelids (Baskin, 1998; Wang et al., 2005; Finarelli, 2008; Ferrusquía-Villafranca & Wang, 2021) The possible explanations for this pattern are: (1) pan-pinnipeds are sister to musteloids, and the shared features between mustelids, *Potamotherium*, and *Puijila* are best explained as plesiomorphies or homoplasy; (2) pan-pinnipeds are nested within musteloids, and the shared features between mustelids, *Potamotherium*, and *Puijila* characterize a more exclusive clade; or (3) *Potamotherium* and/or *Puijila* are incorrectly assigned to Pan-pinnipedia, and should instead be considered mustelids. Hypothesis 2 is only moderately supported in the present analysis and in very few previous studies (Wolsan, 1993), whereas hypothesis 3 disagrees with all present analyses and most prior studies. Therefore, hypothesis 1 is still the most conservative view and is the favored interpretation here.

Discussion 2C: Phylogenetic results of pan-pinnipeds

The following section summarizes the stepwise morphological transitions that occurred from the earliest common ancestor of pan-pinnipeds to the crown clades. Although several robust trees were recovered in our analyses, a single tree must serve as a hypothetical framework on

which to map the synapomorphies of each pan-pinniped clade. One of the maximally parsimonious trees from Trial 4 (see Pan-pinniped Tree) was selected because that analysis yielded the highest overall bootstrap values and this particular tree shows nearly identical pan-pinniped relationships to the also robust Trial 2.

Basal pan-pinnipeds

Several analyses (Trials 1, 2, 3, and a subset of trees in 4) identified *Pachycynodon*, *Allocyon*, *Cephalogale*, and *Amphicticeps* – typically considered more closely related to ursids – as members of the pan-pinniped clade. Although this result is poorly supported, the potential synapomorphies joining these taxa with pan-pinnipeds are discussed below.

The clade including the hypothetical common ancestor of *Pachycynodon* and other pan-pinnipeds is diagnosed by a longer palate with a posteriorly-extended palatal shelf ventral to the choana. The most recent common ancestor of *Allocyon* and later diverging pan-pinnipeds is diagnosed by robust depressions in the basioccipital with tuberosities, prominent mastoid and paroccipital processes, and a medially-deflected M1. The most recent common ancestor of *Cephalogale* and later diverging pan-pinnipeds is diagnosed by antorbital processes constructed from both the maxilla and the frontal sutured in parallel along the orbital rim, and a wider separation of the auditory bulla from the postglenoid process. The most recent common ancestor of *Amphicticeps* and later diverging pan-pinnipeds is diagnosed by slightly enlarged orbits and a more medially placed M2.

Although they are not obviously pinniped-like in appearance, *Potamotherium valletoni* and *Puijila darwini* are consistently supported as part of the pan-pinniped clade in every analysis in this study and in recent literature (Paterson et al., 2020; Everett et al., 2023). Both of these taxa superficially resemble otters and some parsimony trees even recover pan-pinnipeds as nested within mustelids (which has never been supported by molecular evidence), perhaps due to those same similarities. Nevertheless, the synapomorphies discussed below are based on a tree with several branches separating the traditional basal pan-pinnipeds from mustelids.

The clade stemming from the hypothetical common ancestor of *Potamotherium* and later-diverging pan-pinnipeds is characterized by the following synapomorphies. The nasal-frontal suture is more in line with the transverse plane and convoluted, as opposed to the nasals intruding between the frontals. The nasolabialis fossa is deeper with an anterior tuberosity. The postorbital process of the jugal is well-developed. The dorsal surface of the braincase is horizontally flat, as opposed to forming a convex arc. The posterior lacerate foramen is larger than the external auditory meatus. The postglenoid foramen is absent. As in otters, the upper incisors are more posteriorly placed closer to the canines. The M1 is smaller and has lost the postprotocrista. The lower third molar is absent. Only in *Potamotherium* and *Puijila* is the infraorbital foramen triangular and widest at the dorsomedial corner, which, curiously, is convergent with mustelids and unlike the ventromedially wide condition in pinnipedimorphs.

The most recent common ancestor of *Puijila* and later-diverging pan-pinnipeds is diagnosed by a shallower posterodorsal slope of the premaxilla. The sagittal crest is taller and extends farther anteriorly. The palatal process forms a sharp point that extends posteriorly from the

last molar. The epitympanic recess is expanded and the round window is enlarged. P1 is positioned parallel along the toothrow and acquired a narrow lingual cingulum. P2 also has a more expanded lingual cingulum. The lower incisor count is reduced from three to two.

Early Pinnipedimorphs

Pinnipedimorpha, originally coined by Berta (1991) and redefined by Everett et al. (2023), are those pan-pinnipeds that display traits such as flippers which are unmistakably tied to an aquatic lifestyle. Taxa only known from the skull may be diagnosed by the reduced cusps and expanded lingual cingulum of M1. Beginning with the first discovered and most completely known taxon, "*Enaliarctos*" *mealsi* (Mitchell & Tedford, 1973), early pinnipedimorphs acquired unique traits that set them apart from other arctoids, many of which are retained in pinnipeds. These organisms' sensory, locomotory, masticatory, and physiological modifications seem tied to functional adaptations to aquatic environments. The following discussion highlights the phylogenetic relationships of each early pinnipedimorph and presents the sequence of character state transitions that occurred in the lineage leading to pinnipeds, based on the synapomorphies of each corresponding node.

"*Enaliarctos" mealsi* is recovered as the earliest-diverging pinnipedimorph in most trials, although some analyses place *"E." mitchelli* (Trials 6, 8) or *"E." bertae* (Trials 9, 10, 11, 12) before it. Originally, *"E." mealsi* was considered an intermediate form between ursoids and otarioid pinnipeds (Mitchell & Tedford, 1973), but subsequent work demonstrated that "*Enaliarctos*" is a close relative of a monophyletic pinniped clade (Wyss, 1987; Berta & Wyss, 1994). As new species of "*Enaliarctos"* were described, *"E." mealsi* was upheld as

the earliest to diverge, although Barnes (1979) did not use a cladistic framework and Berta (1991) assumed "*Enaliarctos"* species to form a monophyletic group. Few subsequent studies have reassessed the interrelationships of "*Enaliarctos"*, but some identified *"E." mealsi* as possibly the earliest-diverging pinnipedimorph alongside *"E." barnesi* (Paterson et al., 2020) or as having diverged later than *"E." tedfordi*, *"E." barnesi*, or *"E." emlongi* (Everett et al., 2023). Although the branching sequence of "*Enaliarctos*" species is clearly sensitive to sampling and model assumptions, *"E." mealsi* seems to be a reasonable representative of the earliest-diverging pinnipedimorph.

Pinnipedimorphs, represented here by the common ancestor of "*Enaliarctos" mealsi* and all later-diverging pan-pinnipeds, are characterized by the following synapomorphies. The triangular infraorbital foramen is widest at its medioventral corner. The pseudosylvian sulcus is strongly developed. The anterior margin of the braincase became box-shaped, with a sharp corner where it joins the interorbital region and another corner at the anterolateral edge. The auditory bulla is largely continuous with the medial edge of the basioccipital. The tube surrounding the external auditory meatus has been lost. The basal whorl of the scala tympani is enlarged. The upper third premolar's lingual cingulum is expanded. The first upper molar has several innovations, including reduction from three to two roots (the distal of which is bilobed), expansion of the lingual cingulum, loss of the protocone, and narrowing of the parastylar shelf. The lower premolars bear prominent mesial paraconids. The lower first molar has a lingually placed hypoconid. The humerus bears an enlarged, gradually terminating deltopectoral crest, and has lost the entepicondylar foramen. The distal condyle of the femur is significantly inclined medially. The tail is greatly shortened.

"Enaliarctos" barnesi (Berta, 1991) is recovered in several trials as the second pinnipedimorph to diverge, which is reminiscent of its position in Berta's (1991) original tree – though the present topology shows "*Enaliarctos*" as paraphyletic whereas previously it was considered monophyletic. Other trials find *"E." barnesi* to be part of a clade including *"E." emlongi* and *"E." tedfordi* that diverged after *"E." mealsi*. Paterson (2020) found *"E." barnesi* to be one of the earliest diverging forms, alongside *"E." mealsi*. The most recent common ancestor of *"E." barnesi* and later-diverging pinnipedimorphs lost the lacrimal foramen and the parastyle on P4. The protocone shelf on P4 is expanded lingually. The jugal portion of the zygomatic is arched much less strongly dorsoventrally, possibly due to a shift away from mastication and a reduction of the masseter muscles. The pterygoid strut has a concave, rather than flat, lateral margin. The angular process of the mandible is directed medially.

"Enaliarctos" tedfordi (Berta, 1991) is the third pinnipedimorph to diverge in this analysis, although some results place it in a clade with *"E." barnesi* and *"E." emlongi*. Previous work placed *"E." tedfordi* within a paraphyletic grade diverging between *"E." emlongi* and *"E." mitchelli* (Paterson, 2020). The common ancestor of *"E." tedfordi* and later-diverging pinnipedimorphs evolved much larger orbits.

"Enaliarctos" emlongi (Berta, 1991) is the fourth pinnipedimorph to diverge, but as noted previously, it could instead belong to an offshoot clade that includes *"E." barnesi* and *"E." tedfordi*. In a recent study, *"E." emlongi* was somewhat bafflingly resolved as sister to the

littoral ursid *Kolponomos* within a paraphyletic "*Enaliarctos*" grade (Paterson, 2020). The present study finds no evidence for such a connection. The clade including *"E." emlongi* and other later diverging pinnipedimorphs is diagnosed by a supraorbital process positioned more posteriorly, equidistant between the anterior orbital margin and the anterior expansion of the braincase, which probably also corresponds to larger eyes. The stylomastoid foramen and hyoid fossa of the auditory region are separated. The auditory ossicles are also enlarged (see Berta, 1991), though not to the extent of phocids and odobenines.

"Enaliarctos" mitchelli (Barnes, 1979; Berta, 1991) is known from two described specimens which are resolved in this analysis as diverging sequentially along the paraphyletic "*Enaliarctos*" grade. For the sake of simplicity, both specimens are lumped in this discussion, but see Chapter 1 for a more detailed taxonomic examination of this species. Previously, *"E." mitchelli* was found to diverge between *"E." tedfordi* and *Pteronarctos goedertae* (Paterson, 2020). The most recent common ancestor of *"E." mitchelli* and later-diverging pinnipedimorphs is diagnosed by a specialized zygomatic arch wherein the ventral portion of its anterior root is ventrally-placed and flatter, the highest point of dorsal arching is at the postorbital process of the jugal, and the orbital portion of the zygoma forms over one-third of its length. Members of this clade also have a reduced pseudosylvian sulcus.

"Enaliarctos" bertae is the last "*Enaliarctos*" species to diverge along this paraphyletic grade. Some analyses recover it as sister to *Pinnarctidion*, whereas others indicate it diverged even earlier than *"E." mealsi*. This uncertainty likely arises from its missing dentition and posterior portion of the cranium. The most recent common ancestor of *"E." bertae* and later

diverging pan-pinnipeds is diagnosed by a palatal process that is expanded posterolaterally as a shelf. P4 is reduced from three roots to two (the distal of which is bilobed). M1 is oriented parallel to the premolar row as opposed to being deflected medially.

All three recognized species of *Pinnarctidion* (Barnes, 1979; Berta, 1994a; Everett et al., 2023) form a monophyletic group, diverging from other pan-pinnipeds between the "*Enaliarctos*" grade and *Prototaria*. *Pinnarctidion bishopi* was initially considered ancestral to *Allodesmus* (Barnes, 1979). Early cladistic analyses resolved the genus within the phocoid branch of crown pinnipeds, often closely related to desmatophocids (Berta, 1991; Berta, 1994a; Berta & Wyss, 1994). More recent analyses place *Pinnarctidion* outside the crown group, often diverging later than *Pteronarctos* (Paterson, 2020; Everett et al., 2023). Apparently, the inclusion of *Prototaria*, *Proneotherium*, and *Pteronarctos* alongside *Pinnarctidion* changes the polarity of some characters such that *Pinnarctidion* diverges first. The common ancestor of *Pinnarctidion* plus later-diverging pinnipedimorphs is marked by modifications to the palate and dentition. The posterior border of the zygomatic root joins the palate more posteriorly than in earlier diverging taxa, at the level of, or posterior to, M2. The embrasure pits between P4 and M1 are shallower. The metacone of P4 is reduced, and the protocone is posteriorly placed.

The ancestor of the *Prototaria* clade plus later diverging pinnipedimorphs is marked by a posteriorly tapering interorbital constriction, as opposed to being of even thickness along its length. The ancestor of the *Proneotherium* clade plus later diverging pinnipedimorphs has a shortened palate, potentially tied to the simplification of the dentition and a further shift away

from mastication. The clade composed of *Pteronarctos* plus later diverging pinnipedimorphs is diagnosed by nasals that intrude between the frontals. The final node before crown pinnipeds has only a single, undescribed stem representative, LACM 124686, which is labeled *Neotherium sp*. This node is diagnosed by a notched palatal floor ventral to the choana and a reduced paroccipital process.

Crown pinnipeds

Pinnipedia includes all descendants of the common ancestor of extant phocids, otariids, and odobenids. Although evidence for pinniped monophyly is strong, the sequence of branching among the three families is still unclear. Some of the present analyses could not unequivocally resolve the polytomy at the pinniped crown node, but those with sufficient resolution tend to separate phocids from otarioids – otariids plus odobenids (Trials 2, 3, 4, 5, 6, 8, 11). This interpretation is supported by recent work based on morphological (Boessenecker & Churchill, 2018; Paterson et al., 2020; Everett et al., 2023; Park et al., 2024) and molecular (Arnason et al., 2006; Nyakatura & Bininda-Emonds, 2012; Hassanin et al, 2021) evidence.

Pinnipedia is diagnosed by the following cranial and dental synapomorphies: The antorbital process is constructed strictly from the maxilla, as opposed to the frontal or along the suture of the two elements. The lacrimal foramen is lost and the lacrimal bone is fused to the maxilla. The pseudosylvian sulcus is reduced to a shallow impression rather than a deep groove. No embrasure pits occur on the palate between P4 and M1, signifying a complete

loss of carnassial function. P3 has only two simple roots, making the tooth narrow or conical with very limited lingual cingula.

In every analysis, phocids are the best-supported clade of pinnipeds. Even the earliest taxa, *Devinophoca* and *Noriphoca*, which retain many plesiomorphic traits, are firmly upheld as phocids. The distinctive characteristics of this clade include: the posterior extension of the premaxilla sutures with less than half the length of the nasal. The zygomatic arch is widest anterior to the glenoid fossa, rather than adjacent to it. The jugal sutures with the maxilla via an anterodorsal splint; the anteroventral splint is lost. The alisphenoid is diminished to a narrow groove. The ventral floor of the basioccipital is narrower than the flanking auditory region, and the depressions for the rectus capitis muscles have been lost. The ventral surface of the mastoid process is more bulbous and convex. The auditory bulla is largely composed of the caudal entotympanic, and an external auditory tube is present. The basal cochlear whorl is transversely, rather than posterolaterally, directed. The toothrow is more strongly divergent and the palate is more strongly arched transversely than in other pinnipeds. The first premolar is offset medially relative to the canines. The base of the coronoid process of the mandible is anteroposteriorly short and the mandibular condyle is elevated above the level of the toothrow. The tibia and fibula are fused proximally. The astragalus bears a long, caudally-directed calcaneal process.

Phocinae includes most of the extant seals that occupy the Northern Hemisphere, represented here by *Phoca, Cystophora,* and *Erignathus*. This clade can be diagnosed by the following synapomorphies: The zygomatic root of the maxilla is more dorsally placed. The sagittal and

nuchal crests are indistinct. The large auditory bulla underlaps the basioccipital. The first premolar has no cingular heel. The P4 parastyle is absent. The supraspinous fossa of the scapula is smaller than the infraspinous fossa. The distal end of the large deltopectoral crest of the humerus terminates abruptly. The humerus has an entepicondylar foramen, a reversal of its absence in most other pinnipedimorphs. A distally-projecting ledge occurs on the cuneiform, similar to the condition in odobenids. The "counterpart" of phocines, the monachines, have no unambiguous synapomorphies and retain more plesiomorphic characters.

The most robust analyses find that the remaining pinnipeds – otariids, odobenids, and desmatophocids – are united in an otarioid clade. A pairing of otariids and odobenids is the current consensus view, but the inclusion of desmatophocids is more controversial. Otarioids are diagnosed by an uninflated auditory bulla, another reversal from the moderately inflated bulla of earlier pinnipedimorphs. The P4 and M1 lack parastyle cusps. The lower premolars lack mesial paraconid cusps. And the mandibles have a genial tuberosity positioned at, or posterior to, the level of p3.

The otariids are well-supported as a monophyletic group (see Fig. 2.7). They are diagnosed by a convoluted naso-frontal suture. They have prominent antorbital and supraorbital processes. The sagittal crest is pronounced. The basioccipital has depressions for insertion of the rectus capitis muscle with distinct tuberosities. The hypoglossal foramen is closely associated with the posterior lacerate foramen. The posterior carotid canal is posteriorly placed, opening into the same fossa as the posterior lacerate foramen at the posterior wall of

the bulla. The epitympanic recess is small. The P3 lingual cingulum is narrow, and P4 has lost the protocone.

Odobenids form a monophyletic group but with weaker branch support than seen in phocids or otariids. The earliest-diverging odobenid, *Neotherium*, has a very low relative Bremer support of 6 (on a scale of 0-100), and many other branches have scores of less than 50. Notably, odobenids are found to include desmatophocids yet exclude *Prototaria* and *Proneotherium*. This alternate interpretation of the odobenid clade is diagnosed by several features of the cranium and tarsal bones. The antorbital process is made up of both the maxilla and the frontal with their suture oriented perpendicular to the medial edge of the orbit. The supraorbital process is closer to the anterior margin of the orbit than to the braincase. The palatal shelf ventral to the posterior choana is rounded. The pterygoid struts are very broad and bear posterolateral processes. The tympanic bulla contacts the postglenoid process. The calcaneal tuber projects medially rather than parallel to the long axis, and the astragalus has a short caudally-directed calcaneal process. A slightly more exclusive clade unites the desmatophocids with the later-diverging odobenids. In this group, the lateral process of the palate is expanded as a broad shelf, and the I3 is much larger than the other incisors and shaped like a canine.

In a majority of the analyses that produce well-resolved trees, desmatophocids are most closely related to, or nested within, Odobenidae. Desmatophocids were traditionally considered otarioids (Mitchell, 1968; Barnes, 1989), but now are typically recovered closer to phocids (Berta & Wyss, 1994; Deméré & Berta, 2002; Boessenecker & Churchill, 2018).

This incongruity is probably explained by different sampling of characters or taxa across different studies. Desmatophocids are diagnosed by the following synapomorphies: The premaxilla contacts the nasal along less than half of its length. The orbits are more than 20% of the total length of the cranium. The infraorbital foramen is circular–rather than the triangular ventromedial excavation seen in most other pinnipedimorphs. The articulation of the squamosal and jugal is mortised, and the squamosal is dorsoventrally much broader than the jugal. The squamosal fossa is divided. The sagittal crest extends farther anteriorly into the interorbital region. The palate and toothrows are divergent. And the epitympanic recess is greatly enlarged.

The relationships of the remaining odobenids, which may be called Neodobenia (sensu Magellanes et al., 2018), are well-supported and agree closely with other studies (Boessenecker et al., 2024). Neodobenids are diagnosed by the following synapomorphies. The jugal and squamosal are both dorsoventrally broad. The basioccipital bears depressions for insertion of the rectus capitis muscle with distinct tuberosities. The incisors are more posteriorly placed, near or in line with the canines. The canines lack a crista along their posterior edge, and the lower m1 is absent. With the exception of *Osodobenus*, this clade can be split into the dusignathines (Mitchell, 1968) and the true walruses, or odobenines (Mitchell, 1968). The dusignathines have prominent nuchal and sagittal crests. The more inclusive Odobeninae includes *Aivukus*, *Protodobenus*, and Odobenini. In this clade, the premaxilla contacts the nasal along less than half of its length, the orbital vacuities are present and placed more posteriorly than in other pinnipeds, the sagittal crest is lost, the caudal entotympanic contributes significantly to the auditory bulla, and the P3 lingual

cingulum is absent. The most restrictive walrus clade, the Odobenini (Deméré, 1994b), includes *Alachtherium*, *Valenictus*, and *Odobenus*. In this clade, the premaxilla is steeply sloped posterodorsally; the interorbital constriction is nearly as thick at its anterior and posterior ends; the posterior border of zygomatic root of maxilla joins the palate level with or directly posterior to M1; the palate is strongly arched in the transverse plane; the canines are tusk-like; and the mandibular condyle is elevated above the plane of the toothrow.

Pinniped higher order relationships

The relationships among the extant pinniped families agree well with the current consensus, which holds that phocids are basal to otarioids (Delisle & Strobeck, 2005; Flynn et al., 2005; Higdon et al., 2007; Finarelli, 2008; Paterson et al., 2020; Park et al., 2024). Because molecular evidence offers exceptional resolution of the phylogeny of phocids (Davis et al., 2004) and otariids (Wynen et al., 2001; Yonezawa et al., 2009), those details are not reviewed here. However, the positions of fossil phocids and otariids are worth noting.

The earliest-diverging phocids sampled here are *Devinophoca claytoni* (Koretsky & Holec, 2002), *Noriphoca gaudini* (Dewaele et al., 2018), *Piscophoca pacifica* (de Muizon, 1981), and *Acrophoca longirostris* (de Muizon, 1981). *Devinophoca claytoni*, known from an incomplete yet fairly well-preserved cranium from the middle Miocene of Slovakia, has previously been resolved as the earliest-diverging phocid (Koretsky & Holec, 2002; Paterson et al., 2020; Park et al., 2024), though others recover it as a stem-phocine (Dewaele et al., 2018). It possesses many of the cranial features expected of a phocid, but its dentition is more primitive with a triple-rooted M1, suggesting that homodonty evolved independently in

phocids and otarioids. *Noriphoca*, known from an incomplete cranium from the early Miocene of Italy, is another contender for the earliest-diverging phocid (Dewaele et al., 2018) or the earliest monachine (Park et al., 2024). *Piscophoca* and *Acrophoca*, both from the late Miocene of Peru, are typically considered monachines (Dewaele et al., 2018; Paterson et al., 2020; Park et al., 2024). This result is generally supported here, yet in some analyses *Piscophoca* diverges before the common ancestor of phocines and monachines.

The fossil otariids sampled here include *Thalassoleon mexicanus* (Repenning & Tedford, 1977), *Pithanotaria starri* (Kellogg, 1925), and *Callorhinus gilmorei* (Berta & Deméré, 1986). It should be noted that the poorly-known *Eotaria* (Boessenecker & Churchill, 2015; Velez-Juarbe, 2017) is likely the oldest known otariid, but it was excluded from this analysis. *Thallasoleon* and *Pithanotaria*, both known from the late Miocene, are supported as the earliest otariids. *Callorhinus gilmorei* is always recovered as an otariid, but is never sister to *C. ursinus*.

The most surprising result among fossil pinnipeds is that desmatophocids – typically allied with phocids (Berta & Wyss, 1994; Deméré & Berta, 2002; Boessenecker & Churchill, 2018) – are recovered as a monophyletic clade sister to, or nested within, odobenids. Desmatophocids are only sister to phocids in two of the implied weight trials (Trials 9, 10) and none others. Previous studies have considered desmatophocids to be otarioids (Mitchell, 1968; Barnes, 2007; Furbish, 2015), but few have concluded that they are closest to odobenids (Barnes, 1989). Interestingly, functional studies have found that the desmatophocid *Allodesmus* was probably a forelimb swimmer like most otarioids, rather than

a hindlimb swimmer like phocids (Bebej, 2009; Pierce et al., 2011). Modern *Odobenus* predominantly uses its hindlimbs for propulsion while engaging in a head-down posture for benthic feeding (Gordon, 1983), but little is known about the locomotion of early odobenids.

Alternative placement of *Prototaria* and *Proneotherium*

While many of our results agree closely with those of previous workers, notable exceptions include the affinities of *Prototaria* and *Proneotherium*, which were previously considered early otariids (Barnes, 1989) or odobenids (Deméré, 1994b; Kohno et al., 1994; Deméré & Berta, 2001; Boessenecker & Churchill, 2013; Tanaka & Kohno, 2015; Magellanes et al., 2018; Biewer et al., 2020; Boessenecker et al., 2024). Nearly every analysis herein places these two taxa outside of crown pinnipeds, and sometimes within a clade that includes *Pinnarctidion* and *Pteronarctos*. This should not come as a surprise considering previous workers have noted that *Prototaria* and *Proneotherium* are "enaliarctine"-like, lack many of the derived features of odobenids, and have features that, though initially attributed to odobenids, are in fact plesiomorphic (Deméré, 1994b; Kohno et al., 1994; Deméré & Berta, 2001; Boessenecker & Churchill, 2013). Unfortunately, these studies generally sampled very few outgroups when testing the relationships of early odobenids. Some even neglected to include any other crown pinniped lineages in their final analyses (Kohno et al., 1994; Deméré & Berta, 2001), obscuring whether *Prototaria* and *Proneotherium* are members of the crown group. The relatively limited matrices used in those studies favored characters that are diagnostic of odobenids, and this may have also led to biased results. Recent studies that applied only minor modifications to the character matrix from Boessenecker & Churchill (2013) have expectedly reaffirmed prior results (Tanaka & Kohno, 2015; Magellanes et al.,

2018; Biewer et al., 2020). Boessenecker et al. (2024) provided a significant update to their character-taxon matrix, which resulted in a very robust phylogeny of neodobenids but garnered meager support for the branches near the base of the pinniped clade.

Neotherium complicates this story because, in the present analysis, it is variably resolved as either one of the earliest-diverging odobenids or barely outside of Pinnipedia. *Neotherium* retains many plesiomorphic features in common with *Proneotherium*, leading some authors to consider the two to be sister taxa (Repenning & Tedford, 1977). The most notable difference is that *Neotherium* lost the antorbital and supraorbital processes, nasolabialis fossa, lacrimal foramen, and pseudosylvian sulcus. The latter three features are also absent in most crown pinnipeds, and *Neotherium* possesses numerous odobenid synapomorphies, so it is most plausibly an early odobenid.

Looking more closely at the synapomorphies that diagnose odobenids, we suggest amendments to the traditional view. Most early pinnipedimorphs have an antorbital process constructed from both the frontal and the maxilla, but in odobenids the fronto-maxillary suture runs perpendicularly from the lateralmost point of the process to the edge of the orbit (Deméré & Berta, 2001). The broad pterygoid strut with distinct posterolateral process – often attributed to odobenids (Boessenecker & Churchill, 2013) – is also seen in all species of *Pinnarctidion*, but not in *Proneotherium*, *Archaeodobenus*, or *Titanotaria*, so this is not an unequivocal odobenid synapomorphy. The auditory bulla appears to contact the postglenoid process in all odobenids, starting with *Neotherium*, although this is also present in *Desmatophoca oregonensis*, *Allodesmus*, *Mirounga*, and *Otaria*, so it is not walrus-specific.

We do not observe the tympanic bulla contacting the postglenoid in *Proneotherium*, contrary to some previous studies (Deméré & Berta, 2001; Boessenecker et al., 2024). Some authors report that the bony tentorium is appressed to the petrosal in odobenids only (Kohno et al., 1994; Boessenecker & Churchill, 2013), but this character should be examined more closely in non-odobenids before it can serve as a reliable synapomorphy. The particular tarsal morphology of odobenids is challenging to constrain phylogenetically due to how rarely such elements are preserved. The short, caudally-directed calcaneal process of the astragalus is very similar in *Proneotherium*, *Neotherium*, and *Imagotaria*, but differs significantly from the long process present in phocids. The medially-directed calcaneal tuber is also shared by *Proneotherium* and odobenids. Unfortunately, we can only compare these tarsals to those of "*Enaliarctos*" *mealsi* (Berta et al., 1989), a very early-diverging pinnipedimorph that lacks the above tarsal modifications, but without more postcranial material from taxa closer to the crown we can only tentatively infer that these tarsal features are odobenid synapomorphies rather than symplesiomorphies.

Conclusion 2

All of the trial analyses generated consensus trees that disagree with the majority of molecular phylogenetic studies, so finding the interpretation will rely on congruence among different methods. The most unusual result is that pan-pinnipeds are placed within a paraphyletic musteloid clade in several analyses (Trials 5-12). As discussed above, this is likely an artifact of plesiomorphic or convergent similarities between mustelids and *Potamotherium* and *Puijila*, and that we should still consider musteloids and pan-pinnipeds to be distinct clades. The consistency with which pan-pinnipeds are allied with musteloids,

rather than with ursids, reaffirms the results of recent studies (Delisle & Strobeck, 2005; Flynn et al., 2005; Higdon et al., 2007; Finarelli, 2008; Paterson et al., 2020; Park et al., 2024).

The "stem" portion of the pan-pinniped clade consists of *Potamotherium*, *Puijila*, a paraphyletic grade of "*Enaliarctos*," and a variable sequence of *Pinnarctidion*, *Pteronarctos*, *Prototaria*, and *Proneotherium*. In a few analyses, *Pachycynodon*, *Allocyon*, *Cephalogale*, and *Amphicticeps* are identified as pan-pinnipeds, but it seems more likely that these taxa are basal arctoids due to their plesiomorphic basicranium, or closer to ursids due to their robust dentition.

The relationships among crown pinnipeds are largely consistent with recent studies (Delisle & Strobeck, 2005; Flynn et al., 2005; Higdon et al., 2007; Finarelli, 2008; Paterson et al., 2020; Park et al., 2024), with otariids and odobenids forming a clade (otarioids) to the exclusion of phocids. Perhaps the most unexpected result was that desmatophocids were recovered as sister to odobenines. Some of the implied weight analyses (Trials 9, 10, 12) argue for a different arrangement, in which otariids form half the basal pinniped dichotomy, and odobenids, desmatophocids, and phocids form the other.

Despite agreement among previous authors that *Prototaria* and *Proneotherium* are early odobenids, current evidence suggests that they may instead be stem-pinnipeds. This hypothesis is supported by the many plesiomorphies these taxa share with other early pinnipedimorphs such as *Pinnarctidion* and *Pteronarctos*. Although they share features in

common with such bona fide early odobenids as *Neotherium* and *Imagotaria*, those similarities might be better explained as plesiomorphic rather than apomorphic to odobenids. Most strikingly, *Prototaria* and *Proneotherium* retain nasolabialis fossae, lacrimal foramina, and pseudosylvian sulci, which are typically thought to have been lost prior to the common ancestor of pinnipeds. *Proneotherium* also retains plesiomorphic dental characters that have been lost in otarioids. The exclusion of *Prototaria* and *Proneotherium* from Otarioidea and Pinnipedia requires a more detailed examination of all purported early odobenid specimens, a task beyond the scope of this study. Even if this hypothesis does not stand up to scrutiny, it highlights the potential for more comprehensive stem-group sampling to reveal new hypotheses about the origins of various clades.

Figures 2

Figure 2.1. Trial 1

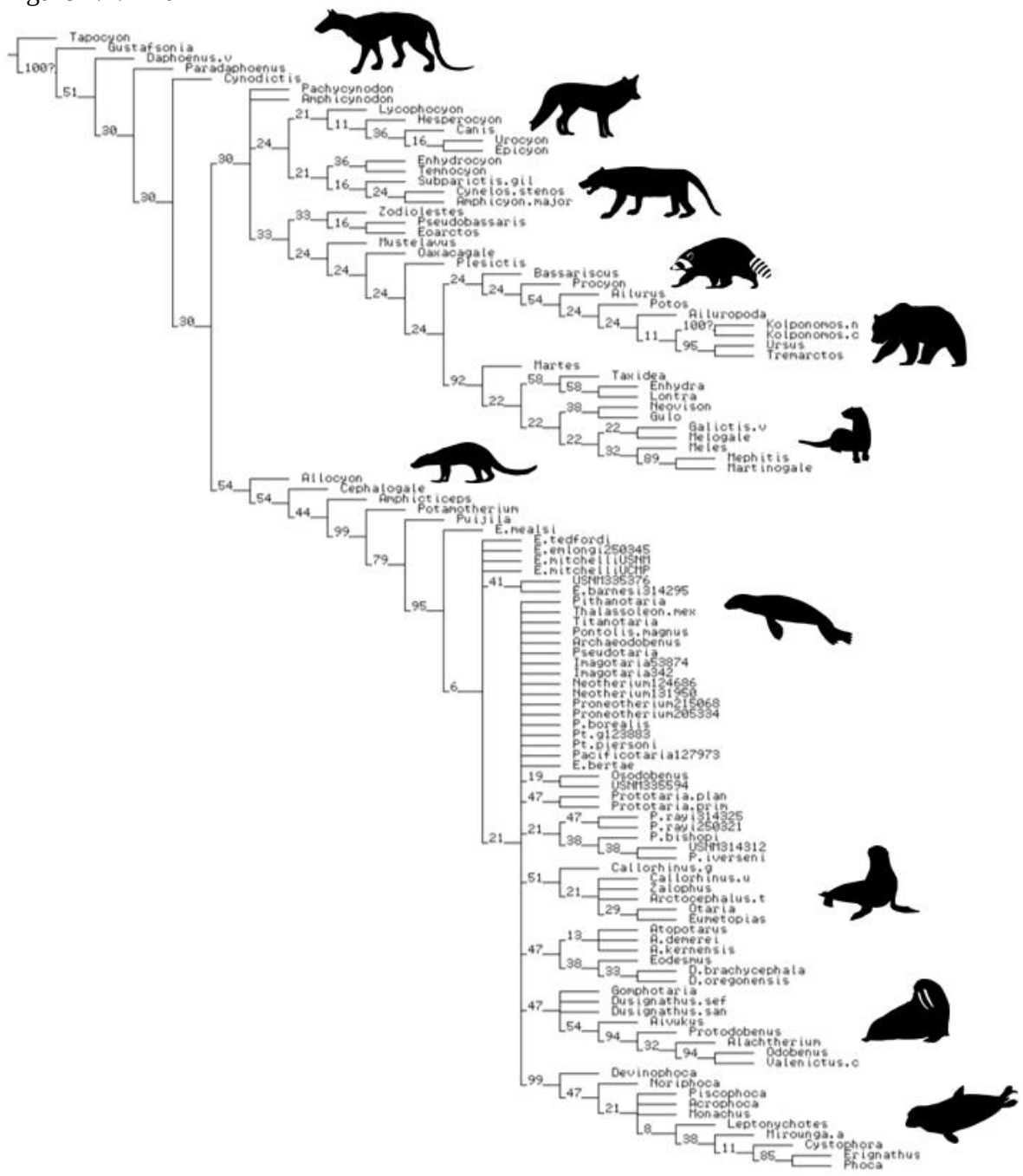

Figure 2.2. Trial 2

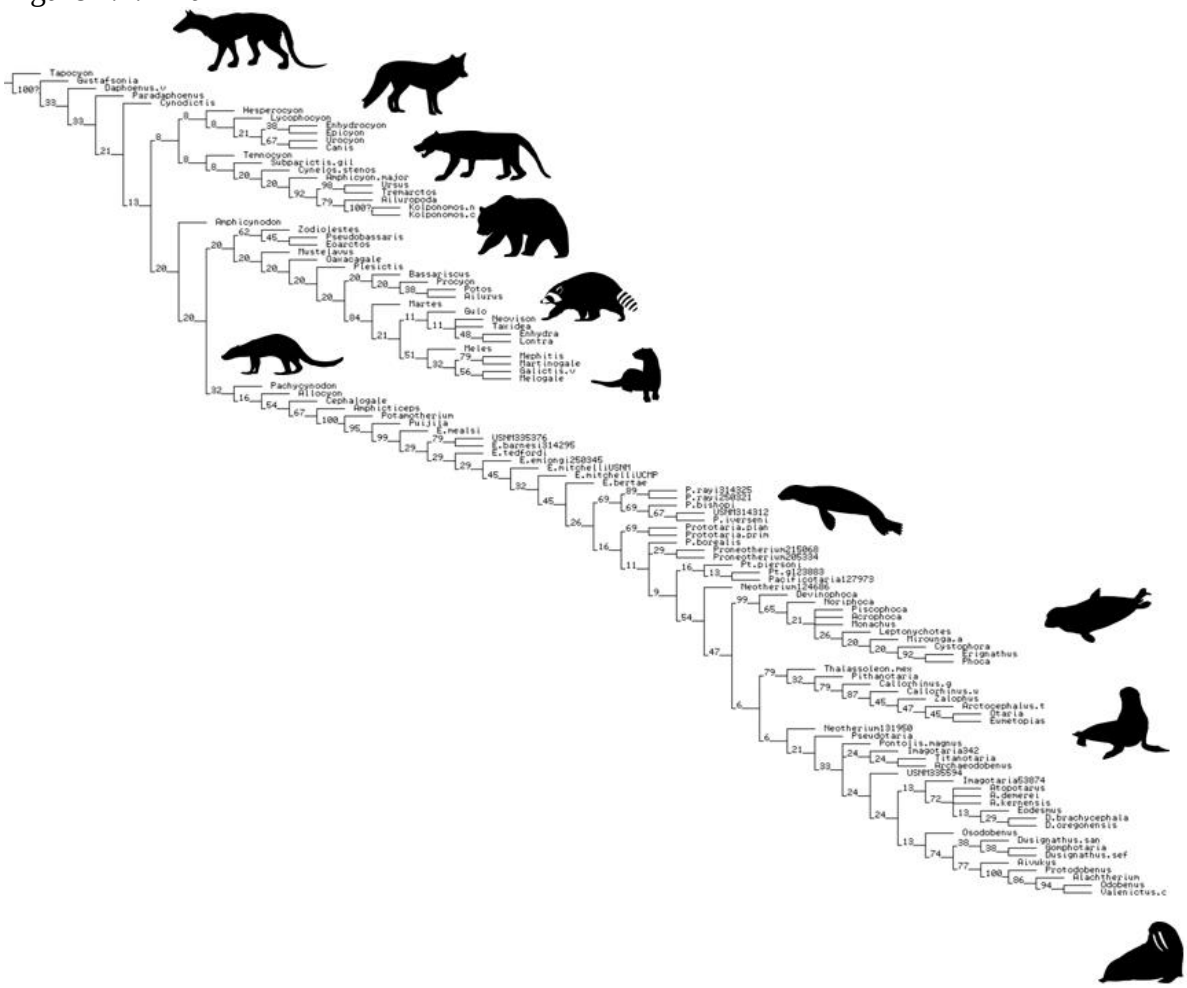

Figure 2.3. Trial 3

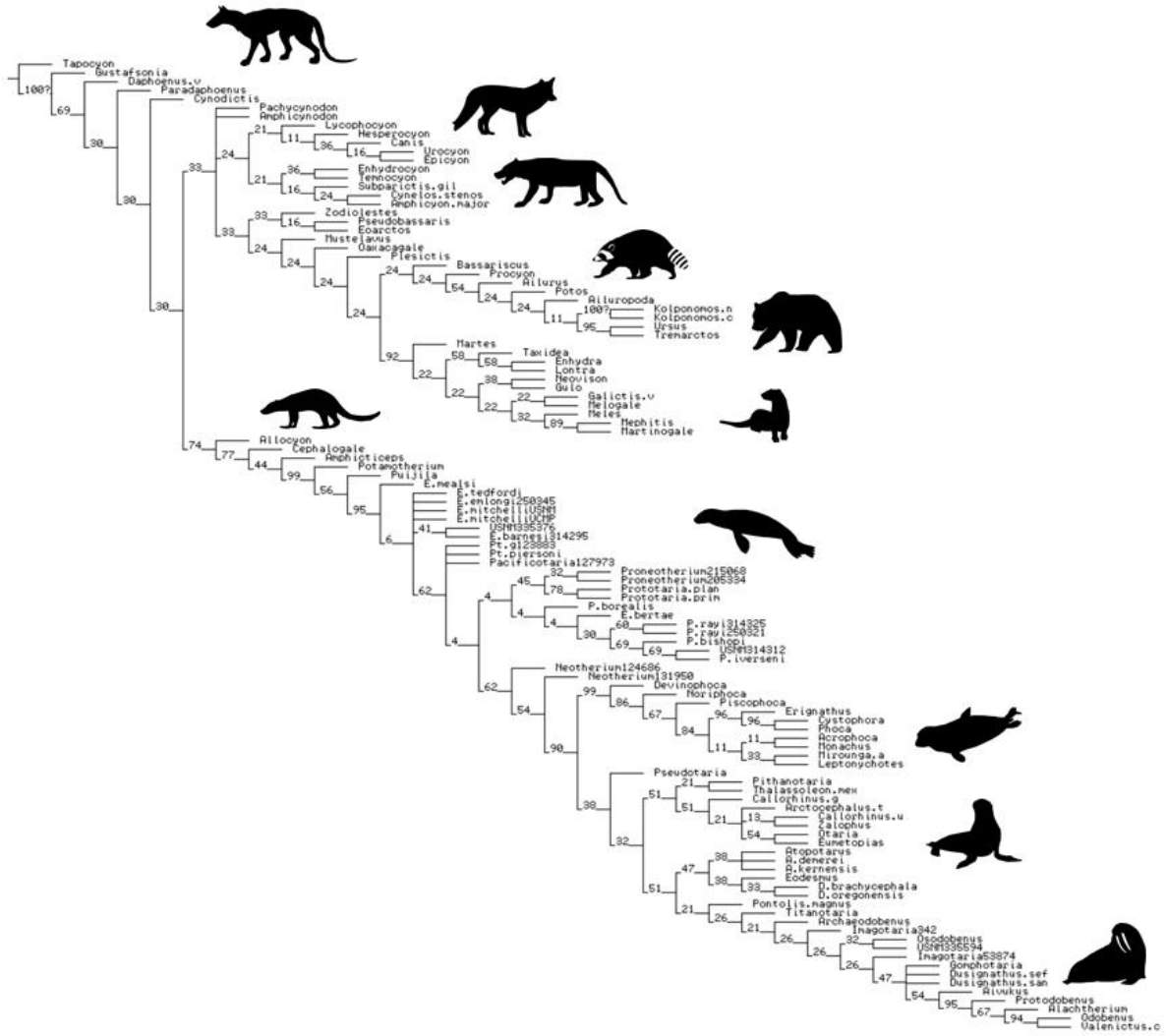

Figure 2.4. Trial 4

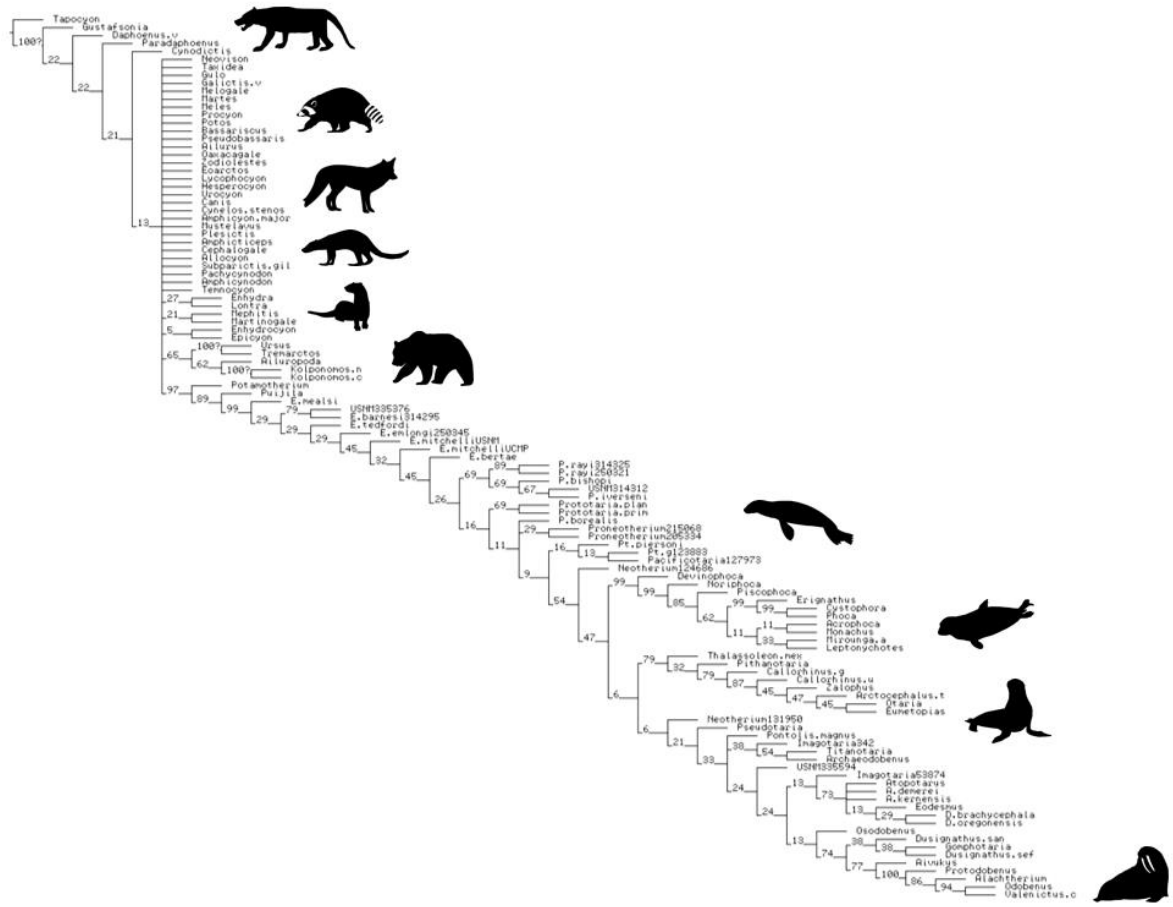

Figure 2.5. Trial 5

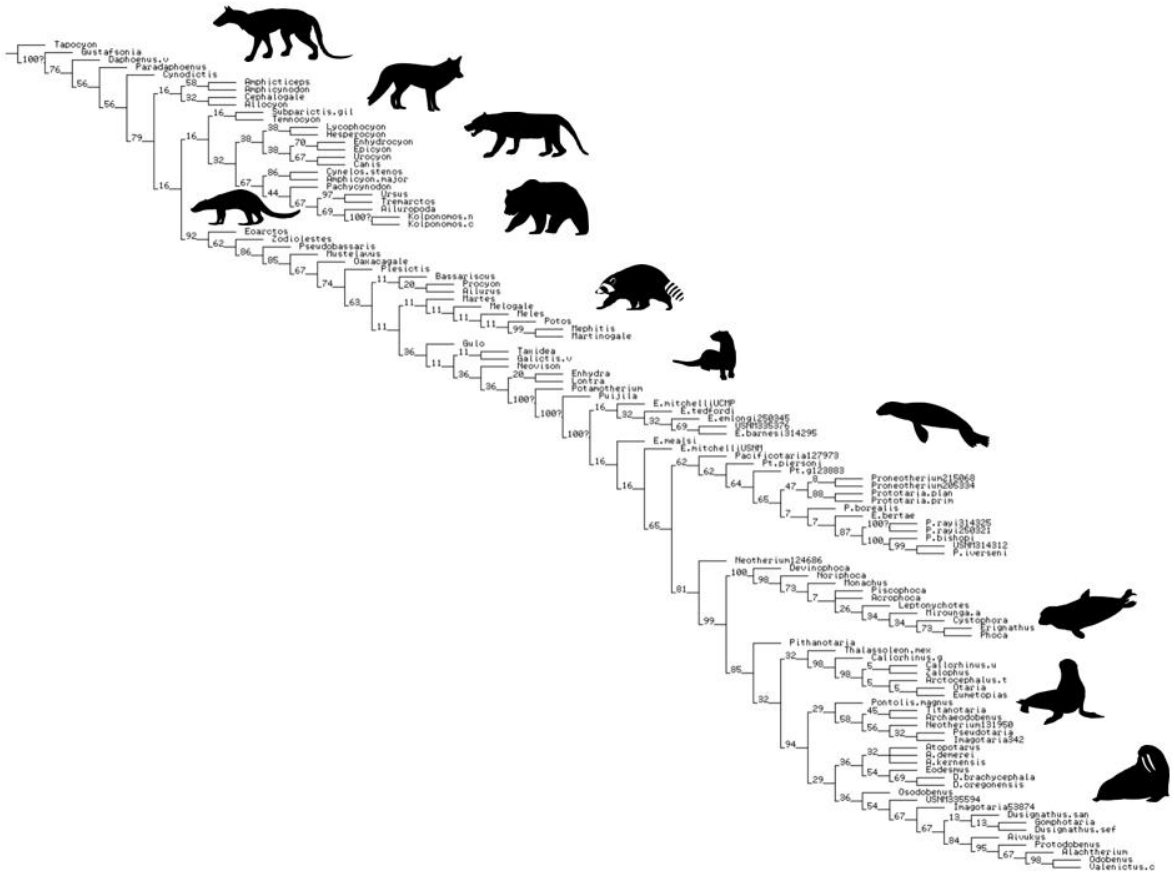

Figure 2.6. Trial 6

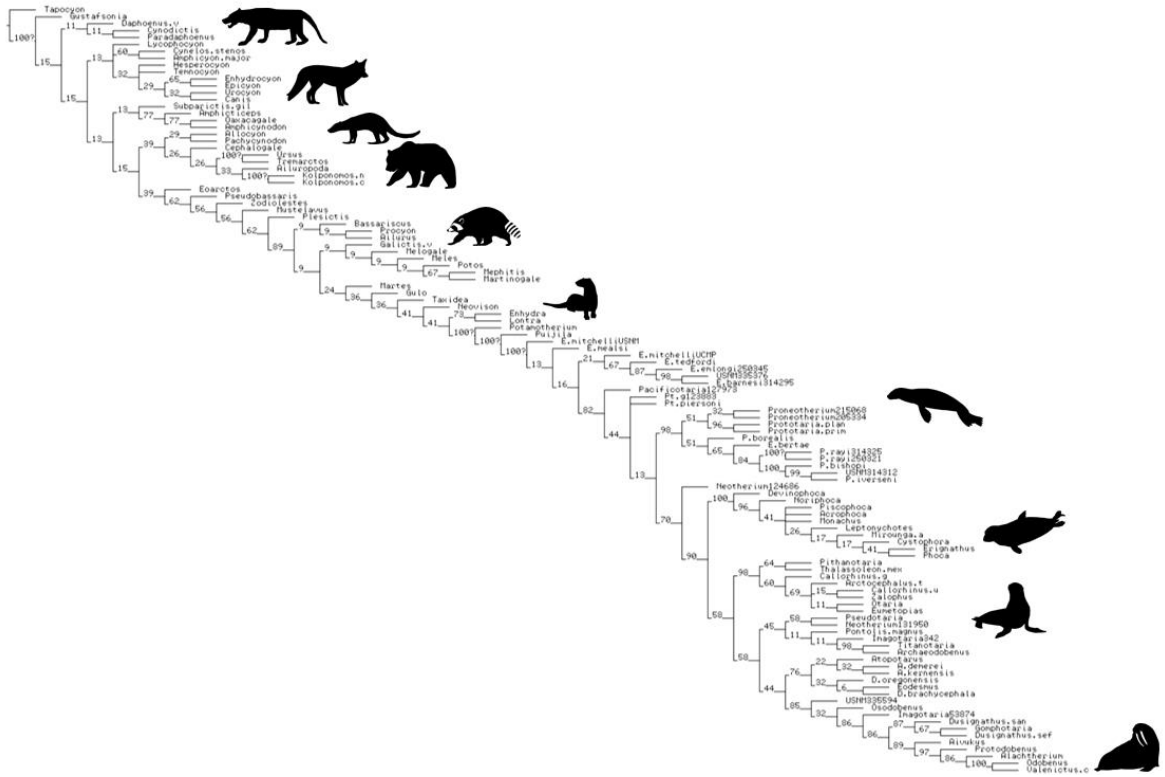

Figure 2.7. Trial 7

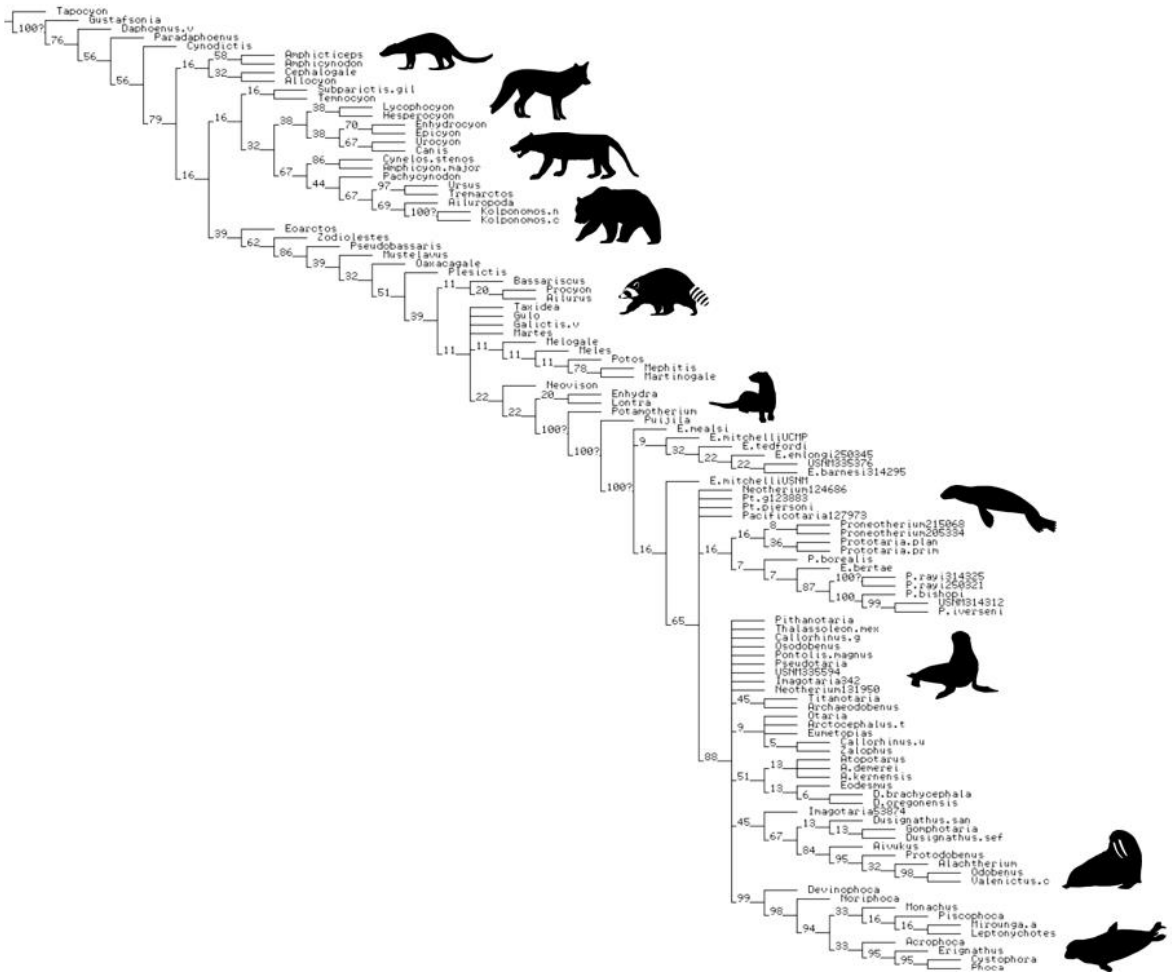

Figure 2.8. Trial 8

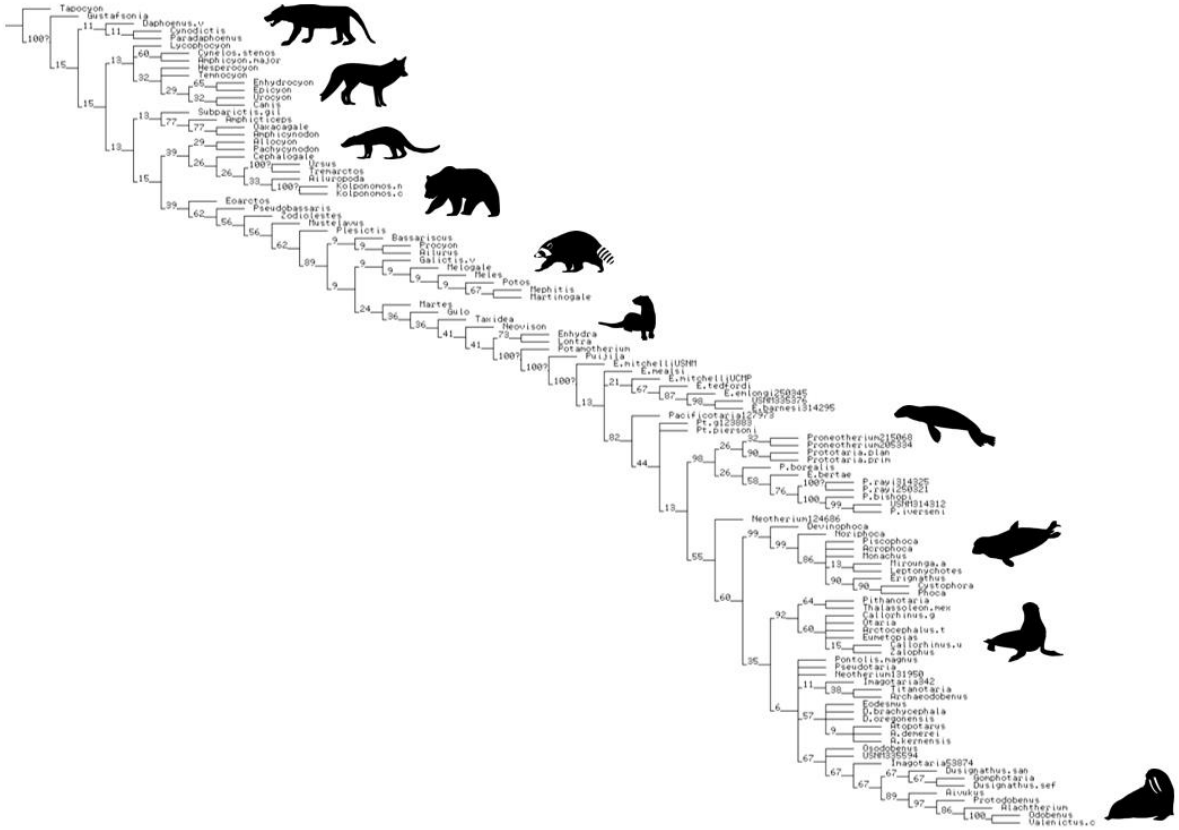

Figure 2.9. Trial 9

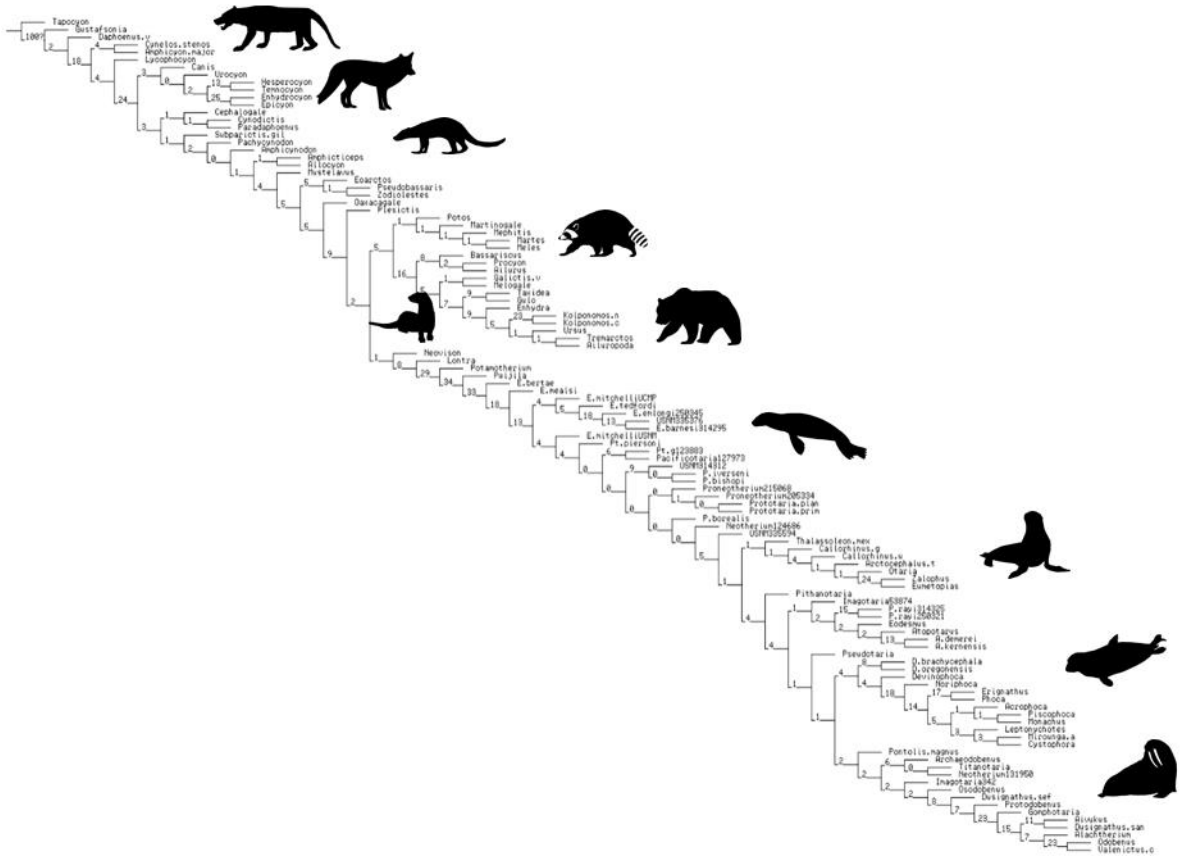

Figure 2.10. Trial 10

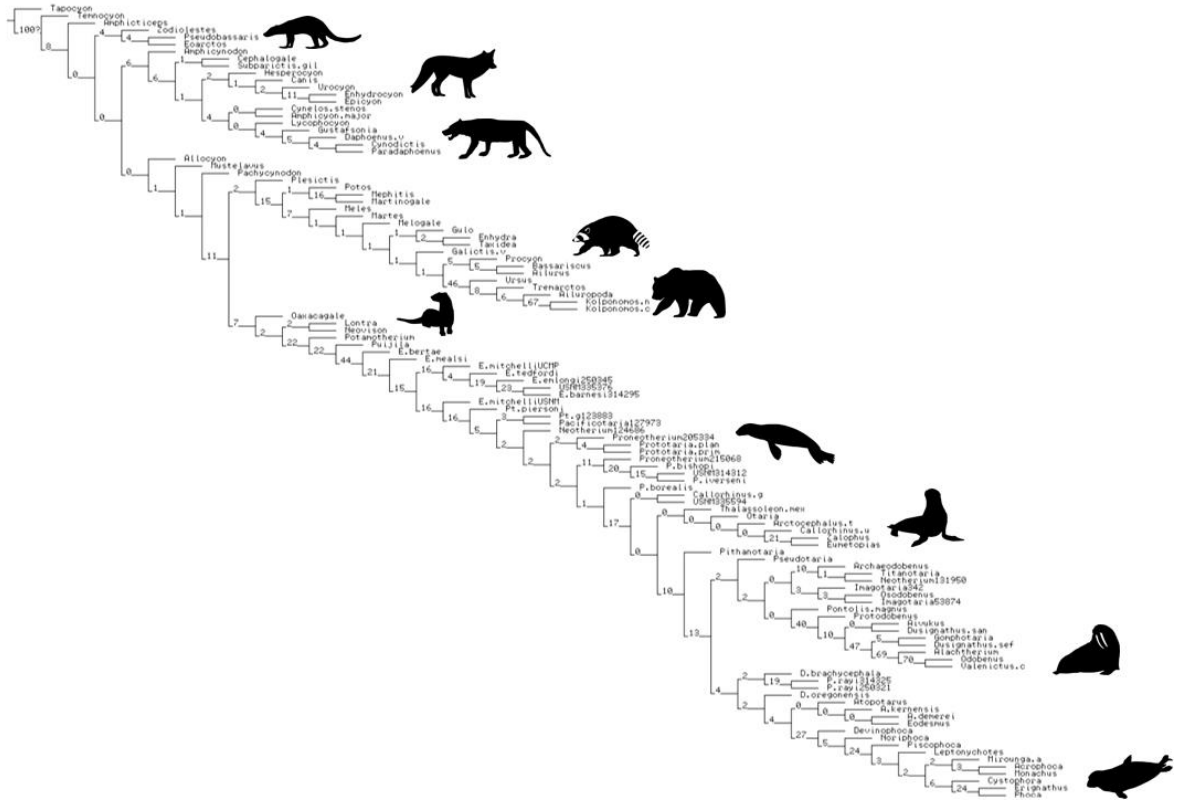

Figure 2.11. Trial 11

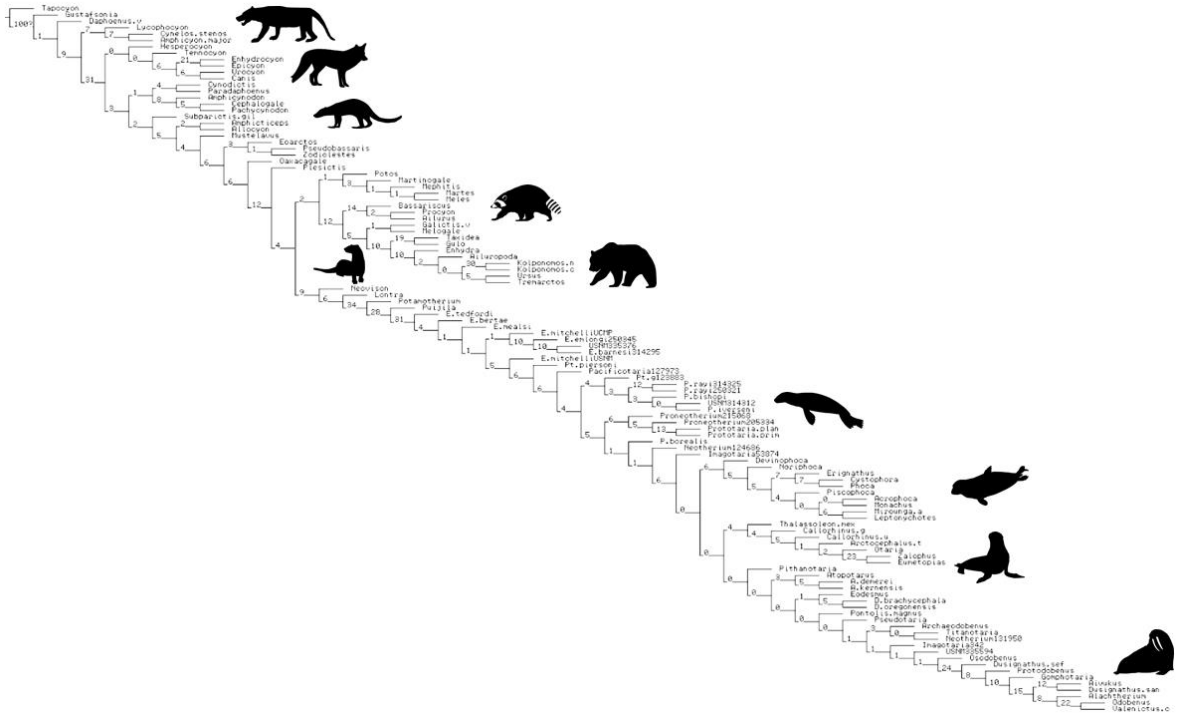

Figure 2.12. Trial 12

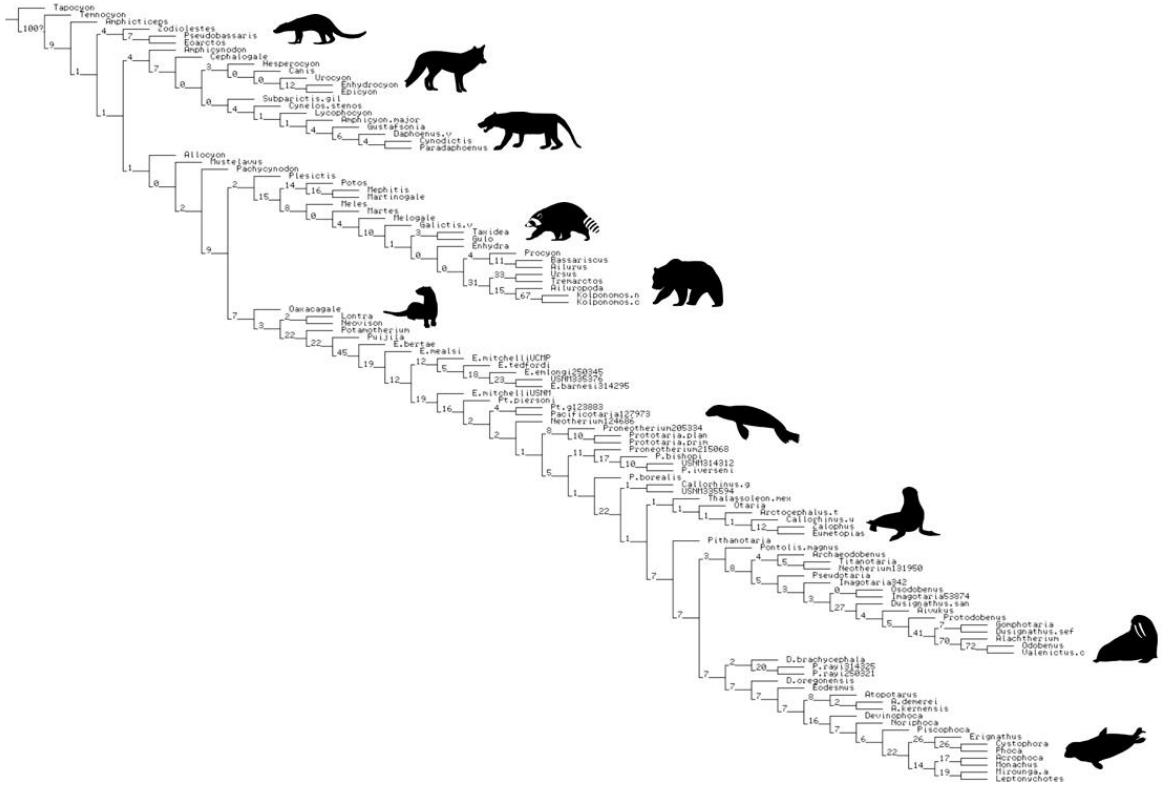

Figure 2.13. Pan-pinniped Tree: Trial 4 parsimony tree #3 out of 11.

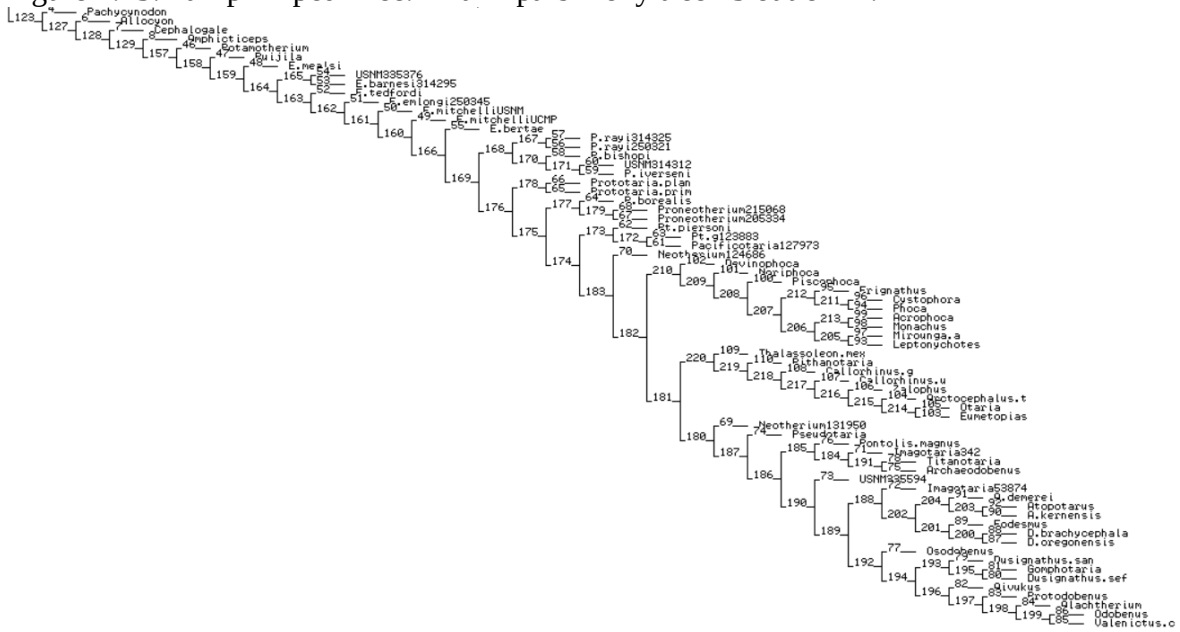

Appendix 2

Character list

1. Anterior narial opening. 0=ovoid vertically or nearly circular. 1=ovoid horizontally. (Boessenecker & Churchill, 2013: character 2)

2. Prenarial process of premaxilla. 0=absent. 1=prominent, protrudes dorsal and anterior to alveolar margin. (Berta & Wyss, 1994: character 3; Boessenecker & Churchill, 2013: character 6)

3. Premaxilla posterodorsal slope in lateral view. 0=shallower or equal to 45 degree slope. 1=steeply sloping or deeply excavated. (Berta & Wyss, 1994: character 2)

4. Premaxilla-nasal contact (ORDERED). 0=less than 50% nasal length, no frontal contact. 1= greater than or equal to 50% nasal length, premaxilla does not contact frontal. 2=premaxilla contacts frontal. (Berta & Wyss, 1994: character 1)

5. Nasal-frontal suture (ORDERED, WEIGHTED). 0=nasals intrude between frontals. 1=suture convoluted or nearly continuous with maxillo-frontal suture. 2=frontal intrudes anteromedially between nasals. (Berta & Wyss, 1994: character 4+5)

6. Nasal length (ORDERED). 0=greater than 18% condylobasal length. 1=18-25% condylobasal length. 2=less than 25% condylobasal length. (Boessenecker et al., 2024: character 22)

7. Frontal process length between nasal and maxilla (ORDERED). 0=greater than 25% nasal length. 1=less than 25% nasal length. 2=no frontal process between nasal and maxilla.

8. Nasolabialis fossa (ORDERED, WEIGHTED). 0=absent. 1=present, shallow. 2=present with anterodorsal tuberosity. (Berta & Wyss, 1994: character 7)

9. Orbit size (ORDERED). 0=15% or less of cranium length. 1=15-20%. 2=20% or more of cranium length. (Boessenecker et al., 2024: character 40)

10. Maxilla contribution to the orbital wall. 0=little to no contribution. 1=significant contribution. (Berta & Wyss, 1994: character 9)

11. Antorbital process size (ORDERED). 0=absent or indistinct. 1=small rounded ridge. 2=prominent. (Berta & Wyss, 1994: character 16)

12. Antorbital process construction (WEIGHTED). 0=frontal only. 1=parallel (along the orbital rim) suture of maxilla and frontal/lacrimal. 2=maxilla or lacrimal only. 3=perpendicular suture of maxilla and frontal.

13. Supraorbital process size (ORDERED). 0=prominent, forms a point. 1=reduced, forms a blunt ridge. 2=absent or indistinct. (Berta & Wyss, 1994: character 17)

14. Supraorbital process position. 0=closer to anterior orbital margin. 1=equidistant or closer to expansion of braincase.

15. Orbital vacuities (WEIGHTED). 0=absent. 1=present anteriorly. 2=present posteriorly. (Berta & Wyss, 1994: character 12; Paterson et al., 2020: character 17)

16. Lacrimal foramen (WEIGHTED). 0=present. 1=absent.

17. Interorbital constriction (ORDERED). 0=thinnest at posterior end. 1=anterior and posterior end of similar thickness. 2=thinnest at the anterior end. (Berta & Wyss, 1994: character 18)

18. Zygomatic transverse width across the skull. 0=widest point at approximate level of anterior border of the glenoid fossa, much wider than orbital width. 1=widest anterior to glenoid fossa, or not significantly wider than orbital.

19. Infraorbital foramen shape (WEIGHTED). 0=small and laterally compressed. 1=large and near-circular with no dorsal or ventral expansion. 2=triangular with the dorsal corner closest to the mid-sagittal plane. 3=triangular with ventral corner closest to mid-sagittal plane. (Berta & Wyss, 1994: character 11; Paterson et al., 2020: character 15)

20. Squamosal-jugal articulation (ORDERED, WEIGHTED). 0=splint-like, contact posterior to postorbital process. 1=mortised, zygomatic process of squamosal fits into the notch in postorbital process of jugal. 2=mortised, zygomatic process of squamosal greatly expanded dorsoventrally. (Berta & Wyss, 1994: character 39)

21. Ventral portion of anterior zygoma. 0=more dorsally placed, steeply inclined anteriorly. 1=lower on skull and flatter.

22. Zygoma highest point of arching. 0=continues arching posterior to postorbital process. 1=at the postorbital process, descends posteriorly.

23. Arching of jugal; greatest ventral arc height divided by length between ventral margins of jugal (ORDERED). 0=less than 20%. 1=20-30%. 2=greater than 30%.

24. Zygoma dorsoventral breadth. 0=thin. 1=both jugal and squamosal broad. 2= squamosal much broader than jugal.

25. Orbital portion of zygoma length. 0=postorbital length greater than 2/3 of zygoma length. 1=orbital length greater than 1/3 of zygoma length.

26. Jugal-maxillary suture (WEIGHTED). 0=jugal with anterodorsal and anteroventral splints. 1=anterodorsal splint only. 2=elongate anteroventral splint extends anteriorly to the level of M1. (Deméré & Berta, 2002: character 12)

27. Ventral tuberosity and/or fossa on anterior zygomatic root. 0=absent. 1=present.

28. Postorbital process of jugal. 0=absent or small. 1=well-developed and pointed medially.

29. The posterior border of the zygomatic root of maxilla joins the palate (ORDERED, WEIGHTED). 0=level with or posterior to M2, or excessively posterior to M1 if M2 is missing. 1=level with or directly posterior to M1. 2=anterior to M1.

30. Pseudosylvian sulcus (ORDERED, WEIGHTED). 0=absent. 1=reduced. 2=strongly developed. (Berta & Wyss, 1994: character 50)

31. Anterolateral margin in dorsal view (ORDERED). 0=sinuously smooth. 1=rounded laterally but cornered medially. 2=box-shaped and cornered laterally.

32. Squamosal fossa. 0=undivided. 1=divided. (Deméré & Berta, 2002: character 18)

33. Shape of dorsal surface of braincase. 0=convex arc; posterior braincase slopes distinctly ventrally. 1=nearly straight, only upturned at occipital shield if applicable. 2=braincase elevated above the interorbital region.

34. Relative length of frontals and parietals at midline (ORDERED). 0=parietal longer. 1=subequal. 2=frontal longer. (Wang et al., 2023: character 15)

35. Nuchal crests (ORDERED). 0=prominent, obscures occipital condyles in dorsal view. 1= weakly prominent, but does not obscure occipital condyles in dorsal view. 2=low or indistinct ridge. (Boessenecker et al., 2024: character 56)

36. Sagittal crest height (ORDERED). 0=no ridge. 1=low ridge. 2=tall ridge. (Boessenecker et al., 2024: character 59)

37. Sagittal crest length (ORDERED). 0=short, restricted to posterior 2/3 of braincase. 1=extends anteriorly to level of anterolateral margin of braincase. 2=extends anteriorly into intertemporal/interorbital region. ((Boessenecker et al., 2024: character 60)

38. Sagittal crest posterior bifurcation along parietal. 0=absent. 1=present. (Boessenecker et al., 2024: character 61)

39. Palatal length (ORDERED). 0=short, <50% of condylobasal length. 1=intermediate, 50-55%. 2=long, >55%. (Boessenecker et al., 2024: character 24)

40. Embrasure pit between P4 and M1 (ORDERED). 0=deep. 1=shallow. 2=absent. (Wang et al., 2023: character 9; Paterson et al., 2020: character 11)

41. Embrasure pit between premolars. 0=absent. 1=present.

42. Incisive foramina position. 0=level with or anterior to canines. 1=extend posterior to canines. (Paterson et al., 2020: character 9)

43. Toothrow alignment, based on lingual borders of tooth crowns (ORDERED). 0=parallel. 1=slightly divergent. 2=strongly divergent. (Berta & Wyss, 1994: character 13)

44. Palatal arching, longitudinal (ORDERED). 0=flat. 1=slightly arched. 2=strongly arched.

45. Palatal arching, transverse (ORDERED). 0=flat. 1=slightly arched. 2=strongly arched. (Paterson et al., 2020: character 8)

46. Palatal lateral process. 0=absent, palatine border terminates directly posterior to the last molar. 1=sharp point or tuberosity near the last molar. (Berta & Wyss, 1994: character 6; Boessenecker et al., 2024: character 15)

47. Palatine posterior border with choana (ORDERED). 0=level with or anterior to last molar. 1=slightly posterior to last molar. 2=extends significantly posterior to last molar. ((Paterson et al., 2020: character 5)

48. Palatal shelf above choana. 0=rounded. 1=notched.

49. Caudal nasal spine of palatal. 0=absent. 1=present.

50. Posterior choana width (between medial pterygoid plates) relative to width between canines. 0=equal width or narrower. 1=wider.

51. Pterygoid strut ventral profile (ORDERED, WEIGHTED). 0=thin. 1=broad. 2=very broad with lateral process. (Boessenecker & Churchill, 2013: character 13)

52. Pterygoid strut lateral margin. 0=flat. 1=concave. 2=convex.

53. Pterygoid hamular process position relative to posterior margin of temporal fossa (ORDERED, WEIGHTED). 0=anterior to margin. 1=level with margin. 2=posterior to margin. (Boessenecker et al., 2024: character 30)

54. Alisphenoid canal (ORDERED, WEIGHTED). 0=present. 1=narrow groove present. 2=absent. (Berta & Wyss, 1994: character 20; Wang et al., 2023: character 32)

55. Basioccipital lateral border with bulla. 0=bulla underlaps. 1=continuous with medial edge of bulla. 2=basioccipital distinct from bulla and flares ventrally. (Berta & Wyss, 1994: character 42)

56. Basioccipital ventral floor width at level of external auditory meatus ventral margin. 0=less than or equal to width of lateral portion of basicranium. 1=greater width than lateral basicranium. (Tomiya & Tseng, 2016: character AC10)

57. Depressions for rectus capitis muscle (ORDERED). 0=absent. 1=present. 2=present with muscular tuberosity.

58. Hypoglossal foramen position relative to PLF. 0=distant, not connected. 1=closely associated by proximity or shared fossa. (Wang et al., 2023: character 28)

59. Hypoglossal foramen position relative to groove between occipital condyle and paroccipital process (ORDERED). 0=well anterior to groove. 1=along anterior border of groove. 2= within or inline with groove. (Wang et al., 2023: character 29)

60. Posterior carotid canal position (ORDERED, WEIGHTED). 0=posteriorly placed, opens into the same fossa as PLF at posterior wall of bulla. 1=posteriorly placed, opens separately from PLF. 2=anteriorly placed, canal shortened. (Wang et al., 2023: character 54)

61. Posterior lacerate foramen (PLF) size. 0=smaller than external auditory meatus. 1=equal to or greater than EAM. (Berta & Wyss, 1994: character 43)

62. Postglenoid foramen (WEIGHTED). 0=present. 1=absent. (Berta & Wyss, 1994: character 40)

63. Retroarticular process (postglenoid process). 0=medial prominence. 1=prominent with minimal directional bias.

64. Articular tubercle (preglenoid process). 0=prominent lip curving ventrally. 1=reduced or indistinct.

65. Mastoid process size. 0=prominent broad projection. 1=small projection. 2=indistinct lateral bulge. (Wang et al., 2023: character 26)

66. Ventral surface of mastoid between lateral edge and bulla. 0=flat or indistinct. 1=concave excavation. 2=convex and bulbous.

67. Paroccipital process (ORDERED). 0=prominent projection. 1=short, narrow projection. 2=indistinct. (Berta & Wyss, 1994: character 45)

68. Mastoid-paroccipital process connection (ORDERED). 0=discontinuous or indirect connection. 1=connected by low or significantly recessed ridge. 2=connected by a prominent continuous ridge. (Berta & Wyss, 1994: character 24; Wang et al., 2023: character 46)

69. Paroccipital process posterodorsal ridge. 0=absent. 1=present.

70. Squamosal suprameatal fossa (WEIGHTED). 0=absent. 1=shallow. 2=deep dorsal expansion. 3=enclosed anterolaterally. (Wang et al., 2023: character 37)

71. Contact with postglenoid process (ORDERED). 0=separated by wide fossa. 1=separated by narrow gap. 2=contacts postglenoid. (Boessenecker et al., 2024: character 67)

72. Entotympanic contribution to bulla (ORDERED). 0=entotympanic unossified. 1=ossified but no significant contribution to bulla. 2=caudal entotympanic contributes significantly. 3=entotympanic greatly inflated. (Berta & Wyss, 1994: character 37)

73. Bulla inflation. 0=uninflated. 1=moderately to greatly inflated. (Deméré & Berta, 2002: character 10)

74. Dorsal region of petrosal (ORDERED). 0=uninflated with pointed apex. 1=inflated with rounded apex. 2=greatly inflated. (Berta & Wyss, 1994: character 29)

75. Inferior petrosal sinus. 0=small. 1=enlarged. 2=deeply excavated into the basioccipital. (Wang et al., 2023: character 44)

76. Pit for tensor tympani. 0=present. 1=absent. (Berta & Wyss, 1994: character 30; Wang et al., 2023: character 52)

77. Stylomastoid foramen and hyoid fossa. 0=closely associated. 1=separated, hyoid fossa is posteromedial. 2=separated, anterolateral. (Berta & Wyss, 1994: character 41; Deméré & Berta, 2002: character 13)

78. Internal auditory meatus (ORDERED). 0=present, canals vestibulocochlear and facial nerves in single foramen. 1=bilobed, canals incipiently separated. 2=canals separated into two foramina. (Berta & Wyss, 1994: character 26)

79. Bony tentorium. 0=separate from petrosal. 1=appressed to petrosal. 2=reduced or absent. (Boessenecker et al., 2024: character 76)

80. Epitympanic recess (ORDERED). 0=small. 1=expanded. 2=greatly enlarged. (Boessenecker et al., 2024: character 68)

81. External auditory meatal tube (WEIGHTED). 0=absent. 1=present. (Wang et al., 2023: character 56)

82. Round window. 0=small. 1=enlarged (much greater area than oval window). (Berta & Wyss, 1994: character 25; Wang et al., 2023: character 58)

83. Basal whorl of scala tympani. 0=small. 1=enlarged. (Berta & Wyss, 1994: character 27)

84. Basal cochlear whorl. 0=posterolateral to long axis of skull. 1=transversely directed. (Berta & Wyss, 1994: character 28)

85. Canal for cochlear aqueduct. 0=separate from round window. 1=merged with the round window. (Berta & Wyss, 1994: character 32)

86. External cochlear foramen. 0=opens into middle ear. 1=opens externally. (Berta & Wyss, 1994: character 33)

87. Auditory ossicles. 0=small. 1=enlarged. (Berta & Wyss, 1994: character 46)

88. Muscular process of malleus (WEIGHTED). 0=present. 1=absent. (Berta & Wyss, 1994: character 47)

89. Processus gracilis (rostral process) and anterior lamina (osseous lamina) of malleus. 0=unreduced. 1=reduced. (Berta & Wyss, 1994: character 48)

90. I3 lingual cingulum. 0=present. 1=absent. (Berta & Wyss, 1994: character 59)

91. I3 size and shape (ORDERED). 0=similar in size to I1-2 or I3 absent. 1=moderately larger than I1-2. 2=much larger (>2x dimensions of I1-2), and canine-like.

92. Upper incisors (ORDERED, WEIGHTED). 0=three. 1=two. 2=one. 3=absent. (Berta & Wyss, 1994: character 55)

93. I1-2 roots. 0=transversely compressed. 1=round. (Berta & Wyss, 1994: character 56)

94. I1-2 transverse grooves. 0=present. 1=absent. (Berta & Wyss, 1994: character 57)

95. I1-2 row shape. 0=curved. 1=straight.

96. I1-2 row position relative to canines. 0=incisors well anterior to canines; I3 alveolus is anterior to canine. 1=incisors slightly anterior to or level with canines.

97. Posterior crista. 0=sharply defined. 1=absent.

98. Canine tusks (ORDERED). 0=proportional canines. 1=tusk-like. 2=tusk-like with globular dentine. (Boessenecker & Churchill, 2013: character 55)

99. Postcanine tooth enamel (ORDERED). 0=well-developed. 1=thin. 2=absent. (Boessenecker & Churchill, 2013: character 62)

100. P1-3 crown shape. 0=laterally compressed. 1=bulbous or conical. (Tanaka & Kohno, 2015: character 63)

101. P1-3 cingulum texture (ORDERED). 0=no cingula. 1=narrow smooth lingual cingulum. 2=narrow cuspate lingual cingulum. 3=well-developed cuspate cingulum.

102. P1 size relative to P2-3 (ORDERED). 0=similar in size. 1=roughly half the size. 2=much less than half the size, nearly vestigial. 3=absent.

103. P1 position along toothrow. 0=parallel. 1=offset medially.

104. P1 distal cingular heel. 0=present. 1=absent.

105. P1 lingual cingulum (ORDERED). 0=absent. 1=narrow. 2=expanded.

106. P2 metacone. 0=absent or indistinguishable. 1=distinct cusp or cingular heel. 2=distinct with accessory cusp present.

107. P2 lingual cingulum (ORDERED). 0=absent. 1=narrow. 2=expanded lingually or protocone cusp present.

108. P2 root (ORDERED). 0=double, posterior bilobed or broadened. 1=double. 2=bilobed. 3=single.

109. P3 metacone. 0=absent or indistinguishable. 1=distinct cusp or cingular heel. 2=accessory cusp present.

110. P3 lingual cingulum (ORDERED). 0=absent. 1=narrow. 2=expanded lingually or protocone cusp present.

111. P3 roots (ORDERED, WEIGHTED). 0=triple. 1=double, posterior bilobed or broadened. 2=double. 3=bilobed. 4=single. (Berta & Wyss, 1994: character 62; Boessenecker et al., 2024: character 116)

112. P4 roots (ORDERED, WEIGHTED). 0=triple. 1=double, posterior bilobed or broadened. 2=double. 3=bilobed. 4=single. (Berta & Wyss, 1994: character 64; Boessenecker et al., 2024: character 117)

113. P4 paracone. 0=simple crest. 1=accessory cusps present.

114. P4 metacone (ORDERED). 0=large. 1=reduced. 2=absent.

115. P4 "carnassial" notch (groove between paracone and metacone). 0=present. 1=absent. (Wang et al., 2023: character 64)

116. P4 parastyle (ORDERED). 0=absent. 1=small bulge on the cingulum. 2=well-developed cusp. (Wang et al., 2023: character 65)

117. P4 lingual cingulum or protocone shelf (ORDERED). 0=absent. 1=very small restricted cingulum. 2=restricted lingual shelf, <50% mesiolingual distance. 3=greatly expanded lingual shelf, >50% mesiolingual distance. (Berta & Wyss, 1994: character 63)

118. P4 protocone position (ORDERED, WEIGHTED). 0=anteriorly, adjacent to paracone. 1=intermediate, forming near-equilateral triangle with paracone and metacone. 2=posteriorly, forming near-right-triangle closer to metacone. 3=absent. (Wang et al., 2023: character 67)

119. P4 hypocone. 0=absent. 1=present.

120. P4 contact with M1. 0=contacts M1. 1=does not contact.

121. M1 size compared to P4 (ORDERED). 0=distinctly larger. 1=similar in area. 2=smaller. 3=absent. (Berta & Wyss, 1994: character 66; Boessenecker et al., 2024: character 120; Wang et al., 2023: character 74)

122. M1 roots (ORDERED, WEIGHTED). 0=triple. 1=double, posterior bilobed or broadened. 2=double. 3=single or M1 absent. (Berta & Wyss, 1994: character 65)

123. M1 hypocone (ORDERED). 0=absent. 1=present as a swelling of the cingulum ridge. 2=present as a distinct cusp. (Wang et al., 2023: character 78)

124. M1 lingual cingulum (ORDERED). 0=absent. 1=narrow or restricted cingulum. 2=expanded, posterior portion only. 3=expanded, continuous. (Wang et al., 2023: character 70)

125. M1 protocone. 0=distinct cusp. 1=absent or indistinct from cingulum.

126. M1 postprotocrista. 0=labial orientation, narrow angle with preprotocrista. 1=posterior orientation, wider angle. 2=absent or indistinct. (Wang et al., 2023: character 82)

127. M1 protocone height compared to paracone. 0=protocone shorter. 1=protocone equal or taller. (Wang et al., 2023: character 71)

128. M1 metacone height compared to paracone. 0=metacone shorter. 1=metacone equal or taller. (Wang et al., 2023: character 76)

129. M1 paraconule and metaconule relative height. 0=paraconule equal or greater. 1=metaconule greater. 2=both indistinct. (Wang et al., 2023: character 77)

130. M1 parastyle position. 0=projects farther labially than metastyle. 1=same level or medial to metastyle. (Wang et al., 2023: character 72)

131. M1 parastylar shelf (ORDERED). 0=absent. 1=narrow. 2=broad. (Wang et al., 2023: character 79)

132. M1 orientation compared to the premolar row. 0=deflected medially. 1=parallel. 2=deflected laterally. (Wang et al., 2005a: character 15)

133. M2 roots (ORDERED, WEIGHTED). 0=triple. 1=double. 2=single. 3=absent. (Berta & Wyss, 1994: character 68; Boessenecker et al., 2024: character 121)

134. M2 size relative to P4 (ORDERED). 0=greater than 50%. 1=25-50%. 2=less than 25% or absent. (Wang et al., 2023: character 84)

135. M2 position (ORDERED). 0=parallel to other cheek teeth. 1=lingually placed, but lingual edge does not meet that of M1. 2=lingually placed, lingual edge is level with or medial to that of M1. (Wang et al., 2023: character 85)

136. M3. 0=present. 1=absent. (Wang et al., 2023: character 87)

137. Lower incisor count (ORDERED). 0=three. 1=two. 2=one. 3=absent. (Berta & Wyss, 1994: character 60)

138. Lower i3. 0=similar size to other incisors. 1=much larger than other incisors. (Boessenecker et al., 2024: character 95)

139. Lower postcanine lingual cingula. 0=mostly smooth. 1=consistently rough or crenulated. (Boessenecker et al., 2024: character 125)

140. Lower premolar mesial paraconid cusps. 0=prominent. 1=small or absent. (Berta & Wyss, 1994: character 70; Boessenecker et al., 2024: character 124)

141. Lower premolar roots. 0=double. 1=all but p4 single. 2=all single. (Boessenecker et al., 2024: character 128)

142. p1 (WEIGHTED). 0=present. 1=absent. (Wang et al., 2023: character 92)

143. p4. 0=present. 1=absent.

144. p4 posterior accessory cuspulid on posterior slope of main cuspid. 0=indistinct or absent. 1=prominent. (Tomiya & Tseng, 2016: character AC7)

145. m1. 0=present. 1=absent.

146. m1 hypoconid position. 0=labial 1/4 of talonid. 1=lingual 3/4 of talonid. 2=hypoconid absent. (Wang et al., 2023: character 97)

147. m2. 0=present. 1=absent. (Berta & Wyss, 1994: character 73; Wang et al., 2023: character 100)

148. m2 elongation. 0=absent. 1=present. (Wang et al., 2023: character 104)

149. m3 (WEIGHTED). 0=present. 1=absent. (Wang et al., 2023: character 105)

150. Mandibular symphysis. 0=unfused. 1=fused.

151. Mandible base of coronoid process (ORDERED). 0=less than 25%. 1=25-30%. 2=30% or greater. (Boessenecker & Churchill, 2013: character 50)

152. Mandible angular process (ORDERED). 0=aligned with ventral margin. 1=slight medial direction or small additional flange. 2=deflected medially and expanded as a shelf. (Berta & Wyss, 1994: character 51)

153. Mandible flange for digastric insertion. 0=absent. 1=present. (Berta & Wyss, 1994: character 52; Boessenecker et al., 2024: character 87)

154. Mandible depth of horizontal ramus. 0=deeper or equal posterior to symphysis. 1=deepest at posterior base of symphysis. ((Boessenecker & Churchill, 2013: character 43)

155. Mandibular condyle. 0=at or near level of tooth row. 1=elevated above the tooth row. (Berta & Wyss, 1994: character 53; Boessenecker et al., 2024: character 88)

156. Mandible genial tuberosity (WEIGHTED). 0=absent. 1=present ventral or anteroventral to p2. 2=present ventral or posteroventral to p3. (Boessenecker et al., 2024: character 84)

157. Scapula posterodorsal process (ORDERED). 0=rounded, blunt edge. 1=simple cornered edge. 2=curves posteriorly to a point. (Berta & Wyss, 1994: character 82)

158. Postscapular fossa for teres major (ORDERED). 0=absent. 1=small, limited to the dorsal 1/2 of the posterior border. 2=large, along at least 1/2 of the posterior border. (Wang et al., 2023: character 107)

159. Scapula metacromion process (ORDERED). 0=absent. 1=small overhang. 2=prominent flange extends posteriorly to the caudal border of the blade. ((Paterson et al., 2020: character 144)

160. Scapula supraspinous fossa. 0=similar area or smaller than infraspinous fossa. 1=significantly larger area than infraspinous fossa. (Berta & Wyss, 1994: character 85; Paterson et al., 2020: character 145)

161. Scapula anterior scapular ridge of supraspinous fossa (ORDERED). 0=absent. 1=weak ridge. 2=prominent ridge. (Berta & Wyss, 1994: character 86; Paterson et al., 2020: character 147)

162. Humerus distal trochlea vs. distal capitulum. 0=trochlea medial lip same or smaller diameter. 1=trochlea medial lip greater diameter. (Deméré, 1994: character 47)

163. Humerus greater tubercle. 0=rises above head distinctly. 1=does not rise above head. (Berta & Wyss, 1994: character 87)

164. Humerus lesser tuberosity. 0=small with no ridge. 1=prominent with a ridge along the shaft. (Paterson et al., 2020: character 152)

165. Humerus deltopectoral crest length. 0=extends less than or equal to 1/2 of humerus length. 1=extends greater than 1/2 humerus length. (Berta & Wyss, 1994: character 88)

166. Humerus deltopectoral crest shape. 0=ridge small. 1=ridge large and terminates gradually. 2=ridge large and terminates abruptly. (Boessenecker & Churchill, 2018: character 75)

167. Humerus entepicondylar foramen (ORDERED, WEIGHTED). 0=present. 1=absent, distinct fossa. 2=absent, no distinct fossa.

168. Ulna olecranon process (ORDERED). 0=knob-like. 1=laterally flattened and posteriorly blunt. 2=laterally flattened and curved posteriorly to a sharp point. (Berta & Wyss, 1994: character 94)

169. Radius pronator teres process. 0=absent. 1=present, proximal. 2=present, distal. (Berta & Wyss, 1994: character 96)

170. Femur lesser trochanter. 0=present, projects medially. 1=present, projects posteriorly. 2=vestigial or absent.

171. Femur greater trochanter height (ORDERED). 0=lower than head. 1=equal or higher than head. 2=significantly higher, noticeable even when the femur is viewed off the long axis. ((Paterson et al., 2020: character 175)

172. Femur trochanteric fossa (ORDERED). 0=deep. 1=shallow. 2=absent. (Berta & Wyss, 1994: character 119; Paterson et al., 2020: character 176)

173. Femur medial inclination relative to shaft (ORDERED). 0=condyle aligned with the long axis. 1=slightly inclined (~10 degrees). 2=significantly inclined >10 degrees. (Berta & Wyss, 1994: character 118; Paterson et al., 2020: character 180)

174. Tibia and fibula. 0=unfused. 1=fused proximally. (Berta & Wyss, 1994: character 122)

175. Calcaneal secondary sustentacular shelf. 0=absent. 1=present. (Berta & Wyss, 1994: character 123)

176. Calcaneal tuber. 0=parallel. 1=medially prominent. (Berta & Wyss, 1994: character 125)

177. Astragalus caudally-directed calcaneal process (ORDERED). 0=absent. 1=present, short. 2=present, long. (Berta & Wyss, 1994: character 126; Boessenecker et al., 2024: character 139)

178. Cuneiform distally projecting ledge. 0=absent. 1=present. (Berta & Wyss, 1994: character 97)

179. Last cervical vs. L1 centrum diameter. 0=cervical wider. 1=lumbar wider. (Berta & Wyss, 1994: character 77; Paterson et al., 2020: character 136)

180. Anterior lumbar transverse processes. 0=shorter than zygapophyses. 1=equal or longer than zygapophyses. (Berta & Wyss, 1994: character 80; Paterson et al., 2020: character 139)

181. Lumbar count (ORDERED). 0=seven. 1=six. 2=five or fewer.

182. Sacrum vertebrae fused (ORDERED, WEIGHTED). 0=three or less. 1=four. 2=five or more. (Paterson et al., 2020: character 140)

183. Tail length. 0=long. 1=short. (Wang et al., 2023: character 108)

184. 2n chromosome count (ORDERED, WEIGHTED). 0=less than 34. 1=34. 2=36. 3=38. 4=over 38. (Arnason, 1974).

185. Biogeographic origin. 0=Pacific/Western NA. 1=Atlantic/Eastern NA. 2=Europe or Africa. 3=Asia. 4=South America/Antarctica.

186. Stratigraphic origin (first appearance). 0=Oligocene or earlier. 1=Early Miocene (Burdigalian/Aquitanian). 2=Middle Miocene (Langhian/Serravallian). 3=Late Miocene (Tortonian/Messinian). 4=Pliocene or more recent.

Taxon and specimen list

Taxon	Specimen	Publication
Acrophoca longirostris	USNM 421632 USNM 559323	de Muizon, 1981
Ailuropoda melanoleuca	IMNH C-302	
Ailurus fulgens	SBMNH MAM 3592	
Aivukus cedrosensis	LACM 154671 (cast of type)	Repenning & Tedford, 1977
Alachtherium	USNM 9343	
Allocyon loganensis		
Allodesmus demerei		
Allodesmus kernensis	LACM 4320	
Amphicticeps shackelfordi	AMNH 19010 AMNH 19017	
Amphicynodon teilhardi		
Amphicyon major		
Archaeodobenus akamatsui	UHR 33282	Tanaka & Kohno, 2015
Arctocephalus townsendi		

Atopotarus courseni	LACM 1376	Downs, 1956
Bassariscus astutus	SBMNH MAM 9317	
Callorhinus gilmorei	SDSNH 25176	Berta & Deméré, 1986
Callorhinus ursinus	UWBM 38921	
Canis lupus	IMHN R-884	
Cephalogale		
Cynelos stenos		
Cynodictis		
Cystophora cristata		
Daphoenus vetus	UCMP 27561	
Desmatophoca brachycephala	USNM 335451	
Desmatophoca oregonensis	USNM 250283	
Devinophoca claytoni	USNM 415624	Koretsky & Holec, 2002
Drassonax harpagops		
Dusignathus santacruzensis		
Dusignathus seftoni		
"Enaliarctos" barnesi	USNM 314295	Berta, 1991
"Enaliarctos" bertae	LACM 128004	This study
"Enaliarctos" emlongi	USNM 250345	Berta, 1991
"Enaliarctos" mealsi	LACM 4321 USNM 374272	Mitchell & Tedford, 1973 Berta et al., 1989
"Enaliarctos" mitchelli	UCMP 100391 UCMP 80943	Barnes, 1979
"Enaliarctos"	USNM 175637	This study

sullivani		
"Enaliarctos" tedfordi	USNM 206273	Berta, 1991
Enhydra lutris	UWBM 38377	
Enhydrocyon basilatus	UCMP 76749 UCMP 76787	
Eoarctos vorax		Wang et al., 2023
Eodesmus condoni	UOMNCH F-68683	Tate-Jones et al., 2020
Epicyon haydeni		
Erignathus barbatus	UAM 21464	
Eumetopias jubatus	SBMNH OS 4038 UWBM 39483	
Galictis vittata		
Gomphotaria pugnax	LACM 121508	
Gulo gulo	UWBM 34936	
Gustafsonia cognita		
Hesperocyon gregarius		
Imagotaria downsi	SBMNH 342	Mitchell, 1968
"imagotarine" incertae sedis	USNM 335594	Boessenecker et al., 2024
Kolponomos clallamensis	UCMP 50056 LACM 131148	Tedford et al., 1994
Kolponomos newportensis	USNM 215070	Tedford et al., 1994
Leptonychotes		
Lontra canadensis	UWBM 32217	
Lycophocyon hutchisoni	UCMP 85202 SDSNH 107442 SDSNH 107659	Tomiya, 2011

Martes americana	SBMNH OS 3644	
Martinogale faulli	LACM 56230	Wang et al., 2005b
Meles meles		
Melogale moschata		
Mephitis mephitis	SBMNH MAM 2026	
Mirounga angustirostris	USNM 21895	
Monachus monachus	USNM 243842	
Mustelavus priscus	YPM 13775	
Neotherium mirum	LACM 131950	Kohno et al., 1994
Neovison vison	UWBM 77427	
Noriphoca gaudini	MSNUN 123	Dewaele et al., 2018
Oaxacagale ruizi	IGM 7998	Ferrusquía-Villafranca & Wang, 2021
Odobenus rosmarus	UAM 12082 UAM 14793 UWBM 35479	
Osodobenus eodon	LACM 118675 LACM 150922 LC 5001	Biewer et al., 2020
Otaria flavescens	USNM 484912	
Pachycynodon sp.		
Pacificotaria hadromma	LACM 127973	Barnes, 1992
Paradaphoenus cuspigerus	AMNH 6853	
Phoca vitulina	UWBM 51215	
Pinnarctidion bishopi	UCMP 86334	Barnes, 1979
Pinnarctidion iverseni	SDSNH 146624	Everett et al., 2023

Pinnarctidion rayi	USNM 314325 USNM 250321	Berta, 1994
Piscophoca pacifica		de Muizon, 1981
Pithanotaria starri	UCMP 86106	Kellogg, 1925
Plesictis sp.		
Pontolis magnus	LACM 4324	
Potamotherium valletoni	AMNH 10085	
Potos flavus	SBMNH MAM 1447	
Procyon lotor	IMNH R-901	
Proneotherium? borealis	LACM 127974	This study
Proneotherium repenningi	USNM 205334 USNM 215068	Deméré & Berta, 2001
Protodobenus japonicus	LACM 140726	Horikawa, 1995
Prototaria planicephala	LACM 134826 (cast of type)	Kohno, 1994
Prototaria primigena	LACM 130432 (cast of type)	Takeyama & Ozawa, 1984
Pseudobassaris riggsi	YPM 11455	
Pseudotaria muramotoi		Kohno, 2006
Pteronarctos goedertae	LACM 123883 USNM 335432	Barnes, 1989
Pteronarctos piersoni	LACM 127972	Barnes, 1990
Puijila darwini	NUFV 405	Rybczynski et al., 2009
Subparictis gilpini	FMNH 22405	Wang et al., 2023
Tapocyon robustus	SDSNH 36000	Wesley & Flynn, 2003
Taxidea taxus	IMNH R-230	

Temnocyon altigens	UCMP 9999	Merriam, 1906
Thalassoleon mexicanus	SDSNH 65155 SDSNH 65163 SDSNH 65172	Deméré & Berta, 2005
Titanotaria orangensis	OCPC 11141	Magellanes et al., 2018
Tremarctos ornatus		
Urocyon cinereoargenteus	SBMNH OS 1759	
Ursus americanus	IMNH R-530 UWBM-33259	
Valenictus chulavistensis		
Zalophus californianus	IMNH R-1000	
Zodiolestes diamonelixensis		

Matrix data

Tapocyon robustus
00100200100000000010001000011O??000110000011001??00?012100100001100100020000000000000000100111000011000000120000001000100100000001102100000000001000022001O??0??1011100?01??00??????00?00

Temnocyon altigens
00000200000201000100000200001O?0100110100010001010000000111O0?011010101?1??01???0????????0100?10000011001011012000012000002300002021011110010001010000000000?????111100000?000???????00?00

Epicyon haydeni
00011111001200000000001100110 1?00202100000100000100010102120000110100 01???000000100000000010100000000110020110200002100010120100001011 11??010101010010000010100100102011100 0????000???01

Amphicynodon teilhardi
00100110?01211000?00???0????10??0??10??00011100010???0?1?????0????????1?11??????0??????0?0100100000011O?000100200001200010120100202111110001000100000001?00100111010000020100O??????0?0?30

Pachycynodon sp.
00100111001210000?1?0???????000001011010000010210001001110120001111?01?1???
????1?????????001?00?000110??111112000023100101201002011000100010001000000010
0000??????????????????????????????20

Subparictis gilpini
00100200?01210000?0?0??0?00?1???0?????000010?00010??????????????????????????????
??????????10???000001101101101200002200000130100002000210001000000000?000?0
??????????????????????????????00

Allocyon loganensis
001001?100121000001?0????0101000010220100000112010000021 2??100010102?0110?20
0???0????????0100010000?10????11210000030001002000?0000011?????0?0?0000?????
??????????????????????????????00

Cephalogale sp.
001?0???0011?000000000110000 1???01????100?1??00000???0?1?021?0010?0??001??20??
??1?????????????????000011101011122000002100001201011000001 1???1000100000001000
0?1???1000000?????????????????00

Amphicticeps shackelfordi
10100221100100000000??0000010?10?11101000101????00??021201100??000201010000
?0?0?00?000????0???0?000111101110110000120001001010020201121?????001000000??0
0?0??????????????????????????????30

Plesictis sp.
00100??000120100012000100 00?10010211210000100020100112101101000111110202 1??
0????1?????????????????0000020??101212000011000100201010020????0001000100001010
0010??????????????????????????????21

Paradaphoenus cuspigerus
00000110001?100000000??00?0010?000110000001110001001001110001001111 2?0001?2
00???00???????110????000001000101111001001000101301110021002100010001000 1000
?0000??????????????????????????????01

Mustelavus priscus
000????000??010?0??0???????0100?01?01111001010201 1????2110?100??2?1102?11?00??
?000???????1100110000011 0????11120000110001002001000202221??0000010000001000
00??????????????????????????????00

Martinogale faulli
0??????0100211?00?0?0??0100010 0?012000000?1??01?100?120000120101201000111???0
???1?????????00???0?00013?????3112000111000001201112020 32?100010100000010??00
00??????????????????????????????03

Amphicyon major
00000200001200000100001001 1?0000010220000011010010011020211010012101 0?1?0??
?????1?????????????1000011001011021000021000001201002111000000010001000000100
0010012001111000210000010 0??????01

Gustafsonia cognita
000??1?0101210000?1?0???????10010?0100000010101011010021210000011011000000200
?01000000???0100010?000110??1?1121000001000001300000021001 0?????0??????????
??????????????????????????????0?00

Daphoenus vetus
00000210001000000000001000000000020220000011120000010021210000011112100000200
???00???????0100110100001000001020000002000101301010021002000010001010000000
0001001110101110121 1??00???11??0?00

Cynodictis sp.
00100210001211000000001000011000001120000010100100000220100010012112001000200
???00????????100110000011001001211000001000101201010021012100010001000000?00
000??????????????????????????????20

Cynelos stenos
00100200000200000000000?0000000000201100000100100100000212 10?000111111?110??0
??????????????100?010000?10??012112000012000001301000111002010010001000000100
0000??????????????????????????????01

Canis lupus
00000201000001000000002100000000010110100010000010000000111000002010001210000
0000010000000001000000000110011112020000020001012010000010011000100010000000
0000101010000000200110000000110004 04

Urocyon cinereoargenteus
00010200101101001000011010010001020121000000010011000000111010011011001210000
0000010000000001000000000110100010120000120000012010001110011000100010000000
0010101010010000 20?10000???????00404

Enhydrocyon basilatus
00120210000100000000001000001000010220000010000010000000111000011011010210000
0000010000000001000110001 13???2112210000020002013000000201211000101010?0010
100000??????????????????????????????00

Hesperocyon gregarius
00000200101201000000001000001000010110000010000010000020011000011111011210000
0000000000000000000010000011010001202000001000101101000000011100010001010000
0000001010010100010110000???11??0?00

Lycophocyon hutchisoni

000002??0???200000?0?0???000?10000?01101000100000100000201010000101110110000000???10????????1001000000110??201202000011000101100000021012 0?001000100000000 0010?????1101000??1000??0???????00

Eoarctos vorax
0010020010020000000010110000100000012002001010001021102120020000111100011?010?0?0????0???1100110100111011010120000003000101201101101002101010000000010110000012110101000001000000000100?00

Ailuropoda melanoleuca
0010111100111100110000120010100000021012000021001001122011101010010112002100 2?1???10000001001000100001321101121220000230100023011101210001000001010001011100100110000011000?0110000011221434

Tremarctos ornatus
0010000100210000000000110101000002011002000001201001202021201001011210110022?0???10000001001000100001201101131140001132100021010101110001000110010001012100000210011010000100 10????01021444

Ursus americanus
0002010100010000000000020101000001021112000001201011202121201001011100010020000010000010010000000012201011301401010321000210101111100010000000000010121000002100010112001000000011121404

Kolponomos clallamensis
0100020100101000011000210011100000??201201122001011100211012110001121022??1???0?????0?0?200?00?0011111?0110?20??1?32100023011101021021???01

Kolponomos newportensis
0000???1001?10000010001101111000 0?0?201201122001011100211110100001110022 0???1???0??????????200?00100111110111022000113110002301110102102110010 00?00011110101?????????????????????????11????01

Zodiolestes diamonelixensis
0011010010121000011000111110110000011000000010101001022110120001110102111?100???00???????0100110000011001011220000002000100202002021121100010001000010100000021011 0?000??10?0????11?00?01

Oaxacagale ruizi
001?0000001201000?1?0??0000?20012120?10000111?????0?1010?11100?11111011?1??0???000000000?1?01100000020????10020000120000???????????0???1???00

Ailurus fulgens

000201120002010011100021001010000101101100100010001011211021000111110121000
00???10000000001011100001 33??011012000002301000220211110100210001000100011 0
1000000220011010102010 00????11100234

Pseudobassaris riggsi
001001011000010001200011100010001101100000111000110110202012000 12?1102221??
00???0????????000011000001100011112100001200010010010000101110001000100011 0?
??????????????????????????????????20

Bassariscus astutus
001001112002010020002010111001020111000000000010210200002200012021021110 0
00???10000000000001100000120000011120000130101022011202101210001000100011 0
1000000110011010000?01010????11000304

Potos flavus
001200101012010020200010001110000211200200000320000112202112100111110221100
00???10000000011001100000 13??002302100012310000130111211210110001010000011 1
2100100110001000000?00000000????00344

Procyon lotor
001201011002010010200021001100210100002100101020101122000112000101100202100
0????10000000001001100001220000120110000230100022011121020021000100010001100
1000100110011000000110 00????11110304

Meles meles
001002000012000001101000001010110202202100000020100112102112011001110?1?1??
01???10000000001001000001121100131120011131000023010011113 2?100010000000010
100100???????????0??????????????0424

Martes americana
001001011012000000200020010111010201101000100020100112002112010011111?0?1??
01???10000000001001100000120100110120011120001013010000203 2?100010001000010
1001000110001000000110000000011100304

Melogale moschata
001002000012010000200020000011010201210000100020100012102022010020111?0?1??
0????10000000001011100000110100011120011131102013010000213 2?100010001000011
20101010200?0?10?0??0?00????1???0?34

Galictis vittata
001001010012010011200010000010010100110000200220100122001022010000111?0?1??
01???10000000001011100001 13???013112000012110202301000121 32?100010100000010
100000???????????0??????????????0?44

Mephitis mephitis

00110200101211001020000001001001010110000001000010011220112201010102002100000?0?1000000000000110000013???013112000103100001201102021 32?100010100000010000100020001011101011000000011100404

Gulo gulo
00100012001200000010002200001001010210100020002000011200111200000110131210001???10000000001001110001121110110120000130102011020020201 2?100010100010010100000020001000000110000000000101404

Taxidea taxus
00100101001200000020000101011001022001100000002000012210111200000111032110?00?1?10000000001001100001 13???002112000013010102301100021 32?100010101010011100000012000000100211000010010101004

Neovison vison
00100100002201000020002000002001021110000010102000112200011200000010030110?0100?1000000?0010011010001 3???012002000022000100302012020 32?100010100010010100000012101100000211000000010100004

Lontra canadensis
00100011002200000020001001102001 1?10000000001020102122001112000001111030100?0100010000000010011100032110012021000013000100201102121 32?100010101000010120100211011000002101000010011100304

Enhydra lutris
00100011002111000020002001101001022001010000102011110200011211001011030200001000100000000100111100113???003020000003110001300100021 32?110010100000110100002121001000002110000000011101304

Potamotherium valletoni
00111022202210000120001000012001 1?10012000101020001022001111111000110002 10?0000010000000101001110000111002112120000131002002020020202221000100010000102001002221000000012011100 00?11100?21

Puijila darwini
000????21?1110000020002 00?1120001?12201100001 12??000?0202??111010?0100021020000111000 0???0100111100011001121111000012100200202002020222110010001000010200002221??00100002010100 00?11100?11

“Enaliarctos” mealsi
1000???2101?100003001101?011220121220?00?10112100100011202111100?1100011020100?011000011????????000???????102100001200021031010201021211000000101001020000021211000012010112000001 1101?01

“Enaliarctos” mitchelli

000????1??1?11?10?3011?0??001?????????00110112000?1????????????????????????????
????????????????10000?10????1??10????31??21????????02221????????????????????????
??????????????????????00

“Enaliarctos” sullivani
000100122?111100113?11201001112012111010001012200011102120111111??1?102110?
0110?0??????????????????0001?0??0202210000031012103120020102221????????????????
????????????????????????????????00

“Enaliarctos” emlongi
000211222011110110100001O?0112201211201010101120101100212001110101010002102
011010110001110100001000011001220221000003100210 3?2?????022211000000101001O
210000?????????????01020??????????01

“Enaliarctos” tedfordi
???????2201110011030000000?00122012122O?00?10112000110011102011110101100 21?20
0??101???0011????????0003????220221000003100 21????????02221????????????????????
????????????????????????????????00

“Enaliarctos” barnesi
11011022??111001013000010??10?2????220?0101011201O????????????????????????????
??????????0100001000021002120121000003100210310002111221110000001010010210000
0????????????????????????????????00

USNM 335376
110010221?11100?113?????????12?012122010101011210011001120111110010 1?0021???
0???01??00????1?????1000210????11120?????1?010?????????12211????????????????????
????????????????????????????00

“Enaliarctos” bertae
0?011?11??11211011201100 1?01112?2??00110112013200021001 12??01011????00110???
???0??????????????000?10????11?11?0???1?021?20??????1112110??000?0?0010???000?
????????????????????????????00

Pinnarctidion rayi (USNM 250321)
00021021111?11011131100010110221121110120110132000210001101110000102100?1?1
?????0?????????10??010000200??120121111103200210310012111221 1????????????????
??2011101111 2??01120??????0???01

Pinnarctidion rayi (USNM 314325)
000210211111110110311000101102211211111101101320102100012001100001010012 1?1
101010110?011101000010000200??120121101013201210310002111220 1????????????????
????????????????????????????????01

Pinnarctidion bishopi

???????11?1?11001131100010011220?2???110?100320012110112011111011020001 1?11
110?0??0?0???????????000?????????1101113201210310002101120 1?????????????????
??????????????????????????????01

Pinnarctidion iverseni
0?0????12?1?11?0213111111?110?2?1????1111211320012110212011111 0?????001101?1
???0110?0???????????0002001112122111111320122031000210122 01?????????????????
???????10112?????????????????00

USNM 314312
?10110111101110020311??0100102202220010201101 32??12110212001110101020002???
111??01???0????100????000210??220121101113201 22??????21012201??00000002001011
1000102110??112??21?20??????????01

Pacificotaria hadromma
0101000221101 00?003011001?1111201?122001000111200011001120011011010200021??
?0???0????????020000100001101202012110101320?11?????????12121?????????????????
??????????????????????????????01

Pteronarctos piersoni
0100010121101 10?003001001001012012121001011012200011001110111?110102000 11?1
10???01??????1?100?010000?10????1??11000?320111?????????12121?????????????????
??????????????????????????????01

Pteronarctos goedertae
0102000121101000003010001001022011022001001003200011001110011001010200111??
10???0????????0100?010000?10????1??11????320122?????????12121?????????????????
??????????????????????????????01

Proneotherium? Borealis
0?121101110110101030110010000120 22?000100101320100100011010111111??00011??
?????0???????????0?0??000?10??110??11?????2?111?2???????12111?????????????????
??????????????????????????????01

Prototaria primigena
0101000211211010013010111001012 01?112011001003200022001120111110010200110??
?11010????????1100001 00???10????11211????320120021??0???12221????????????0????
?00?????????????????????11????32

Prototaria planicephala
0?021002111110100030100100111120121110110001132000220011200110000102000 10??
?11010????????1100001000??10???20??11?????20110?2????????22221?????????????????
??????????????????????????????32

Proneotherium repenningi (USNM 205334)

00010?0?2111101000301000101101201201200100101220001100111010?000102000100?
?1???0??0?????0100?1100013000212022111111320110?????????12111?????????????????
????????????????????????????????02

Proneotherium repenningi (USNM 215068)
0101111111111010003111101001022012011001001113200011001110111000010?0010??
?1???0????????0101101000031002??022111110320120?????????10101?????????????????
????????????????????????????????02

Neotherium mirum (LACM 131950)
01020??01?13201?003011100011002022112001001002200122000110111101011200210??
??1??011???????200?00?0003000111?211?11032011?3???????210211?????0?0?0010?10
10?????????????????011???????01

Neotherium? sp. (LACM 124686)
0101001111100110003011101011112012112001001012210012001110111100011200011??
10???011???????1000001000?10????11211?????1?111?????????12111?????????????????
????????????????????????????????01

Imagotaria downsi
01001??0??232011103011?010?100?0??0?2?1200011?01021?01????11111??12102201?11
111?11010111110001000003?11?2?2123201???201?20????0????1??111100?0?121010?201
01?????10111222?????0111??????03

Imagotaria? sp. 53874
0101???011??20?1103010001001 00?0121000?200011?2?????????1?????1110102102????11
1?1011??0???120??0000012?1??013??4411100301 11?????????10101?????????????????
????????????????????????????????03

USNM 335594
1?0111222123101000301 1001?1100001202101200012220002110211011111101020 02?1??
?1???0????????110???0000120011??3??33??1????123?????????22121?????????????????
????????????????????????????????03

Pseudotaria muramotoi
???10?20?11310111?3?1100101?00?0121120?21?0012?00021?0111??1111101121021 00?1
111101????????1??????0????0????3?222??1?????21?????????11001?????????????????
????????????????????????????????33

Archaeodobenus akamatsui
?1?????0?????????01?11?01?1100?0??0????20?0012???011?01?2??11111??1110211???111
1?????????1200?1?00002?1??1??1?21?????20122?????????2???111100?0?0?0010?2010???
???10?11?????????????????33

Pontolis magnus

0100012201132111003011011001100011022022 0?1012?0?002?001???011010112102 2????1110????0???0100?0101103?01?0?3013201??0??1?20????0???11??121010000021010221112?????1?????????????1???????03

Osodobenus eodon
0101012001132011003011011011010021110110101132000210021211111110102101 10??11??0????0???12000111001200011131133011022012301120 02??02121??1120001210101111102????????????????????????????????03

Titanotaria orangensis
0100012001132011001011010001000012022012000023200011 0?1110201110011210210??11??0????????1200?011001201???12?122????02??22??????????21121??100?00020011211101?????100112?2?????011???????03

Dusignathus santacruzensis
??0???????2???????3??????????????02???????1????????????????????????2??????111??????01???1?????10111?01???3?1?????????????????????????1110120101210102101 02?????10111?22??????????????03

Dusignathus seftoni
0111002201232011003001010011000012020022011102210 12?1?1121101110011210210??????1110????0???11?11111201100110??3??44??11030023?01?002?0220212???2?1?1?101121 1102?????10011?????????11???????03

Gomphotaria pugnax
0101012001232011003001010001?0?0220220?20?1?13???0???????????110??1210?11??1??????0?0???1210??112111?11?0?3014?02??0301?30????????1???13?0?201012101021010 2?????10111222????0011???????03

Aivukus cedrosensis
01000??011232021003011011011 00?02??0???2001112?00121??1?2??111110?11102201?111?1?1?0?01??121110110110?01?0?3104?12??0301230????0???1???12????2?101?1010??0102???????????22??????????????????03

Protodobenus japonicus
011000?0112?20??1?1001100?1110?021?0??220?112?????2???1????11110?1210???????????????10?1011111??0????3104??2??0301?3?????????1???1110120101210102101 12?????????????????????????????34

Alachtherium
0110002011232?2110300101001110?02210??2200122 3?0012???1????111110?1210220???111???0??????21110112210?01?0?3004??????301?30????????1???1110120101210102101 12?????1??1122???????11???????14

Valenictus chulavistensis

01101020112320211030110100 11?0?01?10??2200?223?00121??1?2??111110?12102?01?1
111?????????1?3?1?1122?03???0??00???21003013 3??1???2?0?3??13??1?110121011 1?01
12?????10111?22?????011???????04

Odobenus rosmarus
01101120112320211030111100 11?0202110??220?122320012110112021111101111022010
111110110101111221101122100010003004402100301330?1?002101?2013?012000121011
120112100111011122220220011111101014

Desmatophoca oregonensis
00000200211321010021100212010121121120120010032010101001200111110102102 10??
111?20110?0?1?1200010000100?1112122201 1?0201210????0???122011100000002101 02
211122021000111 22??????????????????01

Desmatophoca brachycephala
0?000121211321010021100212011221121?2?120021132010211111200011010101000200?
?1?1?0????????1200011?00??01???????11????32?123031200212132?1?????????????????
??????????????????????????????01

Eodesmus condoni
11000221210320?11012100210011111120220120010032100101011101111100001100 10??
?1??20??????????0??0??00120011112122201113201 23?????????22111????????????1?????
??????????????????????????????01

Allodesmus kernensis
01000010211221011012110212000 0?1121220220?1123200010100 0?0211111010210210??
112020110?011?0200?00100131010003014401100301230112002101211111012000020010
111101200110111122121120011000211?02

Allodesmus demerei
01000020210211?11112110212010001?20120????11?3????1010101??01111010210210???
1???0??????????0?????001?001???3??33??1????122?????????12101??01?00002001022100
2?????011122?????????????????1?03

Atopotarus
00?????0?1??11??10?211?21?01???1??????????10??????1????????????111??010????????????
?????????20????100???????????3????????1?????????????????1??????0?0?1010?1110??????0
1111?21???????????????02

Leptonychotes
00000100211221111131110111010020221110020110022101120200101111110220?0131??
122??111111111121 11???00010?000130133011113012300120021113??111012000021010
000010??????????2?????????????????1144

Phoca vitulina

000001002102211121320100111100200220010201201321010202010011111122200013 12?
122221111111111100110100001111211202211100301120112002101320110010001021010
101000220000110202122121002111211014

Erignathus barbatus
011001002112210120320101110100200220001201200320010202000021111121211013 12?
122221111111111001111100000 01?00120221210030113 0?120021013201100000000021010
1010122?000011020212222100211121 1114

Cystophora cristata
000001012112101111320101110100202220011201101220110012000021111122101013 12?
122221111111111210110000110011013014302101301130112002101220121012000021010
0010102?000011120212112100211121 1114

Mirounga angustirostris
000000012122 2?111321101111100100200010201101221110?021000211111222010231 2?
122221111111111111111100010011000310441111030113001200 2?0132?121012000021010
201010200100111122220121??????201114

Monachus monachus
000000002122211101320101111110?112010002002002210102021000211111022000131 1?
122221111111111111111100002110111112221112030123011200211132?110100001021010
200100211000110222221221002 0??201124

Acrophoca
0?000100212220110132110011010020221100021110022??10?021001111111222000131 20
?22221?????????????????10000?10????2??22??1??301130?120?21?132?1??100000021010001
01021?100110111221221002 0??201?43

Piscophoca
010001002112101111321101111100201211100201202?2??10?021001111100021010231 2?
122??1?????111?011111000000 1??102??22??1??301230112002101 32?11???000002101000
011121110011112212112 1??????????43

Noriphoca gaudini
0100???0???????1?132110011100?????????020120221101??01?????????????????????????
?????????010101100002110121121 22???????122011200211132?1?????????????????????
??????????????????????????20

Devinophoca claytoni
00000??1211211?10130011011 0?1020222000020120 20???0??0100001111111212101 21???
1???11?1??????100?0??00021102??1122111112201210?120021113 2?11?000001021010000
110?????0010102?2102100 2???????22

Eumetopias jubatus

01112000112300111030110010011020122100120100022010110001211011010112001210011000011000011020001000012001101301430110030123011200210130?110112000021010220101210120011122111220100001201204

Arctocephalus townsendi
01011010212201110030110010011020122120120000122101110010201011110012002100011000011000011020000000012000????3??43??1??301130?120021?120211000200002101022010120101????2?????????????????????????1244

Otaria flavescens
11111010212200110031110110010021222110220100122010111010211011110102002100011000011000011020001000012000???????????1??3011301120021?120011001200002101022110????2?????????????????????????11244

Zalophus californianus
01012000212201110030110010011020122220020100122100010010210011111102000100011000011000011120001000012001101301440210030113011200210130?110102001021010220100220120111122101221100??201204

Callorhinus ursinus
01102010212201111031111110011021122220020001022100010010210011110112000101011000011000011110001100012000101301340110030113001200210120211001000002101022010120011122111120100000211204

Callorhinus gilmorei
??11000????012000101301220111130112011200211020111001100002101021010????????????????????01??1?04

Thalassoleon mexicanus
01011010212201110030110010111020121220120110032100111011211011000102000101011?0011000???120000000002110?111112201 1??301120?120021?110011001000002101022010221100111222212200000??????03

Pithanotaria starri
010?????2??20111?030110010001?202????0120??0022???0100???????1?1????000????????0?????????010000000001000?1?11122011 0?301120?12002101???110010000021010120112????1011112222122000100?211?03

References 2

Arnason, U. (1974). Comparative chromosome studies in Pinnipedia. *Hereditas* 76: 179-226.

Arnason, U., Gullberg, A., Janke, A., Kullberg, M., Lehman, N., Petrov, E.A., & Väinolä, R. (2006). Pinniped phylogeny and a new hypothesis for their origin and dispersal. *Molecular Phylogenetics and Evolution*, 46:345-354.

Barnes, L. G. (1979). Fossil Enaliarctine Pinnipeds (Mammalia: Otariidae) from Pyramid Hill, Kern County, California. *Contributions in Science, Natural History Museum of Los Angeles County 318*, 1–41.

Barnes, L. G. (1987). An Early Miocene Pinniped of the Genus *Desmatophoca* (Mammalia: Otariidae) from Washington. *Natural History Museum of Los Angeles County*, Los Angeles, California, 20 pp.

Barnes, L. G. (1989). A new enaliarctine pinniped from the Astoria Formation, Oregon, and a classification of the Otariidae (Mammalia: Carnivora). *Contributions in Science, Natural History Museum of Los Angeles County 403*, 1–26.

Barnes, L. G. (1990). A new Miocene enaliarctine pinniped of the genus *Pteronarctos* (Mammalia: Otariidae) from the Astoria Formation, Oregon. *Contributions in Science, Natural History Museum of Los Angeles County 422*, 1–20.

Barnes, L. G. (1992). A new genus and species of middle Miocene enaliarctine pinniped (Mammalia, Carnivora, Otariidae) from the Astoria Formation in coastal Oregon. *Contributions in Science, Natural History Museum of Los Angeles County* 431:1–27.

Barnes, L. G. (2007). Otarioidea. *Evolution of Tertiary Mammals of North America* 2:523-541.

Baskin, J. A. (1998). Mustelidae pp. 152–173 in Janis, C.M., Scott, K.M., & Jacobs, L.L. (eds.), Evolution of Tertiary Mammals of North America, Volume 1: Terrestrial

Carnivores, Ungulates, and Ungulate-like Mammals. Cambridge University Press, Cambridge.

Bebej, R. M. (2009). Swimming mode inferred from skeletal proportions in the Fossil Pinnipeds *Enaliarctos* and *Allodesmus* (Mammalia, Carnivora). *Journal of Mammalian Evolution* 16:77-97.

Berta, A. & Deméré, T. A. (1986). *Callorhinus gilmorei* n. sp., (Carnivora: Otariidae) from the San Diego Formation (Blancan) and its implications for otariid phylogeny. *Transactions of the San Diego Society of Natural History* 21(7):111-126.

Berta, A., Ray, C.E.,Wyss, A.R. (1989). Skeleton of the oldest known pinniped, *Enaliarctos mealsi*. *Science 244*:60–62.

Berta, A. (1991). New *Enaliarctos* (Pinnipedimorpha) from the Oligocene and Miocene of Oregon and the role of "Enaliarctids" in pinniped phylogeny. *Smithsonian Contributions to Paleobiology 69*, 1–36.

Berta, A. (1994a). A new species of phocoid pinniped *Pinnarctidion* from the early Miocene of Oregon. *Journal of Vertebrate Paleontology 14*, 405–13.

Berta, A., & Wyss, A. R. (1994). Pinniped phylogeny. In A. Berta & T.A. Deméré (Eds.), *Contributions in marine mammal paleontology honoring Frank C. Whitmore, Jr.* (pp. 33–56) Proceedings of the San Diego Society of Natural History 29.

Berta, A., Churchill, M., & Boessenecker, R. W. (2018). The origin and evolutionary biology of pinnipeds: seals, sea lions, and walruses. Annual Review of Earth and Planetary Sciences, 46(1), 203–228. https://doi.org/10.1146/annurev-earth-082517-010009

Biewer, J. N., Velez-Juarbe, J., and Parham, J. F. (2020). Insights on the dental evolution of walruses based on new fossil specimens from California. *Journal of Vertebrate Paleontology*, 40(5), e1833896. https://doi.org/10.1080/02724634.2020.1833896

Boessenecker, R. W. and Churchill, M. (2015). The oldest known fur seal. *Biology Letters* 11: 20140835.

Boessenecker, R.W., & Churchill, M. (2018). The last of the desmatophocid seals: a new species of *Allodesmus* from the upper Miocene of Washington, USA, and a revision of the taxonomy of Desmatophocidae. *Zoological Journal of the Linnean Society 184*:211–35.

Boessenecker, R., Poust, A., Boessenecker, S., Churchill, M. (2024). Tusked walruses (Carnivora: Odobenidae) from the Miocene-Pliocene Purisima Formation of Santa Cruz, California (U.S.A.): a new species of the toothless walrus *Valenictus* and the oldest records of Odobeninae and Odobenini. *Journal of Vertebrate Paleontology*, DOI: 10.1080/02724634.2023.2296567

Brazeau, M. (2011). Problematic character coding methods in morphology and their effects. *Biological Journal of the Linnean Society* 104:489-498.

Bremer, K. (1994). Branch support and tree stability. *Cladistics* 10:295-304.

Cirot, E., & de Bonis, L. O. U. I. S. (1992). Révision du genre *Amphicynodon*, carnivore de l'Oligocène. *Palaeontographica Abteilung A*, 220(4–6), 103-130.

Congreve, C.R. & Lamsdell, J.C. (2016). Implied weighting and its utility in palaeontological datasets: a study using modelled phylogenetic matrices. *Palaeontology*, 59: 447-462. https://doi.org/10.1111/pala.12236

Davis, C. S., Delisle, I., Stirling, I., Siniff, D. B., & Strobeck, C. (2004). A phylogeny of the extant Phocidae inferred from complete mitochondrial DNA coding regions. *Molecular Phylogenetics and Evolution*, 33(2), 363–377.

Debey, L.M. & Pyenson, N.D. (2012). Osteological correlates and phylogenetic analysis of deep diving in living and extinct pinnipeds: What good are big eyes? *Marine Mammal Science* 29:48–83

Delisle, I., & Strobeck, C. (2005). A phylogeny of the Caniformia (order Carnivora) based on 12 complete protein-coding mitochondrial genes. *Molecular Phylogenetics and Evolution 37*, 192–201.

Deméré, T. A. (1994a). Two new species of fossil walruses (Pinnipedia: Odobenidae) from the Upper Pliocene San Diego Formation, California. *Proceedings of the San Diego Society of Natural History*, 29: 77–98.

Deméré, T. A. (1994b). The family Odobenidae: a phylogenetic analysis of fossil and living taxa. *Proceedings of the San Diego Society of Natural History*, 29: 99–123.

Deméré, T. A. & Berta, A. (2001). A reevaluation of *Proneotherium repenningi* from the Miocene Astoria Formation of Oregon and its position as a basal odobenid (Pinnipedia: Mammalia). *Journal of Vertebrate Paleontology*, 21(2): 279–310.

Deméré, T., and Berta, A. (2002). The Miocene pinniped *Desmatophoca oregonensis* Condon, 1906 (Mammalia: Carnivora), from the Astoria Formation, Oregon. *Smithsonian Contributions to Paleobiology* 93:113–147.

Deméré, T. A. & Berta, A. (2005). New skeletal material of *Thalassoleon* (Otariidae: Pinnipedia) from the late Miocene-early Pliocene (Hemphillian) of California. *Bulletin of the Florida Museum of Natural History* 45(4):379–411.

de Muizon, C. (1981). Les vertebres fossiles de la Formation Pisco (Perou). Premiere parti: Deux nouveaux Monachina (Phocidae, Mammalia) du Pliocene de Sud-Sacaco. *Recherche sur les grandes civilisations Memoire* 6:1–150.

Domning, D. P. (2018). Sirenian Evolution; pp. 856–859 in Würsig, B., Thewissen, J.G.M., Kovacs, K.M. Encyclopedia of Marine Mammals (Third Edition), Academic Press

Downs, T. (1956). A New Pinniped from the Miocene of Southern California: With Remarks on the Otariidae. *Journal of Paleontology* 30(1): 115–131.

Esteban, J. M., Martín-Serra, A., Pérez-Ramos, A., Mulot, B., Jones, K., & Figueirido, B. (2023). The impact of the land-to-sea transition on evolutionary integration and modularity of the pinniped backbone. *Communications Biology*, 6(1): 1141.

Everett, C. J., Deméré, T. A., & Wyss, A. R. (2023). A New Species of Pinnarctidion from the Pysht Formation of Washington State (U.S.A.) and a Phylogenetic Analysis of Basal Pan-Pinnipeds (Eutheria, Carnivora). *Journal of Vertebrate Paleontology 42(3)*.

Farris, J. S. (1969). A successive approximations approach to character weighting. *Systematic Zoology*, 18(4), 374-385.

Felsenstein, J. (1985). Confidence limits on phylogenies: an approach using the bootstrap. *Evolution* 39, 783–791.

Ferrusquía-Villafranca, I., & Wang, X. (2021). The first Paleogene mustelid (mammalia, Carnivora) from southern North America and its paleontologic significance. *Journal of South American Earth Sciences*, 109, 103236.

Finarelli, J. A. (2008). A total evidence phylogeny of the Arctoidea (Carnivora: Mammalia): Relationships among basal taxa. *Journal of Mammal Evolution 15*, 231–259.

Flynn, J. J., Neff, N. A., & Tedford, R. H. (1988). Phylogeny of the Carnivora; pp. 73–116 in M. J. Benton (ed.) *The Phylogeny and Classification of the Tetrapods, Vol. 2: Mammals*. Oxford: Clarendon.

Flynn, J. J., & Nedbal, M. A. (1998). Phylogeny of the Carnivora (Mammalia): congruence vs incompatibility among multiple datasets. *Molecular Phylogenetics and Evolution 9*, 414–426.

Flynn, J. J., Finarelli, J. A., Zehr, S., Hsu, J., & Nedbal, M. A. (2005). Molecular Phylogeny of the Carnivora (Mammalia): Assessing the Impact of Increased Sampling on Resolving Enigmatic Relationships. *Systematic Biology 54*, 317–337.

Flynn, J. J., Finarelli,J. A., & Spaulding, M. (2010). Phylogeny of the Carnivora and Carnivoramorpha, and the use of the fossil record to enhance understanding of evolutionary transformations; pp. 25–63 in A. Goswami and A. Friscia (eds.), *Carnivoran Evolution: New Views on Phylogeny, Form and Function*. Cambridge University Press, Cambridge.

Fulton, T. L., & Strobeck, C. (2006). Molecular phylogeny of the Arctoidea (Carnivora): effect of missing data on supertree and supermatrix analyses of multiple gene data sets. *Molecular Phylogenetics and Evolution 41*, 165–81.

Furbish, R. (2015). Something Old, Something New, Something Swimming in the Blue: An Analysis of the Pinniped Family Desmatophocidae, its Phylogenetic Position and Swimming Mode. M.S. Thesis, San Diego State University.

Goloboff, P.A. (2014). Oblong, a program to analyse phylogenomic data sets with millions of characters, requiring negligible amounts of RAM. *Cladistics* 30: 273–281.

Goloboff, P.A., Torres, A., & Arias, J.S. (2018). Weighted parsimony outperforms other methods of phylogenetic inference under models appropriate for morphology. *Cladistics* 34:407-437.

Goloboff, P. A. & Morales, M. E. (2023). TNT version 1.6, with a graphical interface for MacOS and Linux, including new routines in parallel. *Cladistics*, 39: 144-153.

Gordon, K. R. (1983). Mechanics of the limbs of the walrus (*Odobenus rosmarus*) and the California sea lion (*Zalophus californianus*). *Journal of Morphology* 175:73-90.

Hassanin, A., Veron, G., Ropiquet, A., Jansen van Vuuren, B., Lecu, A., Goodman, S.M., et al. (2021). Evolutionary history of Carnivora (Mammalia, Laurasiatheria) inferred from mitochondrial genomes. *PLoS ONE* 16(2): e0240770.

Higdon, J. W., Bininda-Emonds, O. R., Beck, R. M., & Ferguson, S. H. (2007). Phylogeny and divergence of the pinnipeds (Carnivora: Mammalia) assessed using a multigene dataset. *BMC Evolutionary Biology*, 7, 1–19.

Holmes S. (2003). Bootstrapping phylogenetic trees: theory and methods. *Statistical Science* 18, 241-255.

Horikawa, H. (1995). A primitive odobenine walrus of Early Pliocene age from Japan. *Island Arc* 3(4):309–328.

Hunt, R. M., Jr. (1998a). Ursidae; pp. 174–195 in Janis, C.M., Scott, K.M., & Jacobs, L.L. (eds.), Evolution of Tertiary Mammals of North America, Volume 1: Terrestrial Carnivores, Ungulates, and Ungulate-like Mammals. Cambridge University Press, Cambridge.

Hunt, R. M., Jr. (1998b). Amphicyonidae; pp. 196–227 in Janis, C.M., Scott, K.M., & Jacobs, L.L. (eds.), Evolution of Tertiary Mammals of North America, Volume 1:

Terrestrial Carnivores, Ungulates, and Ungulate-like Mammals. Cambridge University Press, Cambridge.

Hunter, L. (2019). Carnivores of the world (second ed.). Princeton University Press.

Kellogg, R. (1925). New pinnipeds from the Miocene diatomaceous earth near Lompoc, California. *Contributions to Palaeontology from the Carnegie Institution of Washington* 348:71-95.

Kohno, N., Barnes, L. G., & Hirota, K. (1994). Miocene fossil pinnipeds of the genera *Prototaria* and *Neotherium* (Carnivora; Otariidae; Imagotariinae) in the North Pacific Ocean: evolution, relationships and distribution. *Island Arc* 3:285–308.

Kohno, N. (2006). A new Miocene odobenid (Mammalia: Carnivora) from Hokkaido, Japan, and its implications for odobenid phylogeny. *Journal of Vertebrate Paleontology*, 26(2), 411–421.

Koretsky, I.A & Holec, P. (2002). A Primitive Seal (Mammalia: Phocidae) from the Early Middle Miocene of Central Paratethys. *Smithsonian Contributions to Paleobiology* 93:163–178.

Law, C. J., G. J. Slater, & Mehta, R. S. (2017). Lineage diversity and size disparity in Musteloidea: Testing patterns of adaptive radiation using molecular and fossil-based methods. *Systematic Biology 67*:127–144.

Luan, P. T., Ryder, O. A., Davis, H., Zhang, Y. P., & Yu, L. (2013). Incorporating indels as phylogenetic characters: impact for interfamilial relationships within Arctoidea (Mammalia: Carnivora). *Molecular Phylogenetics and Evolution* 66: 748–756.

Marjanovic, D., Maddin, H. C., Olori, J. C., & Laurin, M. (2023). The new problem of Chinlestegophis and the origin of caecilians (Amphibia, Gymnophionomorpha) is

highly sensitive to old problems of sampling and character construction. *HAL Open Science*. Hal-04238145

Matthew, W.D., & Granger, W. (1924). New Carnivora from the Tertiary of Mongolia. *American Museum Novitates* 104: 1–9.

McKenna, M. C., & Bell, S. K. (1997). *Classification of mammals: above the species level*. Columbia University Press.

Mitchell, E. (1968). The Mio–Pliocene pinniped *Imagotaria*. Journal of the Fisheries Board of Canada, 25, 1843–1900.

Mitchell, E. D., & Tedford, R. H. (1973). The Enaliarctinae: a new group of extinct aquatic Carnivora and a consideration of the origin of the Otariidae. *Bulletin of the American Museum of Natural History 151*, 201–284.

Nyakatura, K. & Bininda-Emonds, O. R. P. (2012). Updating the evolutionary history of Carnivora (Mammalia): a new species-level supertree complete with divergence time estimates. *BMC Evolutionary Biology 10*.

Park, T., Burin, G., Lazo-Cancino, D., Rees, J. P. G., Rule, J. P., Slater, G. J., Cooper, N. (2024). Charting the course of pinniped evolution: insights from molecular phylogeny and fossil record integration. *Evolution* 78(7):1212-1226.

Paterson, R. S., Rybczynski, N., Kohno, N., & Maddin, H. C. (2020). A total evidence phylogenetic analysis of pinniped phylogeny and the possibility of parallel evolution within a monophyletic framework. *Frontiers in Evolutionary Biology 7*.

Pierce, S. E., Clack, J. A., & Hutchinson, J. R. (2011). Comparative axial morphology in pinnipeds and its correlation with aquatic locomotory behaviour. *Journal of Anatomy* 219:502-514.

Reichmuth, C., Holt, M. M., Mulsow, J., Sills, J. M., & Southall, B. L. (2013). Comparative assessment of amphibious hearing in pinnipeds. *Journal of Comparative Physiology A*, 199, 491-507.

Rule, J. P., Adams, J. W., Rovinsky, D. S., Hocking, D. P., Evans, A. R., & Fitzgerald, E. M. G. 2020. A new large-bodied Pliocene seal with unusual cutting teeth. *Royal Society Open Science* 7201591201591.

Rybczynski N, Dawson, M. R., & Tedford, R. H. (2009). A semi-aquatic Arctic mammalian carnivore from the Miocene epoch and origin of Pinnipedia. *Nature 458*, 1021–24.

Sato, J. J., M.Wolsan, S. Minami, T. Hosoda, M. H. Sinaga, K. Hiyama, Y. Yamaguchi, and H. Suzuki. (2009). Deciphering and dating the red panda's ancestry and early adaptive radiation of Musteloidea. *Molecular Phylogenetics and Evolution 53*:907–922.

Sereno, P. C. (2007). Logical basis for morphological characters in phylogenetics. *Cladistics*, 23(6), 565-587.

Simões, T. R., Caldwell, M. W. , Palci, A., & Nydam, R. L. (2017). Giant taxon-character matrices: quality of character constructions remains critical regardless of size. *Cladistics 33*, 198–219.

Simpson, G. G. (1945). The principles of classification and a classification of mammals. *Bulletin of the American Museum of Natural History* 85:1–350.

Stirton, R. A. (1960). A marine carnivore from the Clallam Miocene Formation, Washington. Its correlation with nonmarine faunas. *University of California Publications in Geological Sciences* 36:345-368.

Tanaka, Y., & Kohno, N. (2015). A New Late Miocene Odobenid (Mammalia: Carnivora) from Hokkaido, Japan Suggests Rapid Diversification of Basal Miocene Odobenids. *PLoS ONE 10(8)*: e0131856.

Tate-Jones M.K., Peredo, C.M., Marshall, C.D., Hopkins, S.S.B. (2020). The dawn of Desmatophocidae: a new species of basal desmatophocid seal (Mammalia, Carnivora) from the Miocene of Oregon, U.S.A. *Journal of Vertebrate Paleontology* 40(4).

Tedford, R. H. (1976). Relationships of pinnipeds to other carnivores (Mammalia). *Systematic Zoology 25*, 363–74.

Tennett, K. A., Costa, D. P., Nicastro, A. J., & Fish, F. E. (2018). Terrestrial locomotion of the northern elephant seal (*Mirounga angustirostris*): limitation of large aquatically adapted seals on land? *Journal of Experimental Biology*, 221(18), jeb180117.

Tomiya, S. (2011). A new basal caniform (Mammalia: Carnivora) from the middle Eocene of North America and remarks on the phylogeny of early carnivorans. *PLoS one*, 6(9), e24146.

Tomiya, S., & Tseng, Z. J. (2016). Whence the beardogs? Reappraisal of the Middle to Late Eocene 'Miacis' from Texas, USA, and the origin of Amphicyonidae (Mammalia, Carnivora). *Royal Society open science 3*: 160518.

Trouessart, E. L. (1885). Catalogue des mammifères vivants et fossiles (Carnivores). *Bulletin de la Société d'Études Scientifiques d'Angers* 14, 1–108.

Velez-Juarbe, J. (2017). *Eotaria citrica*, sp. nov., a new stem otariid from the "Topanga" formation of Southern California. *PeerJ* 5:e3022

Uhen, M. D. (2010). The origin(s) of whales. *Annual Review of Earth and Planetary Sciences*, 38(1), 189–219.

Wang, X. M., McKenna, M. C., & Dashzeveg, D. (2005a). *Amphicticeps* and *Amphicynodon* (Arctoidea, Carnivora) from Hsanda Gol Formation, central Mongolia, and phylogeny of basal arctoids with comments on zoogeography. *American Museum Novitates 3483*, 1–57.

Wang, X. M., Whistler, D. P., & Takeuchi, G. T. (2005b). A new basal skunk *Martinogale* (Carnivora, Mephitinae) from late Miocene Dove Spring Formation, California, and origin of new world mephitines. *Journal of Vertebrate Paleontology*, 25(4), 936–949.

Wang, X. M., Emry, R. J., Boyd, C. A., Person, J. J., White, S. C., & Tedford, R. H. (2023). An exquisitely preserved skeleton of *Eoarctos vorax* (nov. gen. et sp.) from Fitterer Ranch, North Dakota (early Oligocene) and systematics and phylogeny of North American early arctoids (Carnivora, Caniformia). *Journal of Vertebrate Paleontology Memoir 42:sup1,* 1–123.

Wesley, G. D., & Flynn, J. J. (2003). A revision of *Tapocyon* (Carnivoramorpha), including analysis of the first cranial specimens and identification of a new species. *Journal of Paleontology*, 77(4), 769–783.

Wesley-Hunt, G. D., & Flynn, J. J. (2005). Phylogeny of the carnivora: Basal relationships among the carnivoramorphans, and assessment of the position of 'miacoidea' relative to carnivora. *Journal of Systematic Palaeontology*, 3:1, 1–28.

Wheeler, Q. D. (1986). Character weighting and cladistic analysis. *Systematic Biology*, 35(1): 102-109.

Wolsan, M. (1993). Phylogeny and classification of early European Mustelida (Mammalia: Carnivora). *Acta Theriologica. 38*(4), 345–384.

Wolsan, M., Wyss, A. R., Berta, A., & Flynn, J. J. (2020). Pan-Pinnipedia, new clade name. *Phylonyms: A Companion to PhyloCode.*

Wright, A., & Hillis, D. (2014). Bayesian Analysis Using a Simple Likelihood Model Outperforms Parsimony for Estimation of Phylogeny from Discrete Morphological Data. *PLoS ONE* 9(10): e109210

Wynen, L. P., Goldsworthy, S. D., Insley, S. J., Adams, M., Bickham, J. W., Francis, J., Gallo, J. P., Hoelzel, A. R., Majluf, P., White, R. W., & Slade, R. (2001). Phylogenetic relationships within the eared seals (Otariidae: Carnivora): Implications for the historical biogeography of the family. *Molecular Phylogenetics and Evolution*, 21(2), 270–284.

Wyss, A. R., & Flynn, J. J. (1993). A phylogenetic analysis and definition of the Carnivora. In F. S. Szalay, M. J. Novacek & M. C. McKenna, (Eds.), *Mammal phylogeny: Placentals* (pp. 32–52). Springer-Verlag, New York, NY.

Yonezawa, T., N. Kohno, and M. Hasegawa. 2009. The monophyletic origin of sea lions and fur seals (Carnivora; Otariidae) in the Southern Hemisphere. *Gene* 441:89–99.

Yu, L., Zhang, Ya-ping. (2006). Phylogeny of the caniform carnivora: evidence from multiple genes. *Genetica*, 127, 65–79.

Zharkikh, A., & Li, W.-H. (1992). Statistical properties of bootstrap estimation of phylogenetic variability from nucleotide sequences. Four taxa with a molecular clock. *Molecular Biological Evolution* 9, 1119-1147.

Chapter 3: Morphometric analysis of upper carnassial dentition to infer diets of fossil arctoids

Introduction 3

Carnivorans primitively possess an enlarged upper fourth premolar (P4) that operates in concert with the lower first molar (m1), producing a shearing bite. In several clades, the P4/m1 pair are modified to produce various masticatory functions, ranging from durophagy, to folivory, to pierce feeding. Oligocene and early Miocene arctoids, such as Amphicyonidae,

early pan-pinnipeds, early ursoids, and early musteloids, exhibit a high degree of dental disparity that presumably corresponds with unique dietary functions. The dentition of extant carnivorans can be used to establish a model for how dental morphology corresponds to dietary function, which can inform hypotheses of functional morphology in these extinct carnivorans. The diets of extinct mammals can also be inferred using other tools such as microwear, finite element analysis, stable isotopes, coprolites, or preserved gut contents. Morphometric analysis, however, provides an opportunity to efficiently and non-destructively sample a wide range of taxa and characterize their dental variability in order to test hypotheses of phylogenetic signal and dietary niche.

Craniodental morphology has been demonstrated to correspond with dietary ecology in carnivorans. A classic metric is the relative blade length (RBL) of the lower m1 talonid, taken as a fraction of total crown length (Van Valkenberg, 1989). The RBL positively correlates with the proportion of meat in a terrestrial carnivoran's diet, but it is not ideal for assessing taxa with a variety of specialized diets. With the advent of geometric morphometrics, more comprehensive tools for dietary assessment became possible (Adams et al., 2004). Cranial and mandibular 2D landmarks have been used to correlate tooth shape with diet among extinct and extant ursids (Figueirido et al., 2009) and 2D landmarks and linear measurements of carnivoran crania have revealed that the relative distance from the jaw joint to certain teeth correlates with diet but varies by clade (Harano & Asahara, 2022). The application of 3D morphometrics has similarly demonstrated that diet, phylogenetic affinity, and lower molar shape are strongly correlated in living carnivorous mammals (Tarquini et al., 2020). However, use of these tools is complicated by the fact that

preservation of complete mandibles, let alone lower dentitions, is rare among fossil arctoids, and even then, much of the upper dentition tends to disarticulate. Therefore, the simple approach of focusing on a single highly functional tooth, the upper fourth premolar, is advantageous.

The diets of extinct arctoids have received considerable attention. The feeding modes of extinct pan-pinnipeds were scrutinized using discrete anatomical characters (Adam & Berta, 2002), yet the statistical significance of the results were mixed. Morphometric studies using extant specimens have yielded more consistent results (Jones et al., 2013; Kienle & Berta, 2015). These studies identify important functional morphological trends that distinguish different feeding modes within pinnipeds, but they do not thoroughly examine stem-pinnipeds or other arctoids. Further, their methods cannot be consistently applied to partially preserved fossils. This study aims to compare a comprehensive sample of terrestrial and aquatic carnivorans in order to assess the dietary shift that presumably took place during the transition of pan-pinnipeds from terrestrial to aquatic environments, and to explore dietary trends in other extinct arctoids.

Methods 3

In this study I examine the upper fourth premolar because this tooth is frequently preserved in fossils and is highly functional in food processing, therefore providing a simple and consistent tool for comparing diet in a wide variety of taxa. Landmarks were captured in the occlusal view to avoid the more pronounced effects of tooth wear and abrasion when landmarks are captured in labial or lingual view. Ideal landmarks are homologous anatomical

structures that provide adequate coverage of form and can be reliably replicated. Landmark quality can be divided into Types I, II, and III (Zelditch et al., 2012). Type I landmarks (Table 3.1: 1, 2, 3, and 7) correspond to homologous structures or clear intersections of two or more structures. Type II landmarks (5, 6, 8, and 9) correspond to definable points such as local maxima or minima, but are not strictly homologous in different taxa. Type III landmarks, the lowest in quality, were not used in this study. Some landmarks used here could be considered Type I depending on the presence of a carnassial notch (3), parastyle (4), protocone (8), or hypocone (12). Otherwise they are based on relative positions like Type II landmarks. Landmarks were placed on specimen images using tpsDig2 version 2.32 (Rohlf, 2006).

After the landmarks were recorded, the coordinate data from the TPS file was uploaded to MorphoJ version 1.08.01 (Klingenberg, 2011) to read in the classifier variables, perform Procrustes fit, and carry out further analyses. Procrustes superimposition brings all specimens into alignment relative to the centroid, or focal point. Classifiers such as clade, extinction status, and diet category (if known) were included alongside the landmark data. See Table 3.2 for a complete list of taxa and corresponding references.

The first steps in analyzing the data involved the generation of a covariance matrix and performance of a principal component analysis (PCA). This allowed visualization of shape differences along two axes which represented the simplest way to separate all the multidimensional variation in the sample. To more rigorously separate taxa based on classifier groups, canonical variate analysis (CVA) was performed. Segregation based on

clade and diet, relative to shape, were tested in two separate analyses. The goal of the clade identity CVA was to determine the morphological distinctiveness of each clade. Ursids and pinnipeds would be expected to separate more distinctly than the others because of their highly modified dentition.

The initial steps of the analysis were complicated by the fact that the diet of the extinct taxa was unknown and consequently the initial dietary category was "unknown". However, this categorization is necessary as the first step in determining which categories these fossil taxa are most similar to. A diet category CVA was used initially to differentiate groupings among modern taxa. Then a discriminant function analysis (DFA) was used to determine how likely each fossil taxon of unknown diet was to cluster reliably with an existing dietary category. Taxa fitting better into a known category than into the unknown category are reclassified as such, and a new CVA is run. Iterating between the CVA results and DFA cross-validations allows gradual placement of fossil taxa into dietary categories which can later be statistically tested.

Results 3

A plot of principal component axes 1 and 2 (Figure 3.1) reveals substantial overlap among early-diverging caniforms and more apparent separation among ursids, pan-pinnipeds, and later-diverging musteloids. Both clade identity and diet category had significant effects on the Procrustes distances separating the sample.

Canonical variate analysis of shape and clade identity (Figure 3.2) predictably shows the greatest separation between pan-pinnipeds and ursids, as well as more overlap between other clades. Permutation tests demonstrate that both ursids and pan-pinnipeds can be significantly distinguished from basal arctoids and musteloids, and that pan-pinnipeds can be distinguished from canids, and ursids from pan-pinnipeds.

CVA of shape and diet category (Figure 3.3) fully distinguishes piscivores (pan-pinnipeds) and mostly separates the carnivores, yet leaves considerable overlap of the other categories (folivores, frugivore, invertebrate consumers, and omnivores), with frugivores overlapping slightly with each of them. Permutation tests show that carnivores are significantly distinct from the other categories except frugivores, folivores overlap with all other categories except carnivores, while omnivores and invertebrate consumers are both distinct from piscivores.

Discussion 3

The dietary niches occupied by extinct carnivorans can be inferred from the diet CVA plot. Fossil taxa were initially categorized as "unknown" but many were placed tentatively within diet categories based on significant overlap observed from DFA results. Some fossil taxa that occupy presently empty morphospace may represent transitional stages between two or more dietary specializations. Due to their tight clustering around the carnivorous diet morphospace, many extinct taxa were assigned that diet category. These likely early-diverging carnivores include *Amphicticeps, Amphicynodon, Amphicyon, Cynodictis, Cynelos, Daphoenus, Drassonax, Enhydrocyon, Epicyon, Gustafsonia, Hesperocyon, Lycophocyon, Martinogale, Mustelavus, Oaxacagale, Pachycynodon, Paradaphoenus, Plesictis,*

Subparictis, *Tapocyon*, *Temnocyon*, and *Zodiolestes* (see Table 3.2). *Allocyon* was scored as an omnivore, although it is somewhat of an outlier relative to the modern omnivores.

The two specimens of *Cephalogale sp.* fall outside of the space occupied by carnivores, but only one overlaps with omnivores and frugivores. Because of that overlap, and because of this taxon's likely close relationship with *Allocyon* and ursids (Wang et al., 2005; Wang et al., 2023), omnivory would be the most logical hypothesized diet for *Cephalogale*.

Eoarctos does not occupy the carnivore morphospace, instead falling along the border of omnivores and in the middle of frugivores. The analysis places *Eoarctos* very close to the modern generalist omnivore mustelid, *Mellivora*, which prefers to eat vertebrates, but will supplement its diet with melons and other water- or nutrient-rich plants during the dry season (Begg et al., 2003). Several *Eoarctos* fossils have molars that are conspicuously damaged, missing, and subsequently healed, which indicates a durophagous habit (Wang et al., 2023). Although it was initially argued that the observed trauma occurred from consuming shelled molluscs, as observed in *Enhydra* (Winer et al., 2013), one cannot rule out the possibility that it resulted from crushing robust seeds or nuts.

Perhaps the most unusual fossil taxon considered here is *Kolponomos*, a littoral ursoid from the Oligo-Miocene of Washington (Stirton, 1960; Tedford, et al., 1994). The cheek teeth are extremely broad, but their cusp morphology is incompletely understood because all known specimens are worn nearly to the roots. The present analysis places *Kolponomos* within the folivore and frugivore morphospace, although it is closest in landmark shape to some early

pan-pinnipeds. It has been argued that *Kolponomos* was a durophagous molluscivore because its teeth resemble those of *Enhydra*, the sea otter (Tedford et al., 1994). Finite element analysis indicates that its jaw structure seems suited to prying, like the motion thought to have been employed by *Smilodon* (Tseng et al., 2016), a notion supported by cranial morphometrics (Modafferi et al., 2023). It is also plausible, however, that *Kolponomos* developed such tooth wear from mastication of marine macroalgae or seagrass. Evidence for the presence of kelp forests in the Pacific Northwest as early as 32 million years ago (Kiel et al., 2024) and the co-occurrence of many desmostylian fossils in the same units as *Kolponomos* suggests that marine plant matter was abundant in their ecosystem. Additionally, *Kolponomos* is most closely related to *Ailuropoda* within Ursida in almost all phylogenetic analyses tested in Chapter 2 of this work, so the propensity for a plant-rich diet may be ancestral for this taxon.

The simplified dentition of many extinct pan-pinnipeds, such as *Desmatophoca*, *Devinophoca, Eodesmus, Hadrokirus, Imagotaria*, *Osodobenus,* and species of *Pinnarctidion*, causes them to overlap significantly with the morphospace occupied by modern pinnipeds. Accordingly, they are inferred to have had a piscivorous diet. *Proneotherium*, *Pacificotaria*, and species of "*Enaliarctos"* plot in a more intermediate range, so they may have had a varied diet that included more invertebrates. *Proneotherium* was thought to have a piscivorous diet similar to otariids (Kohno et al., 1994).

The fossil pan-pinnipeds that occupy intermediate positions in morphospace between carnivores, invertebrate consumers, and piscivores are distributed in a quasi arc bridging the

three categories. This spectrum of transitional forms nearly follows the sequence of branching presented in Chapter 2. *"Enaliarctos" mealsi* and *tedfordi* are nearest to the plesiomorphic carnivore condition; *Potamotherium* and *Puijila* are intermediate between carnivores and invertebrate consumers; *"Enaliarctos" emlongi*, *"E." barnesi*, and *Proneotherium* are closest to the invertebrate consumers; and *Pacificotaria, "Enaliarctos" mitchelli,* and *Pinnarctidion* are closest to the piscivorous pinnipeds.

Conclusion 3

Landmark morphometric analysis allows arctoid carnassial variation to be visualized in multivariate morphospace, with the clustering of taxa by evolutionary and dietary category permitting estimation of the most likely diet for extinct taxa. As expected, the caniforms that retain more carnassial-like P4s form a cluster that represents the carnivorous diet category. There is substantial overlap among the hypocarnivorous omnivores, insectivores, and folivores, making it difficult to confidently separate these diet categories. Despite some uncertainty, the position of two enigmatic early arctoids, *Eoarctos* and *Kolponomos*, challenges previous hypotheses about their diets. The P4 morphology of *Eoarctos* appears more similar to omnivores such as the modern *Mellivora* and *Ursus* than to durophagous invertebrate consumers such as *Enhydra*, suggesting the taxon may not have relied on crushing hard-shelled molluscs as previously hypothesized (Wang et al., 2023). On a similar note, the dentition of the littoral ursid *Kolponomos* compares better with the folivorous *Tremarctos* and *Ailuropoda* and the transitional piscivores *"Enaliarctos" emlongi* and *"E." barnesi* than it does to the durophagous *Enhydra*. This pattern suggests *Kolponomos* may

have been more omnivorous than previously thought (Tedford et al., 1994), potentially even consuming kelp or other marine foliage to supplement its diet.

The piscivore category occupies a distinct morphospace. Later-diverging pinnipedimorphs cluster together as piscivores, whereas the transitional early pan-pinnipeds bridge the gap between carnivores, insectivores, and piscivores. The observed pattern suggests that pan-pinnipeds may have undergone a two-phased shift in dietary preference over evolutionary time. The first phase was a transition from carnivory to invertebrate consumption, characterized by a retention of the carnassial apparatus and broadening of the protocone shelf for greater masticatory function. The second phase was a transition from invertebrate consumption to piscivory, characterized by a loss of carnassial features in favor of a more simplified tooth for piercing and tearing soft tissue without mastication.

Figures 3

Table 3.1. List of P4 landmark points.

Landmark	Anatomical structure	Type
1	Paracone, or primary cusp	Type I
2	Metacone, or distal heel of crown	Type I
3	Carnassial notch, or minima between paracone and metacone	Type I or II
4	Parastyle, or mesial-most prominence of crown	Type I or II
5	Labial base of paracone	Type II
6	Labial base of metacone	Type II
7	Posterolabial corner of crown	Type II
8	Protocone, or center of lingual cingulum	Type I or II

9	Mesial origin of lingual cingulum	Type II
10	Lingual-most point along cingulum	Type II
11	Distal termination of lingual cingulum	Type II
12	Hypocone, or center of distal cingulum	Type I or II

Table 3.2. List of specimens used in landmark morphometric analysis of upper fourth premolar. Diet references listed where known.

Species	ID	Clade	Extant	Diet category	Diet ref. (if known)
Ailuropoda melanoleuca	Ai1	Ursoid	y	Folivore	Meloro & Tamagnini, 2022
Ailuropoda melanoleuca	Ai2	Ursoid	y	Folivore	Meloro & Tamagnini, 2022
Ailurus fulgens	Ail	Musteloid	y	Folivore	Meloro & Tamagnini, 2022
Allocyon loganensis	All	Arctoid	n	Unknown	
Amphicticeps shackelfordi	Ams	Arctoid	n	Unknown, carnivore?	Morlo et al., 2010
Amphicynodon teilhardi	At1	Arctoid	n	Unknown, carnivore?	Morlo et al., 2010
Amphicynodon teilhardi	At2	Arctoid	n	Unknown, carnivore?	Morlo et al., 2010
Amphicynodon teilhardi	At3	Arctoid	n	Unknown, carnivore?	Morlo et al., 2010
Amphicyon major	Amn	Arctoid	n	Unknown, carnivore?	Morlo et al., 2010
Aonyx capensis	Aon	Musteloid	y	Invertebrates	Meloro & Tamagnini, 2022
Artocephalus townsendi	Arc	Pinniped	y	Piscivore	Meloro & Tamagnini, 2022
Bassariscus astuta	Ba1	Musteloid	y	Omnivore	Morlo et al., 2010
Bassariscus astuta	Ba2	Musteloid	y	Omnivore	Morlo et al., 2010
Callorhinus ursinus	Ca1	Pinniped	y	Piscivore	Meloro & Tamagnini, 2022
Callorhinus ursinus	Ca2	Pinniped	y	Piscivore	Meloro & Tamagnini, 2022
Canis latrans	Cla	Canid	y	Carnivore	Meloro & Tamagnini, 2022
Canis lupus	Clu	Canid	y	Carnivore	Meloro & Tamagnini, 2022

Cephalogale sp.	Cg1	Arctoid	n	Unknown, omnivore?	Morlo et al., 2010
Cephalogale sp.	Cg2	Arctoid	n	Unknown, omnivore?	Morlo et al., 2010
Cynodictis sp.	Cy1	Arctoid	n	Unknown	
Cynodictis sp.	Cy2	Arctoid	n	Unknown	
Cynelos lemanensis	Cyn	Arctoid	n	Unknown	
Cystophora cristata	Cys	Pinniped	y	Piscivore	Meloro & Tamagnini, 2022
Daphoenus vetus	Dap	Arctoid	n	Unknown	
Desmatophoca oregonensis	Dp1	Pinniped	n	Unknown	
Desmatophoca oregonensis	Dp1	Pinniped	n	Unknown	
Devinophoca claytoni	Dev	Pinniped	n	Unknown	
Drassonax harpagops	Dh1	Arctoid	n	Unknown	
Drassonax harpagops	Dh2	Arctoid	n	Unknown	
"Enaliarctos" barnesi	Eba	Pinniped	n	Unknown	
"Enaliarctos" emlongi	Eem	Pinniped	n	Unknown	
"Enaliarctos" mealsi	Eme	Pinniped	n	Unknown	
"Enaliarctos" mitchelli	Emi	Pinniped	n	Unknown	
"Enaliarctos" tedfordi	Ete	Pinniped	n	Unknown	
Enhydra lutris	En1	Musteloid	y	Invertebrates	Meloro & Tamagnini, 2022
Enhydra lutris	En2	Musteloid	y	Invertebrates	Meloro & Tamagnini, 2022
Enhydra lutris	En3	Musteloid	y	Invertebrates	Meloro & Tamagnini, 2022
Enhydra lutris	En4	Musteloid	y	Invertebrates	Meloro & Tamagnini, 2022
Enhydrocyon	Enc	Canid	n	Unknown	
Eoarctos vorax	Eo1	Arctoid	n	Unknown	
Eoarctos vorax	Eo2	Arctoid	n	Unknown	
Eodesmus condoni	Eod	Pinniped	n	Unknown	

Epicyon haydeni	Epi	Canid	n	Unknown	
Eumetopias jubatus	Eu1	Pinniped	y	Piscivore	Meloro & Tamagnini, 2022
Eumetopias jubatus	Eu2	Pinniped	y	Piscivore	Meloro & Tamagnini, 2022
Eumetopias jubatus	Eu3	Pinniped	y	Piscivore	Meloro & Tamagnini, 2022
Galictis vittata	Gal	Musteloid	y	Carnivore	Morlo et al., 2010
Gulo gulo	Gul	Musteloid	y	Carnivore	Meloro & Tamagnini, 2022
Gustafsonia cognita	Gus	Arctoid	n	Unknown	
Hadrokirus martini	Had	Pinniped	n	Unknown	
Hesperocyon gregarius	Hes	Canid	n	Unknown	
Imagotaria downsi	Ima	Pinniped	n	Unknown	
Kolponomos newportensis	Kol	Ursoid	n	Unknown	
Lontra canadensis	Lo1	Musteloid	y	Invertebrates	Meloro & Tamagnini, 2022
Lontra canadensis	Lo2	Musteloid	y	Invertebrates	Meloro & Tamagnini, 2022
Lontra canadensis	Lo3	Musteloid	y	Invertebrates	Meloro & Tamagnini, 2022
Lutra lutra	Lut	Musteloid	y	Invertebrates	Meloro & Tamagnini, 2022
Lycophocyon hutchisoni	Ly1	Canid	n	Unknown	
Lycophocyon hutchisoni	Ly2	Canid	n	Unknown	
Martes americana	Mam	Musteloid	y	Carnivore	Meloro & Tamagnini, 2022
Martinogale faulli	Mar	Musteloid	n	Unknown	
Meles meles	Mls	Musteloid	y	Omnivore	Meloro & Tamagnini, 2022
Mellivora capensis	Mca	Musteloid	y	Omnivore	Begg et al., 2003
Melogale moschata	Mel	Musteloid	y	Omnivore	Meloro & Tamagnini, 2022
Mephitis mephitis	Me1	Musteloid	y	Invertebrates	Meloro & Tamagnini, 2022

Mephitis mephitis	Me2	Musteloid	y	Invertebrates	Meloro & Tamagnini, 2022
Mephitis mephitis	Me3	Musteloid	y	Invertebrates	Meloro & Tamagnini, 2022
Monachus monachus	Mon	Pinniped	y	Piscivore	Meloro & Tamagnini, 2022
Mustelavus priscus	Mpr	Musteloid	n	Unknown	
Nandinia binotata	Na1	Carnivoran	y	Frugivore	Meloro & Tamagnini, 2022
Nandinia binotata	Na2	Carnivoran	y	Frugivore	Meloro & Tamagnini, 2022
Neovison vison	Nv1	Musteloid	y	Carnivore	Meloro & Tamagnini, 2022
Neovison vison	Nv2	Musteloid	y	Carnivore	Meloro & Tamagnini, 2022
Oaxacagale ruizi	Oax	Musteloid	n	Unknown	
Osodobenus eodon	Oso	Pinniped	n	Unknown	
Pachycynodon sp.	Pch	Arctoid	n	Unknown	
Pacificotaria hadromma	Pac	Pinniped	n	Unknown	
Paradaphoenus cuspigerus	Par	Arctoid	n	Unknown	
Phoca vitulina	Ph1	Pinniped	y	Piscivore	Meloro & Tamagnini, 2022
Phoca vitulina	Ph2	Pinniped	y	Piscivore	Meloro & Tamagnini, 2022
Pinnarctidion bishopi	Pbi	Pinniped	n	Unknown	
Pinnarctidion iverseni	Piv	Pinniped	n	Unknown	
Pinnarctidion rayi	Pr1	Pinniped	n	Unknown	
Pinnarctidion rayi	Pr2	Pinniped	n	Unknown	
Pinnarctidion sp.	Psp	Pinniped	n	Unknown	
Plesictis sp.	Ple	Musteloid	n	Unknown	
Potamotherium valletoni	Pot	Pinniped	n	Unknown	
Potos flavus	Pfl	Musteloid	y	Frugivore	Morlo et al., 2010

Procyon lotor	Pl1	Musteloid	y	Omnivore	Meloro & Tamagnini, 2022
Procyon lotor	Pl2	Musteloid	y	Omnivore	Meloro & Tamagnini, 2022
Procyon lotor	Pl3	Musteloid	y	Omnivore	Meloro & Tamagnini, 2022
Proneotherium repenningi	Pn1	Pinniped	n	Unknown	
Proneotherium repenningi	Pn2	Pinniped	n	Unknown	
Puijila darwini	Pui	Pinniped	n	Unknown	
Pusa hispida	Pus	Pinniped	y	Piscivore	
Subparictis gilpini	Sp1	Arctoid	n	Unknown	
Subparictis gilpini	Sp2	Arctoid	n	Unknown	
Subparictis gilpini	Sp3	Arctoid	n	Unknown	
Tapocyon robustus	Tap	Carnivoran	n	Unknown	
Taxidea taxus	Tt1	Musteloid	y	Omnivore	Meloro & Tamagnini, 2022
Taxidea taxus	Tt2	Musteloid	y	Omnivore	Meloro & Tamagnini, 2022
Temnocyon ferox	Tem	Canid	n	Unknown	
Tremarctos ornatus	Tre	Ursoid	y	Folivore	Meloro & Tamagnini, 2022
Urocyon cinereoargenteus	Uro	Canid	y	Omnivore	Meloro & Tamagnini, 2022
Ursus americanus	UAm	Ursoid	y	Omnivore	Meloro & Tamagnini, 2022
Ursus maritimus	UMF	Ursoid	y	Carnivore	Meloro & Tamagnini, 2022
Ursus maritimus	UMM	Ursoid	y	Carnivore	Meloro & Tamagnini, 2022
Vulpes vulpes	Vul	Canid	y	Carnivore	Meloro & Tamagnini, 2022
Zodiolestes diamonelixensis	Zod	Arctoid	n	Unknown	

Figure 3.1. Principal Components Analysis, plotting axes 1 and 2.

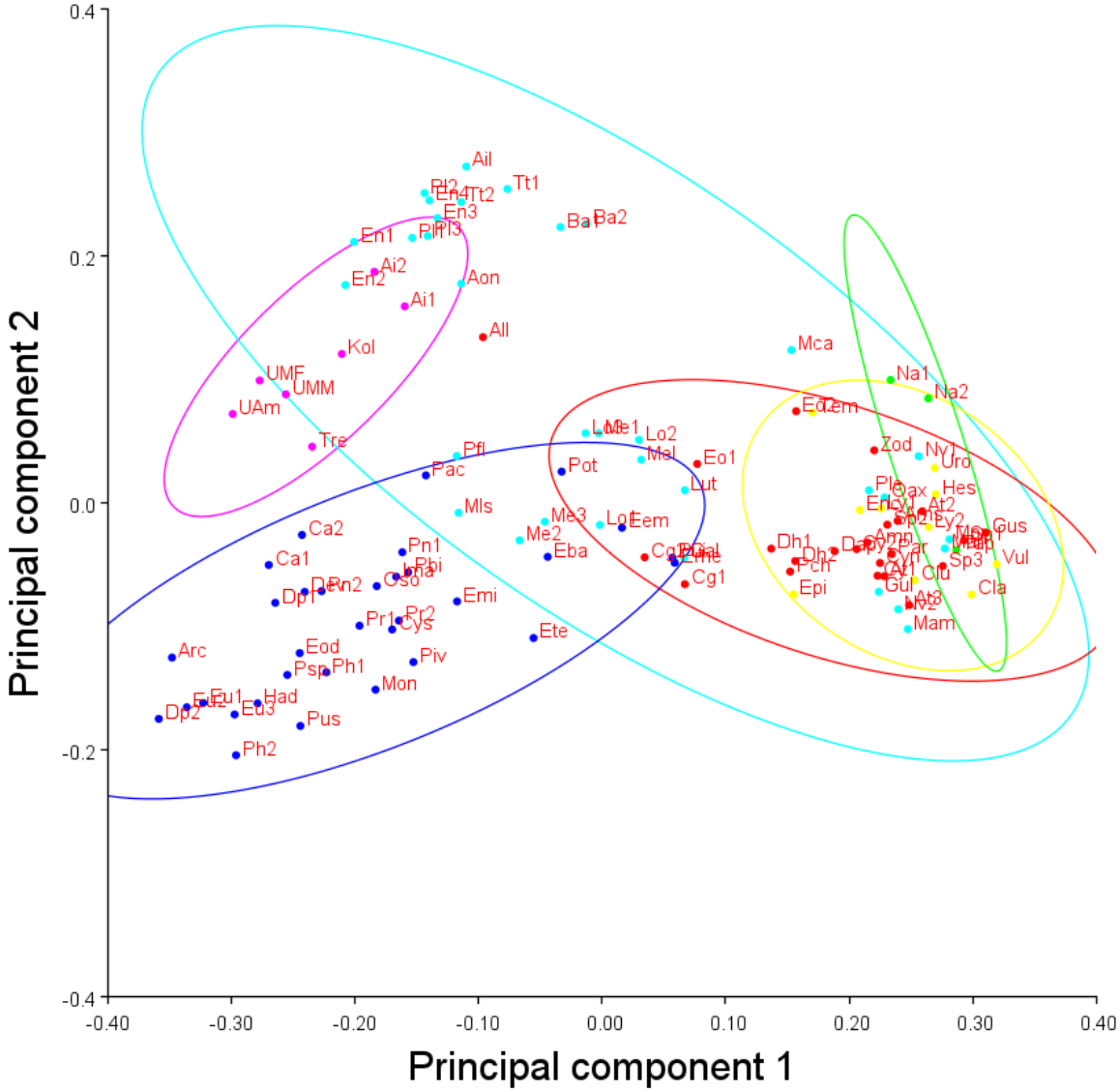

PC1 accounts for 51.8% of the total variance of the sample and PC2 accounts for 15.3%. Clades are represented by color and surrounded by 95% confidence ellipses. Basal carnivorans are green, enigmatic arctoids are red, canids are yellow, ursids are pink, musteloids are light blue, and pinnipeds are dark blue.

Figure 3.2. Canonical Variate Analysis of shape and clade identity.

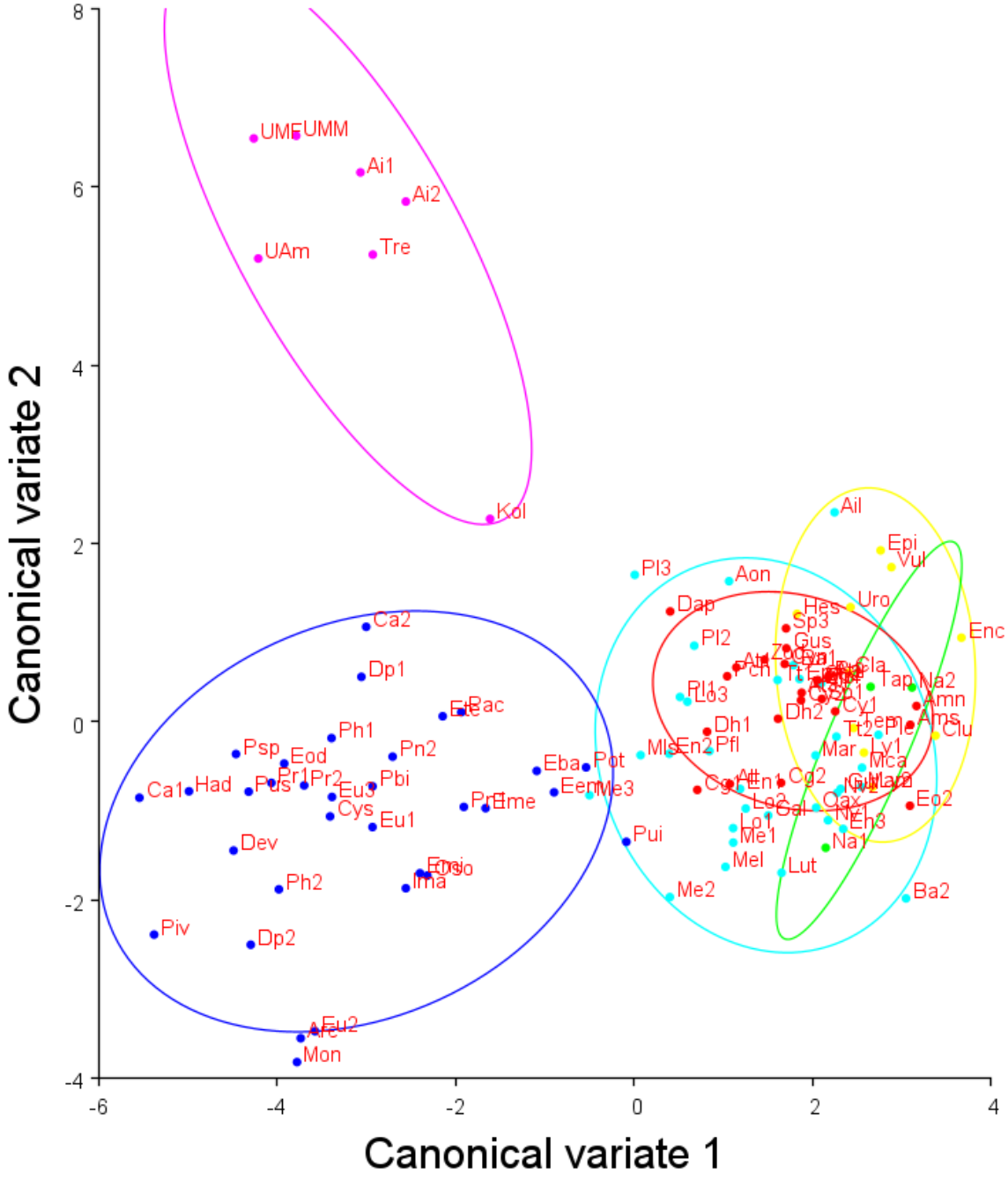

Clades are represented by color and surrounded by 95% confidence ellipses. Basal carnivorans are green, enigmatic arctoids are red, canids are yellow, ursids are pink, musteloids are light blue, and pinnipeds are dark blue.

Figure 3.3. Canonical Variate Analysis of shape and diet category.

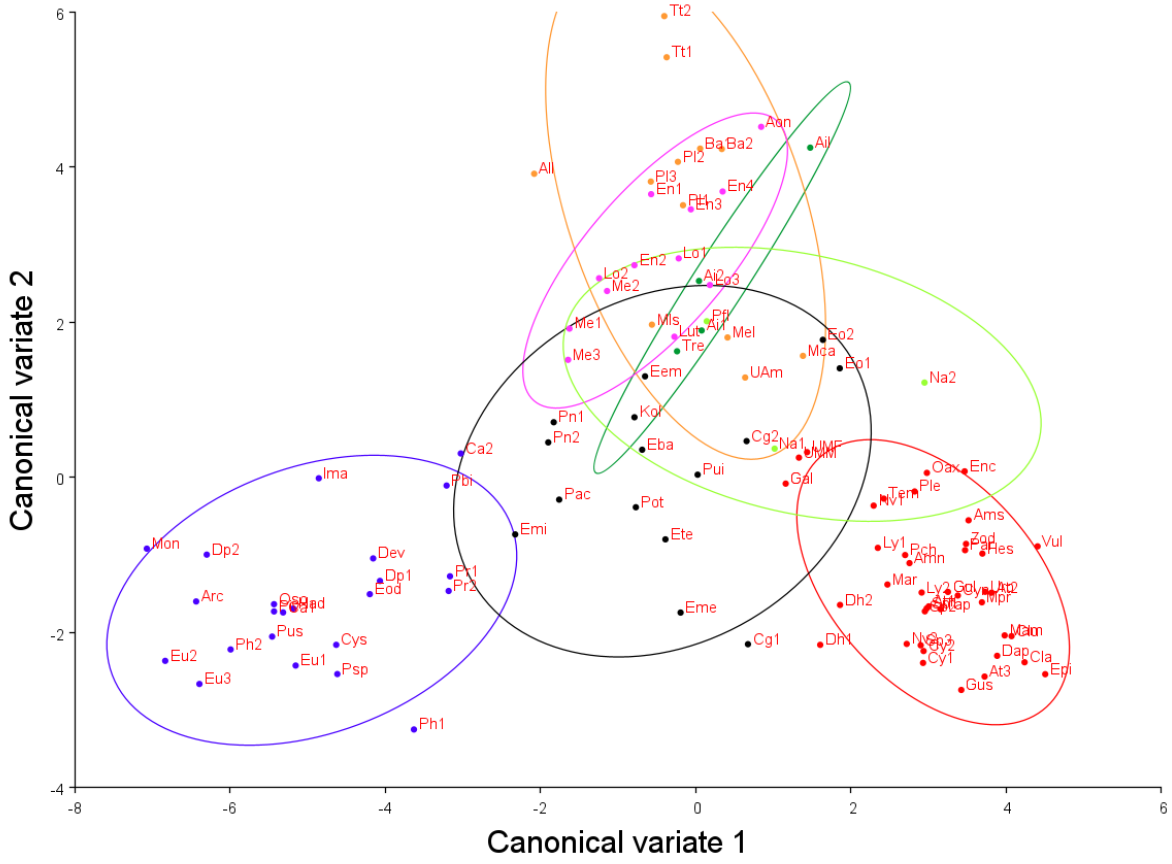

Dietary categories are represented by color and surrounded by 95% confidence ellipses. Carnivores are red, folivores are dark green, frugivores are light green, invertebrates consumers are pink, omnivores are orange, piscivores are blue, and taxa with yet unknown diets are black.

References 3

Adam, J., & Berta, A. (2002). Evolution of prey capture strategies and diet in the Pinnipedimorpha (Mammalia, Carnivora). *Oryctos* 4, 83-107.

Adams, D. C., Rohlf, F. J., & Slice, D. E. (2004). Geometric morphometrics: ten years of progress following the 'revolution'. *Italian Journal of Zoology*, 71(1), 5-16.

Begg, C. M., Begg, K. S., Du Toit, J. T., & Mills, M. G. L. (2003). Sexual and seasonal variation in the diet and foraging behaviour of a sexually dimorphic carnivore, the honey badger (*Mellivora capensis*). *Journal of Zoology*, 260(3), 301-316.

Figueirido, B., Plamqvist, P., & Perez-Claros, J. A. (2009). Ecomorphological correlates of craniodental variation in bears and paleobiological implications for extinct taxa: an approach based on geometric morphometrics. *Journal of Zoology 277*, 70-80.

Harano, T., & Asahara, M. (2022). Correlated evolution of craniodental morphology and feeding ecology in carnivorans: a comparative analysis of jaw lever arms at tooth positions. *Journal of Zoology 318*, 135-145.

Jones, K. E., Ruff, C. B., & Goswami, A. (2013). Morphology and biomechanics of the pinniped jaw: mandibular evolution without mastication. *The Anatomical Record*, 296(7), 1049-1063.

Kiel, S, Goedert, J.L., Huynh, T.L., & Looy, C.V. (2024). Early Oligocene kelp holdfasts and stepwise evolution of the kelp ecosystem in the North Pacific. *Proceedings of the National Academy of Sciences* 121(4).

Klingenberg, C. P. 2011. MorphoJ: an integrated software package for geometric morphometrics. *Molecular Ecology Resources* 11: 353-357

Meloro, C., & Tamagnini, D. (2022). Macroevolutionary ecomorphology of the Carnivora skull: adaptations and constraints in the extant species. *Zoological Journal of the Linnean Society*, 196(3), 1054-1068.

Modafferi, M., Melchionna, M., Castiglione, S., Tamagnini, D., Maiorano, L., Sansalone, G., Profico, A., Girardi, G. & Raia, P. (2022). One among many: the enigmatic case of

the Miocene mammal, *Kolponomos newportensis*. *Biological Journal of the Linnean Society*, 136(3), 477-487.

Morlo, M., Gunnell, G. F., & Nagel, D. (2010). Ecomorphological analysis of carnivore guilds in the Eocene through Miocene of Laurasia; pp. 269-310 in A. Goswami and A. Friscia (eds.), *Carnivoran Evolution: New Views on Phylogeny, Form and Function*. Cambridge University Press, Cambridge.

Rohlf, F. J. (2021). tpsDig, digitize landmarks and outlines, ver. 2.32. Department of Ecology and Evolution, State University of New York at Stony Brook.

Stirton, R. A. (1960). A marine carnivore from the Clallam Miocene Formation, Washington. Its correlation with nonmarine faunas. *University of California Publications in Geological Sciences* 36:345-368.

Tarquini, S. D., Chemisquy, M. A. & Prevosti, F. J. (2020). Evolution of the Carnassial in Living Mammalian Carnivores (Carnivora, Didelphimorphia, Dasyuromorphia): Diet, Phylogeny, and Allometry. *Journal of Mammalian Evolution 27*, 95-109.

Tedford, R. H., Barnes, L. G., Ray, C. E. (1994). The early Miocene littoral ursoid carnivoran *Kolponomos*: systematics and mode of life; pp. 11-32 in: A. Berta & T. A. Deméré (eds.), *Contributions in marine mammal paleontology honoring Frank C. Whitmore Jr.* San Proceedings of the San Diego Society of Natural History, San Diego.

Tseng, Z. J., Grohé, C., & Flynn, J. J. (2016). A unique feeding strategy of the extinct marine mammal *Kolponomos*: convergence on sabretooths and sea otters. *Proceedings of the Royal Society B: Biological Sciences*, 283(1826), 20160044.

Van Valkenburgh, B. (1989). Carnivore dental adaptations and diet: a study of trophic diversity within guilds. Pages 410–436 in J. L. Gittleman, ed. *Carnivore behavior, ecology, and evolution. Vol. 1*. Cornell University Press, Ithaca, NY.

Wang, X. M., Emry, R. J., Boyd, C. A., Person, J. J., White, S. C., & Tedford, R. H. (2023). An exquisitely preserved skeleton of *Eoarctos vorax* (nov. gen. et sp.) from Fitterer Ranch, North Dakota (early Oligocene) and systematics and phylogeny of North American early arctoids (Carnivora, Caniformia). *Journal of Vertebrate Paleontology Memoir 42:sup1,* 1-123.

Winer, J. N., Liong, S. M., & Verstraete, F. J. M. (2013). The dental pathology of southern sea otters (*Enhydra lutris nereis*). *Journal of Comparative Pathology*, 149(2-3), 346-355.

Zelditch, M. L., Swiderski, D. L., & Sheets, H. D. (2012). Geometric Morphometrics for Biologists: A Primer, Second Edition. Academic Press.